The Role of Soil Moisture Conditions in the Occurrence of Floods and Droughts over the Mississippi Basin

by

Jeremy S. Pal

A.S., Santa Monica College (1991)
B.S., Loyola Marymount University (1994)

Submitted to the Department of Civil and Environmental Engineering
in partial fulfillment of the requirements for the degree of

Master of Science in Civil and Environmental Engineering

at the

MASSACHUSETTS INSTITUTE OF TECHNOLOGY

May 1997

Author .....
Department of Civil and Environmental Engineering
19 May, 1997

Certified by .....
Elfatih A. B. Eltahir
Assistant Professor
Thesis Supervisor

Accepted by .....
Joseph M. Sussman
Chair, Departmental Committee on Graduate Studies

The Role of Soil Moisture Conditions in the Occurrence of Floods and Droughts over the Mississippi Basin

by

Jeremy S. Pal

Submitted to the Department of Civil and Environmental Engineering
on 19 May, 1997, in partial fulfillment of the
requirements for the degree of
Master of Science in Civil and Environmental Engineering

Abstract

In this study, we investigated the role that soil moisture conditions played in the drought of 1988 and the flood of 1993 over the Mississippi basin using a regional climate model. Simulations were initialized with different magnitudes of soil moisture to develop an understanding of the role of soil moisture in the atmospheric dynamics of these events. Additional simulations were performed with different initialization dates to see how the timing of the soil moisture anomaly affected climate. Furthermore, we used two different convective parameterizations (Kuo-Anthes and Grell) to determine whether the sensitivity of soil moisture to precipitation is influenced by the choice of convective scheme. Overall, regardless of the convection scheme used, the model did an adequate job in simulating the spatial patterns of precipitation in May and September of both years. However, in July, when convective activity in mid-latitudes is at a maximum, both convective parameterizations do an unsatifactory job of simulating the spatial distributions of rainfall. We found that neither improving the boundary condition resolution nor adjusting some of the convection scheme's parameters significantly improved the simulation of precipitation. The magnitude and timing of the soil moisture anomaly does play a large role in the sensitivity of precipitation to soil moisture. The two convective parameterizations, however, give significantly different results. Results from the Kuo-Anthes scheme suggest that soil moisture did play a major role in the persistence of the drought of 1988 and the flood of 1993. On the other hand, results from the Grell scheme indicate that the persistence of these events were primarily a result of large-scale circulation anomalies. The contrasting differences in soil moisture - precipitation sensitivities between the two convective parameterizations raises many questions about the results of previous numerical modeling studies.

Thesis Supervisor: Elfatih A. B. Eltahir
Title: Assistant Professor

Acknowledgments

Research support for this thesis was provided by the Alliance for Global Sustainability.

First and foremost, I would like to thank my advisor, Professor Elfatih Eltahir for his guidance and support through this reaserch. We have grown together; he as professor and I as student. In addition, I would like to thank all of those of the Eltahir Research Group for their help as friends and colleagues: Kirsten Findell, Cuiling Gong, Jim Humphries, Bassam Kassab, Julie Kiang, Guiling Wang, and Xinyu Zheng. Lynn (the true computer guru) Reid has not only been a friend, but she has also taught me how to be a system administator for the research group and Parsons Lab; something I can not place value on. I would also like to thank Gary Bates of NCAR for teaching me how to use and providing me with RegCM2 and for his patience with me. In addition, thanks to Steve Hollinger and Jin Huang for providing me with the soil moisture data used in this study.

I would like to acknowledge Mara Pereira for believing in me. Without her, I would not be where I am today. Thanks to my best friends, Joey Ancrile and Steve Avooski, for simply being my best friends. Ziad Zakharia has also been a great friend and teacher, here and at LMU. Jenny Jay has been my friend and counsellor. She has always been there for me when times have been tough. Richard (Romeo) Camilli, Paolo (Casanova) Sammarco, Kirsten (Guru Hildy) Findell and David (Jambalaya) Senn have all been great friends. I would like to thank Garbo, my wonderful dog, for being a shoulder to cry on and for listening to me all these years when no one else would listen. I deeply appreciate my parents, David and Marie-Luise Pal, and my grandparents, George (in spirit) and Elisabeth Pal for all their love and support. And, of course, I would like to thank Nicole Gasparini for bringing happiness back into my life and for being such a wonderful person.

Just in case I forgot someone, thanks to my friends and family, all of the people of the Parsons Laboratory, and anyone who has helped me in this research.

Contents

List of Figures

List of Tables

Chapter 1

Introduction

1.1 Objective/Overview

Eagleson (1994) writes that "drought and flood have driven the search for understanding of water since the first civilizations formed along the banks of rivers." Figure 1-1 (taken from Dooge (1988)) is a water-level gage for the Nile River (Nilometer) built over four thousand years ago. It was calibrated by Pliny the Elder to demonstrate the social and economic consequences of river stage. Notice that adversity is associated with both extremes: flood and drought.

The 1988 summer drought over the United States was the worst in recent decades. According to Ropelewski (1988), the summer of 1988 was the warmest and driest since 1936. It resulted in approximately 10,000 deaths from heat stress and caused an estimated $30 billion in agricultural damage (Trenberth and Branstator 1992). The 1993 summer flooding over the Midwestern United States was one of the most devastating floods in modern history (Kunkel et al. 1994). Record high rainfall and flooding occurred throughout much of the Upper Mississippi River basin and persisted for long periods. The National Oceanic and Atmospheric Administration (NOAA) estimated that the flood caused $15-20 billion in damages (NOAA 1993). Such extreme events result in large financial losses for the agricultural community and cause additional hardship and personal loss in many urban communities.

Figure 1-2 shows maps of observed United States Historical Climatology Network

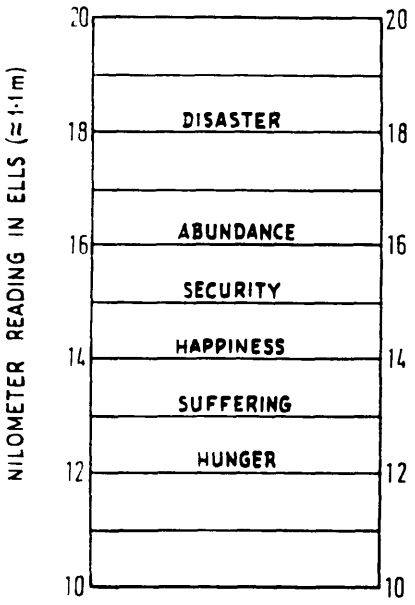

Figure 1-1: Pliny the Elder's social calibration of the Nile River's stages. Taken from Dooge (1988).

accumulated precipitation and precipitation anomalies (May, June, and July) for the Midwestern U.S. during 1988 and 1993. Note the large negative anomalies (light shading) over the Midwest during 1988 and the large positive anomalies (dark shading) during 1993. Associated with these extreme rainfall conditions were extreme soil moisture conditions over the Midwest. Figure 1-3 shows a time series (1981 through 1993) of Illinois State Water Survey soil saturation from zero to ten centimeters averaged over the state of Illinois. Clearly, 1988 (lower solid line) and 1993 (upper solid line) are the most extreme on record. Kerr (1989) suggests that global warming due to increased levels of CO_2 may be responsible for extreme events such as these. Trenberth and Guillemot (1996) concluded that these extremes are initiated by tropical sea surface temperatures (SSTs). Still others think that the severity of floods and droughts is amplified by soil moisture anomalies (for example, Atlas et al. (1993); Betts et al. (1996)). This study attempts to determine whether the extreme soil moisture conditions observed in 1988 and 1993 played a role in initiating and enhancing these extremes in observed precipitation or whether they were simply a bi-product of these extremes.

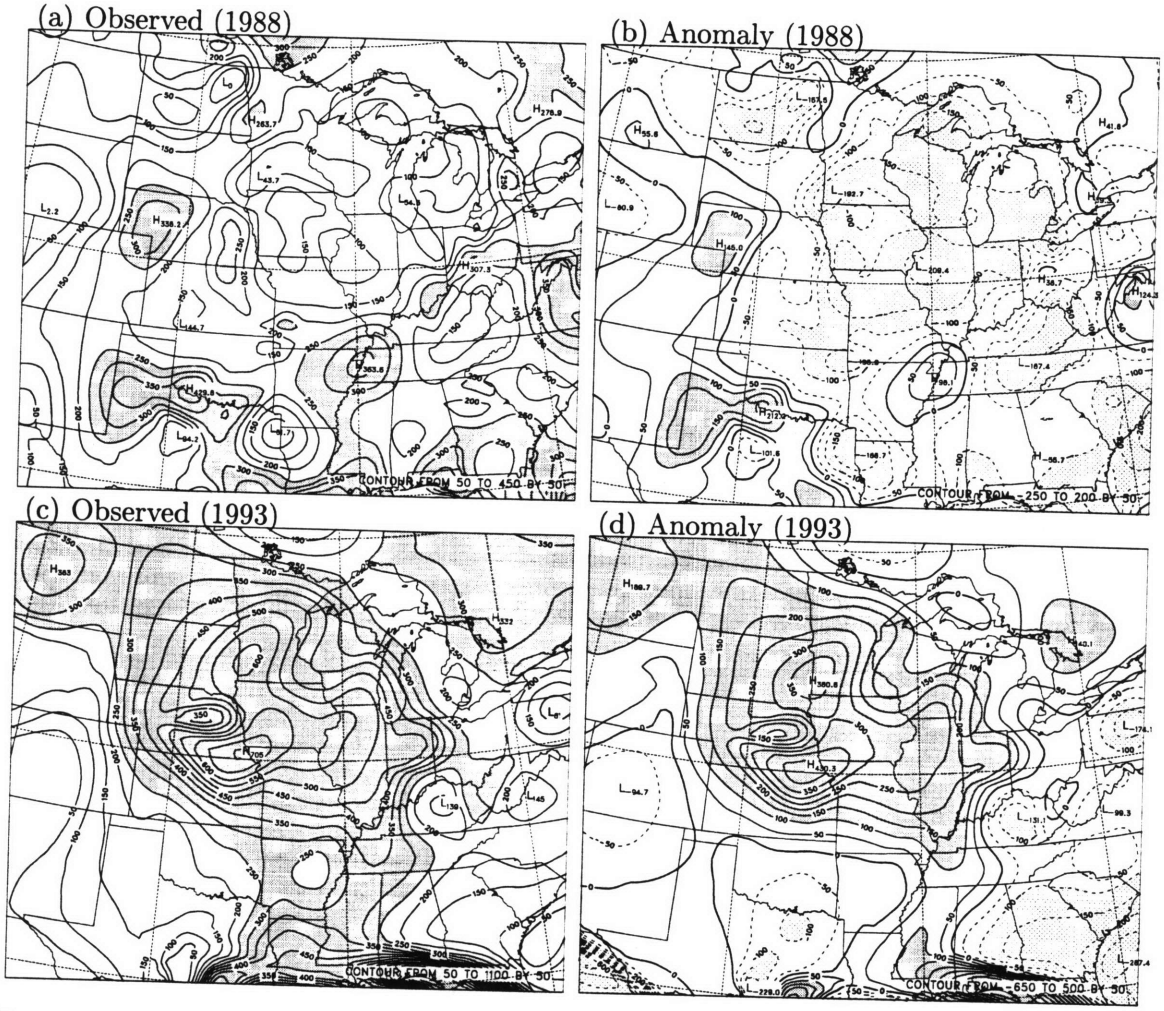

Figure 1-2: May, June, and July observed precipitation and precipitation anomalies (mm) for 1988 and 1993 based on the U.S. Historical Climatology Network Dataset. Shading occurs for observations over 250 mm and anomalies above 100 mm.

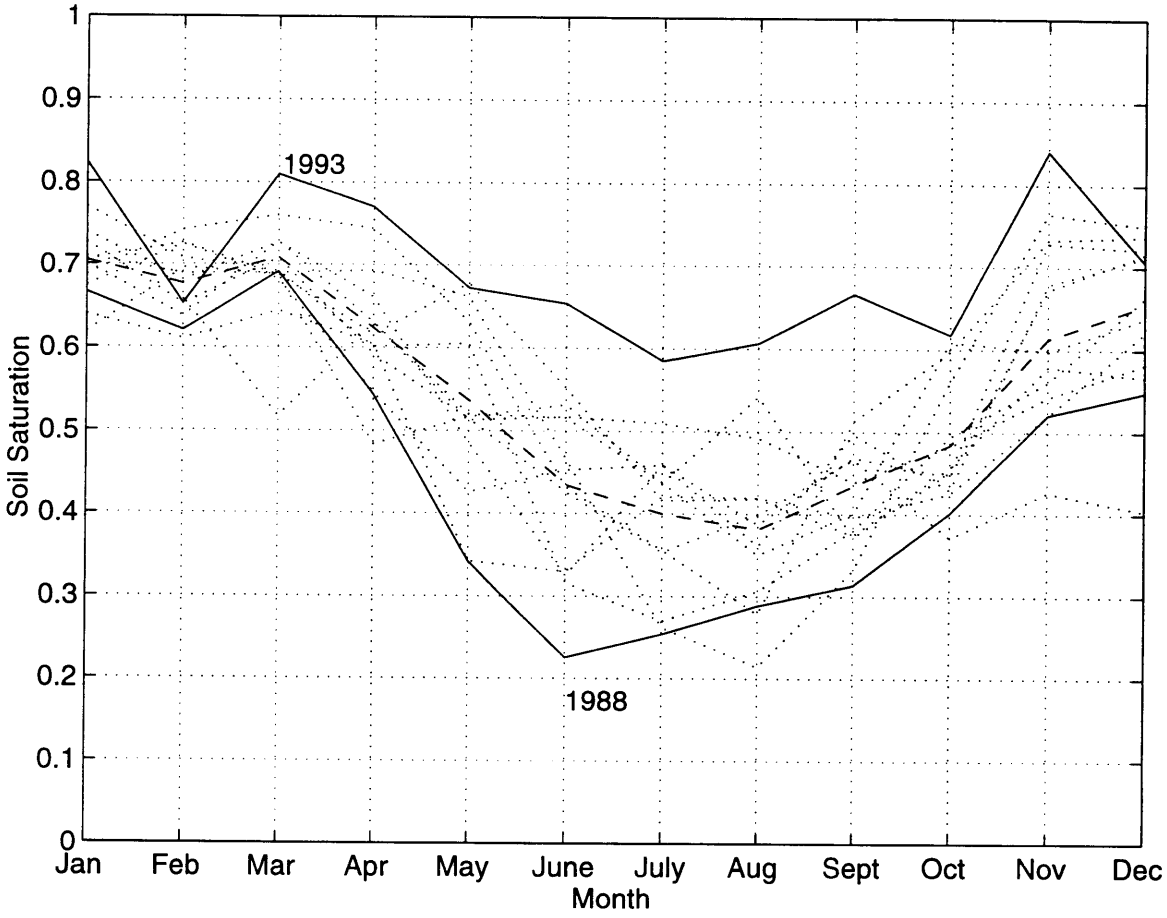

Figure 1-3: Illinois State Water Survey monthly averaged soil saturation from 0 to 10 cm for 1981 to 1993. Lower solid line is the soil saturation for 1988, upper solid line is for 1993, dotted lines are the rest of the years, and dashed line is the average of all of the years.

This study focuses on the drought of 1988 and the flood of 1993 in the Midwestern United States with the objective of studying the role of soil moisture conditions in initiation and maintenance of droughts and floods. It is well recognized that soil moisture is an important element in the climate system. It has many implications on the surface energy and water balance. The main hypothesis of this study is that soil moisture not only affects the water balance through the recycling of precipitation, but it also affects the energy balance via the Bowen ratio and albedo changes. More specifically, an increase in soil moisture yields an increase in moist static energy which yields an increase in convection and hence rainfall. A recent study by Eltahir and Pal (1996) showed that an increase in wet-bulb temperature (a measure of moist static energy) increases the frequency and magnitude of rainfall events in convective regimes such as those occurring in the tropics and mid-latitudes during the summer. Therefore, an increase in soil moisture should lead to an increase in the frequency and volume of rainfall.

In trying to understand of the role of soil moisture in the extreme events of 1988 and 1993, this study investigates the predictability of summer rainfall based on spring initial soil moisture conditions using a regional climate model (RCM). In other words, it assesses whether or not the extreme events of 1988 and 1993 were a result of local or large-scale forcings by using the Second Generation Regional Climate Model (RegCM2) developed by the National Center for Atmospheric Research (NCAR) and the Pennsylvania State University (PSU). Futhermore, it attempts to determine if and and how the magnitude of the soil moisture anomaly affects future precipitation over the Midwestern U.S.

Many General Circulation Model (GCM) studies, such as Shukla and Mintz (1982), Oglesby (1991), and Betts et al. (1996) have shown that soil moisture plays an important role in the climate of mid-latitude summers. They, in general, show that low soil moisture conditions produce less future rainfall than high soil moisture conditions. On the other hand, regional climate models have shown conflicting results. For example, a recent study by Giorgi et al. (1996) concludes that there is a negative feedback between soil moisture and precipitation while Pan et al. (1995) show mixed

results depending on the year. The credibility of these models depends on their ability to simulate precipitation processes. Precipitation, however, is one of the most difficult fields to simulate due to unresolvable convection and cloud processes even at RCM spatial resolutions. If precipitation is simulated poorly, the water balance will be simulated incorrectly which then affects the energy balance (see Chapter 2). This study aims to shed some light on the reasons for the inconsistencies in numerical model results by testing the sensitivity of the model simulations to the selection of the convective parameterization in RegCM2. This will help to further define some of the limitations and uncertainties in numerical weather prediction.

1.2 Summary of Previous Studies

Over the past twenty years, extensive work has gone into the study of how soil moisture affects boundary layer, surface, and atmospheric fields. Most of this work has been performed by numerical models such as General Circulation Models. This chapter gives a brief description of the previous observational and numerical modeling studies relevant to the 1988 drought and the 1993 flood.

1.2.1 Observational Studies

Kunkel et al. (1994), from their analysis of the National Climatic Data Center (NCDC) precipitation data, found that the summer rainfall totals for 1993 over the upper Midwestern United States exceeded the 200 year return period event. By several measures, the summer of 1993 was, by far, the wettest on record. They concluded that above average rainfall over the previous year helped to set the stage for summer flooding by June 1, 1993. That is, the highly saturated soils and the full rivers across the Midwest enhanced the effects of the record rainfall when it occurred during the summer.

Bell and Janowiak (1995) presented an observational analysis of the large-scale atmospheric circulation associated with the flood of 1993. They found that an El Niño related mid-spring breakdown of the ridge over the western U.S. enhanced zonal

flow from the western North Pacific to the eastern U.S. in early June. The zonal flow configuration provided a "duct" for intense cyclones to propagate into the Midwest. The cyclones then triggered intense convective complexes over the Midwest initiating major flooding.

Trenberth and Guillemot (1996) concluded that tropical SSTs induce atmospheric circulation changes across North America and hence, were the primary cause of the drought of 1988 and the flood of 1993. In 1988, they found that the strong La Niña and warm SST anomaly southeast of Hawaii caused a northward shift in the intertropical convergence zone (ITCZ), which in turn caused a northward shift in the storm track across North America. In contrast, for 1993 they found that the El Niño shifted the ITCZ south of normal which shifted the storm track southward. They concluded that the southern storm track of 1993 created a link to the moisture from the Gulf of Mexico via transient eddies. This link is what they believe to be responsible for the record rainfall observed over the Midwest in 1993. This link did not exist in 1988 due to the northward shift in the storm track and hence the lack of observed precipitation. Paegle et al. (1996) discuss this link in further detail. Lastly, Trenberth and Guillemot (1996) concluded that soil moisture may have played a role in the maintenance and persistence of these events after they were established.

Recently, using observed soil moisture and precipitation data over the state of Illinois, Findell and Eltahir (1997) found that the feedback of soil moisture and precipitation is a function of the time of year. More specifically, they found that soil moisture and subsequent precipitation show a significant correlation in the summer while little or no correlation is shown for the rest of the year. This summertime correlation is stronger than the serial correlation of precipitation, indicating that there is a positive feedback between soil moisture and precipitation over the state of Illinois during summer months.

1.2.2 GCM Studies

Most GCM studies of how soil moisture affects precipitation indicate that the climate of the U.S. and other regions are sensitive to soil moisture during months that are

dominated by convective storms. The following is a review of GCM sensitivity studies that were performed over the past 15 years.

Shukla and Mintz (1982) found that precipitation increased and temperature decreased for most of the globe for simulations with evapotranspiration equal to the potential evapotranspiration, as opposed to simulations where evapotranspiration equaled zero. Rowntree and Bolton (1983), in a similar study, found similar results for their simulations over Europe.

Oglesby (1991) used the NCAR Community Climate Model version 1 (CCM1) GCM to run two reduced soil moisture simulations (soil moisture saturation equal to 0.01) over North America: one where the perturbation occurred on March 1 and the other occurring on May 1. By comparing their results to the control run, they found that "a mid- to late-spring soil moisture anomaly could have a significant impact on the climate of the following summer and could help induce drought conditions." However, the late-winter, early-spring soil moisture anomaly could be corrected. Therefore, the timing of the soil moisture anomaly is crucial for the onset and/or persistence of a drought.

Atlas et al. (1993) found from their GCM simulations that 1988 tropical SST anomalies decreased precipitation over the Great Plains but did not increase temperature while SST anomalies in high latitudes had little effect. In contrast, their results showed that anomalous soil moisture conditions (derived values based upon 1988 surface conditions) produced a larger reduction in precipitation and a significant increase in surface air temperature over the Great Plains, as observed. Hence, they concluded that soil moisture deficit contributed to the severity of the hot and dry drought of 1988 via a positive feedback on rainfall and temperature.

Beljaars et al. (1996) performed soil moisture sensitivity simulations for the flood of 1993 using the European Centre for Medium Range Weather Forecasts (ECMWF) model. They found that the moist runs, where soil moisture was initialized at the field capacity, produced much more precipitation than dry runs where soil moisture was initialized at 25% of the availability. They concluded that the persistence in precipitation indicates that "there may be a seasonal predictability potential related

to the depletion timescale of the soil moisture reservoir." Betts et al. (1996) drew further conclusions from these simulations by asserting that soil moisture enhanced precipitation during the flooding of 1993. They found that the increased sensible heat flux associated with dry soil moisture conditions increases entrainment of air of lower equivalent potential temperature from the boundary layer top and therefore decreases convection.

1.2.3 RCM Studies

Unlike the results of most GCM studies, RCMs give mixed results on how soil moisture affected precipitation for the drought of 1988 and the flood of 1993. In addition, very few soil moisture sensitivity simulations have been performed using RCMs. The following gives a brief description of each of these studies and their conclusions.

Pan et al. (1995) performed a series of one-day sensitivity simulations on the drought of 1988 and the flood of 1993 to investigate how evapotranspiration affected rainfall in the Midwestern United States. The control runs used crop moisture and Palmer drought indices to infer surface evaporation. For the saturated runs, they maintained surface evaporation at 99% of the potential evaporation and for the dry runs, they maintained surface evaporation at 1% of the potential evaporation. A few rainfall events from each of the two years were chosen for simulation. Their results suggest that a large-scale circulation was responsible for deficient rainfall observed in the drought of 1988. In contrast, their simulations suggest that local evapotranspiration contributed to the flooding that occurred in 1993. Additional simulations were performed with surface evaporation over the drought- and flood-stricken regions prescribed at the saturated case and the rest of the domain at the psuedo-observed values to see if the contrast between the wet north and dry south enhanced rainfall during these years. The results of these simulations did not significantly change from the control runs.

A later study by Pan et al. (1996) tested how the sensitivity of different convection schemes (Kuo and Grell) and surface flux schemes (Simple Biosphere Model and aerodynamic formulation) affect the soil moisture-precipitation feedback. They found

that increased soil moisture enhanced total rainfall over the Midwest for isolated 24-hour rainfall events in July 1993. They further added that higher soil moisture enhanced local rainfall when the lower atmosphere was dry and unstable. In contrast, high soil moisture decreased rainfall when the atmosphere was moist and stable. In addition, they found the Kuo scheme exhibited a greater sensitivity to soil moisture than did the Grell scheme. They believe that the different sensitivities are due to how the schemes partition rainfall between convective and stable forms, and due to the different closure assumption in each scheme. Lastly, the different surface flux schemes had little impact on the results of their 24-hour simulations.

Paegle et al. (1996) attempted to simulate the summertime atmospheric conditions of 1993 with the University of Utah Local Area Model (ULAM). Their control run used evaporation forecasts from the Global Data Assimilation System of the NCEP/NWS/NOAA. Two perturbed experiments were run: one with high southern evapotranspiration and the other with high northern evapotranspiration. They found that the low-level jet that travels from the Gulf of Mexico northward into the Midwest was enhanced by dry southwestern conditions. The enhanced low-level jet results from an increase surface temperature which decreases static stability and enhances low-level moisture which then amplifies precipitation over the flood region. They also found that moist southwest conditions weakened the low-level jet and decreased precipitation in the flood region. Furthermore, moist northern conditions tended to spread out the precipitation over the Midwest. They concluded that the low-level jet is a more important mechanism for rainfall release over the flood region than moistening through local evapotranspiration.

Giorgi et al. (1996), in study using RegCM2, found that local evaporated water played a minor role in the drought of 1988 and the flood of 1993. They concluded that the extreme weather events were due to large-scale circulations and that dry soil moisture conditions actually enhanced convection due to an increased buoyancy from the increased sensible heat flux. Therefore, they believe that there is actually a negative feedback between soil moisture and precipitation. Their control runs had soil moisture initialized at the field capacity of the soil, and their perturbed runs were

initialized at the wilting point of the soil.

Finally, Entekhabi et al. (1992) investigate the occurrence and persistence of droughts using a simple model that couples the water balance of continental landmasses and the overlying atmosphere. Precipitation over the land is derived from atmospheric moisture that is supplied by local evapotranspiration and external advection. They represent the synoptic scale features that initiate droughts as simple white noise random perturbations. The solution to their stochastic model exhibits a bimodal probability distribution for soil moisture and precipitation. They conclude that, due the soil moisture-rainfall feedback, "climate persists in one mode and occasionally transitions to the other mode in the presence of strong inducements" (p. 812). Clearly, simple mechanistic models can be useful for developing a qualitative understanding of the feedbacks associated with soil moisture anomalies.

1.3 Scope of the Study

This study uses a regional climate model to investigate the impact of initial soil moisture on precipitation. Accurate simulation of rainfall requires a precise knowledge of soil moisture coupled with an accurate representation of hydrologic processes. This study takes advantage of two soil moisture datasets to initialize soil moisture at more realistic values. Pairs of simulations are performed using pseudo-observed atmospheric initial and boundary conditions. The only difference between the pairs is the initial soil moisture. Most previous modeling studies prescribe the worst possible scenario (see Section 1.2). In many instances, evapotranspiration is considered to be a surrogate for soil moisture and is maintained with no dynamic feedback at values close to zero for the dry simulations and close to the potential evapotranspiration for the wet runs. In less extreme cases, soil moisture is prescribed at the wilting point for the dry runs and at the field capacity for the wet runs where two-way interaction is allowed. These extreme conditions are not observed in nature. One aspect of this study is to investigate the impact of specifying soil moisture at these extreme values. We expect that the larger the soil moisture anomaly, the more pronounced impact

it has on precipitation. It is conceivable that precipitation may show sensitivity to extreme soil moisture changes and show no sensitivity to changes comparable in magnitude to those observed in nature.

This study will also investigate the seasonal dependence of the soil moisture-rainfall feedback. Soil moisture would be expected to affect precipitation over mid-latitudes during the summer when convective activity is at a maximum. In contrast, soil moisture would be expected to have little or no impact on precipitation in the winter when large-scale synoptic conditions dominate. A data analysis study by Findell and Eltahir (1997) concluded that soil moisture has a significant impact on future precipitation during summer (convective) months and has little or no impact during rest of the year when large-scale conditions dominate. In contrast, a recent modeling study by Castelli and Rodriguez-Iturbe (1996), found that heterogeneous soil moisture conditions can modify the dynamics of large-scale circulations. This study focuses on comparing the impact of local conditions (interior) versus boundary conditions (large-scale). By doing this, we aim to understand the some of the limitations and uncertainties of the seasonal predictability of precipitation based on the timing of the initial soil moisture conditions.

Several questions are being addressed in this study: Were the extreme events of 1988 and 1993 initiated and maintained by external forcings or were they due to internal mechanisms such as soil moisture? What role does the magnitude of the soil moisture anomaly play? How does the timing of the soil moisture anomaly affect the onset of such events? What role does the convective parameterization play in the results of numerical modeling studies? And how do the spatial and temporal resolution of the boundary conditions affect the results of the RCM simulations?

This thesis is organized into 6 chapters. Chapter 2 discusses the role of soil moisture and gives a description of the soil moisture datasets used in this study. A brief description of RegCM2 and its components is given in Chapter 3. Chapter 4 gives a detailed description of the model domain, initial and boundary conditions, and numerical experiments. Chapter 5 discusses the results of the numerical experiments. Finally, Chapter 6 summarizes the findings and gives possible future

research directions.

Chapter 2

Soil Moisture and Soil Moisture Datasets

2.1 Role of Soil Moisture

It is well recognized that soil moisture plays an important role in the climate system. Paul Dirmeyer (Dirmeyer 1995) states that soil moisture is a "source of moisture (latent heat) for the atmosphere, it acts to stabilize surface temperature (via sensible heating and longwave radiation), it affects surface runoff rates, it changes the color and radiative properties of the soil (through albedo changes), it affects transpiration rates in vegetation (latent heat), it affects vegetation physiology and distribution (surface roughness, albedo, etc.) on long times scales, it recharges groundwater (water table level), and it affects geochemical and biochemical cycles (carbon, pollutants, tracers, etc.)." Although some may not exactly agree with his description of soil moisture, Dirmeyer's statement shows that soil moisture plays many important roles.

Soil moisture plays many important roles in the climate system. Studies by Eltahir (1997), Betts et al. (1996), Entekhabi et al. (1996), among others, suggest that soil moisture not only impacts the water balance of the boundary layer, but it also impacts the energy balance. These studies indicate that soil moisture affects that partitioning of heat fluxes from the ground into latent and sensible forms. The following is a description of the mechanisms involved in how soil moisture affects

boundary layers processes as described in Eltahir (1997). Increased soil moisture increases net solar radiation at the surface via a decrease in albedo; wet soil absorbs more than dry soil. In addition, it also decreases the Bowen ratio by increasing latent heat flux and decreasing sensible heat flux. The increased latent heat moistens the lower atmosphere while the decreased sensible heat cools the surface. Both yield an increase in net longwave radiation at the surface. Therefore, with all else being equal, wet soil moisture conditions increase net radiation at the surface. Furthermore, wet soil moisture conditions imply a shallow boundary layer due to the decreased sensible heat flux. The increase in net radiation (total heat flux) and the shallower boundary layer should generate more moist static energy per unit depth. In contrast, Betts et al. (1996) proposed different mechanism of how soil moisture impacts the boundary layer. They suggest that drier soil moisture conditions increase turbulence, and, hence, entrain more air from above the boundary layer of lower equivalent potential temperature (a quantity proportional to moist static energy). Eltahir (1997) and Betts et al. (1996) disagree on the dominant mechanisms involved in how soil moisture impacts the boundary layer. However, they agree that soil moisture increases the moist static energy of the boundary layer per unit depth. A recent study by Eltahir and Pal (1996) shows that an increase in wet-bulb temperature (a quantity proportional to moist static energy) increases the frequency and magnitude of rainfall events in convective regimes such as the tropics and mid-latitudes during the summer. Hence, an increase in soil moisture should lead to an increase in the frequency and volume of rainfall. In addition to the implications soil moisture has on the surface energy and water balance, soil moisture directly affects runoff rates. For example, Kunkel et al. (1994) found that the high soil moisture in 1993 amplified the flooding that occurred over the Mississippi basin.

According to Giorgi et al. (1996), surface sensible and latent heat flux have two opposing effects on summer precipitation in mid-latitudes. First, as mentioned above, wet soil moisture conditions provide more moisture for evaporation (latent heat) which provides increased moisture for convective storms. This would result in more precipitation and hence a positive feedback for extreme conditions such as the drought

of 1988 and the flood of 1993. On the other hand, dry soil moisture conditions result in a reduction in evaporation and an increase in sensible heat. This increase in sensible heat provides additional buoyancy that enhances convection and broadens cyclonic systems and hence, is a negative feedback in extreme conditions.

The above remarks imply the importance of an accurate representation of soil moisture. Unfortunately, knowledge of soil moisture is virtually non-existent on both high spatial and temporal scales. For this reason, most studies that focus on the impacts of soil moisture on climate have performed sensitivity simulations using soil moisture initialized at extreme values such as the wilting point of the soil or no moisture for the dry runs and the field capacity or saturated for the wet runs. In fact, in some cases, evapotranspiration is used as a surrogate for soil moisture and is held constant throughout the simulation.

An excellent soil moisture dataset exists for 19 different locations over the state of Illinois (see Hollinger and Isard (1994)). It was developed by the Illinois State Water Survey (ISWS) and was also used in Findell and Eltahir (1997). This dataset, however, does not cover a wide spatial range. A recent modeled dataset, based on station precipitation and temperature was developed by Huang et al. (1996) (hereafter referred to as HDG data). This is a monthly dataset for 344 stations over the entire U.S. since 1931. These datasets provide the most spatially and temporally extensive soil moisture data over the entire U.S. and hence can be more realistically used to initialize model simulations. The remaining sections describe both of these datasets in greater detail.

2.2 Datasets

The initialization of soil moisture in models is very important for an accurate representation of the land surface energy balance. This study takes advantage of two excellent datasets to initialize soil moisture in each simulation.

2.2.1 Illinois State Water Survey (ISWS) Data

The ISWS is responsible for a network of direct soil moisture measurement stations across the state of Illinois (see Hollinger and Isard (1994)). To date, it provides the most accurate and the most spatially and temporally extensive soil moisture dataset of its kind. Since 1981, biweekly measurements, using a neutron probe, have been taken at 11 depths down to two meters (0-10, 10-30, 30-50, 50-70, 70-90, 90-110, 110-130, 130-150, 150-170, 170-190, and 190-200 cm) over a number of grass-covered sites across Illinois. When the project started in 1981, there were eight sites. Seven more were added in 1982, two more in 1986, and by 1992 the number of stations totalled 19. Figure 2-1 is a map of the 17 soil moisture measurement locations that existed between 1986 and 1992. Although this is the best data set we have, it does not cover a large enough spatial range to initialize the entire domain of an RCM.

Figure 2-2 shows how soil saturation varies annually. Clearly, for the surface layer, 1988 and 1993 are the most extreme summers of the dataset. However, when the deeper zones are included, much less seasonal and interannual variablity is displayed. In fact, 1988 is no longer the driest year in terms of soil saturation. In addition, the winter variability is much lower than the remainder of the year, especially the summer. It appears that in the mid- to late-spring substantial drying occurs during the "spring green up." The amount of drying varies from year to year. Notice that extreme drying occurred in 1988 while little or no drying occurred in 1993. Apparently, some sort of phenomena determines the amount of drying that occurs in a given year. One of the objectives of this study is to decipher whether large-scale or internal forcings are responsible for the initiation, maintenance, and persistence of the drought of 1988 and the flood of 1993. Figure 2-3 shows soil moisture as it varies with depth for each season. There is little difference between each of the years during the winter months (DJF). When comparing Figure 2-3(b) and Figure 2-3(c) it is noticable that extreme drying occurred in the spring of 1988. Note that the difference in soil moisture at lower depths between years becomes less apparent. In fact, for 1988, below 1.4 meters, the soil moisture closely follows the mean profile. Therefore, if there is a lot

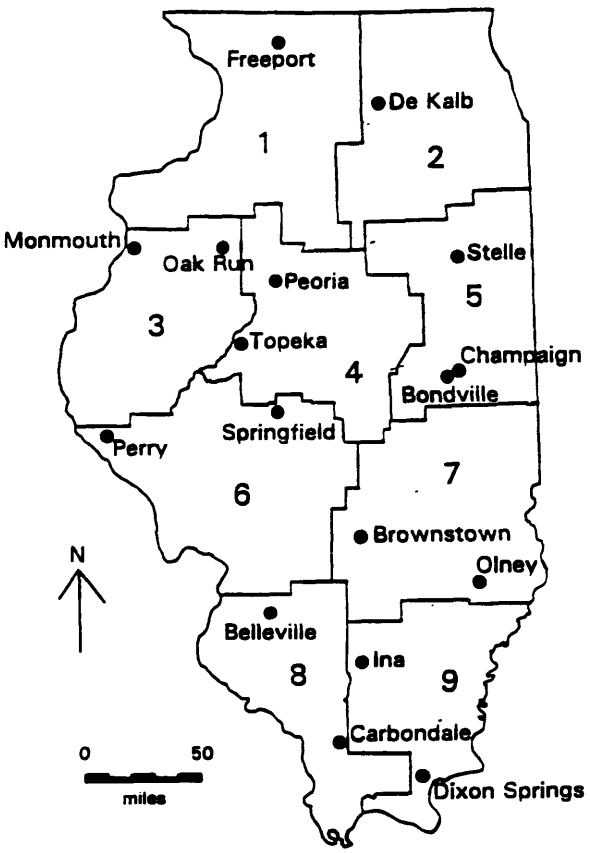

Figure 2-1: Map of the 17 Illinois State Water Survey soil measurment stations across the state of Illinois that existed between 1986 and 1993. Taken from Hollinger and Isard (1994).

of vegetation with deep roots, 1988 may not show much sensitivity to soil moisture. However, most of the Midwest is crop land and therefore has shallow roots. Hence, when evapotranspiration occurs more moisture is extracted from the upper zones.

2.2.2 Huang et al. (1996) (HDG) Soil Moisture Data

The HDG soil moisture data used in this study comes from a simulated dataset created over the continental United States (Huang et al. 1996). It spans the period from 1931 to 1993. The model used to generate data is based on the water budget of the soil and uses monthly precipitation and monthly temperature as inputs. Its four parameters were calibrated using observed precipitation, temperature, and runoff from an area in Oklahoma. The model performed remarkably well when compared to the ISWS soil moisture data (correlation coefficient = 0.84). Therefore, this dataset should be adequate in initializing the domain of a RCM. The following gives a description of the governing equations of the HDG simulated soil moisture dataset.

The dynamics of soil moisture over an area, A, is expressed as follows:

$$\frac{dW(t)}{dt} = P(t) - E(t) - R(t) - G(t), \tag{2.1}$$

where $W(t)$ is the soil water content at time t, $P(t)$ is the mean areal precipitation, $E(t)$ is the mean areal evaporation, $R(t)$ is the net streamflow divergence, and Gt) is the net groundwater loss (through deep percolation).

Surface runoff $S(t)$ and baseflow $B(t)$ are parameterized as follows:

$$S(t) = P(t)[\frac{W(t)}{W_{\max}}]^m \tag{2.2}$$

$$B(t) = \frac{\alpha}{1+\mu} W(t), \tag{2.3}$$

where $W_{\max}$ is a measure of the capacity of soil to hold water in millimeters, m is a parameter with values greater than 1, α is the inverse response time of the baseflow, and μ dimensionless parameter that determines the portion of the subsurface flow

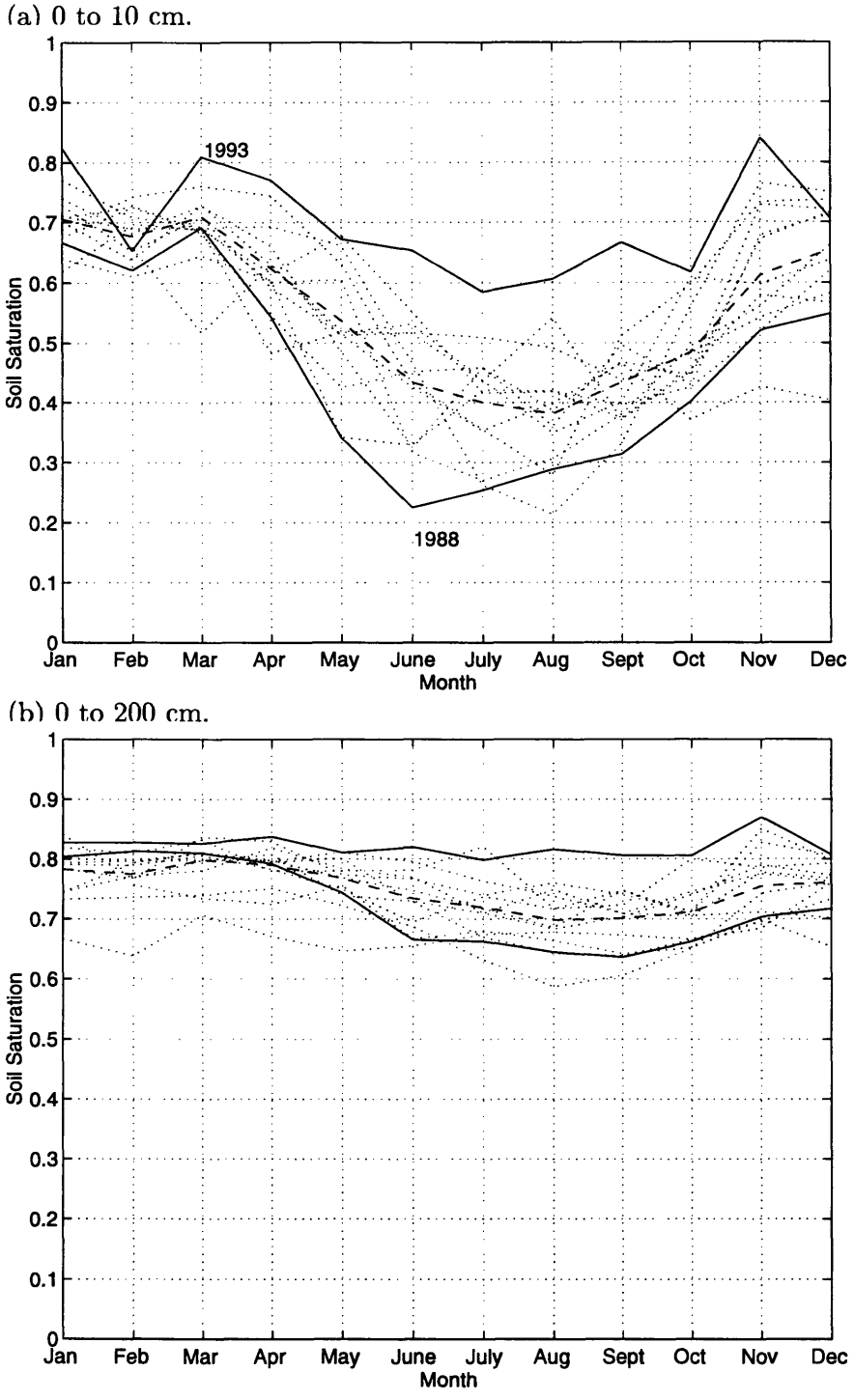

Figure 2-2: Illinois State Water Survey monthly averaged soil saturation from (a) 0 to 10 cm and (b) 0 to 200 cm for 1981 to 1993. Lower solid line is the soil saturation for 1988, upper solid line is for 1993, dotted lines are the rest of the years, and dashed line is the average of all of the years.

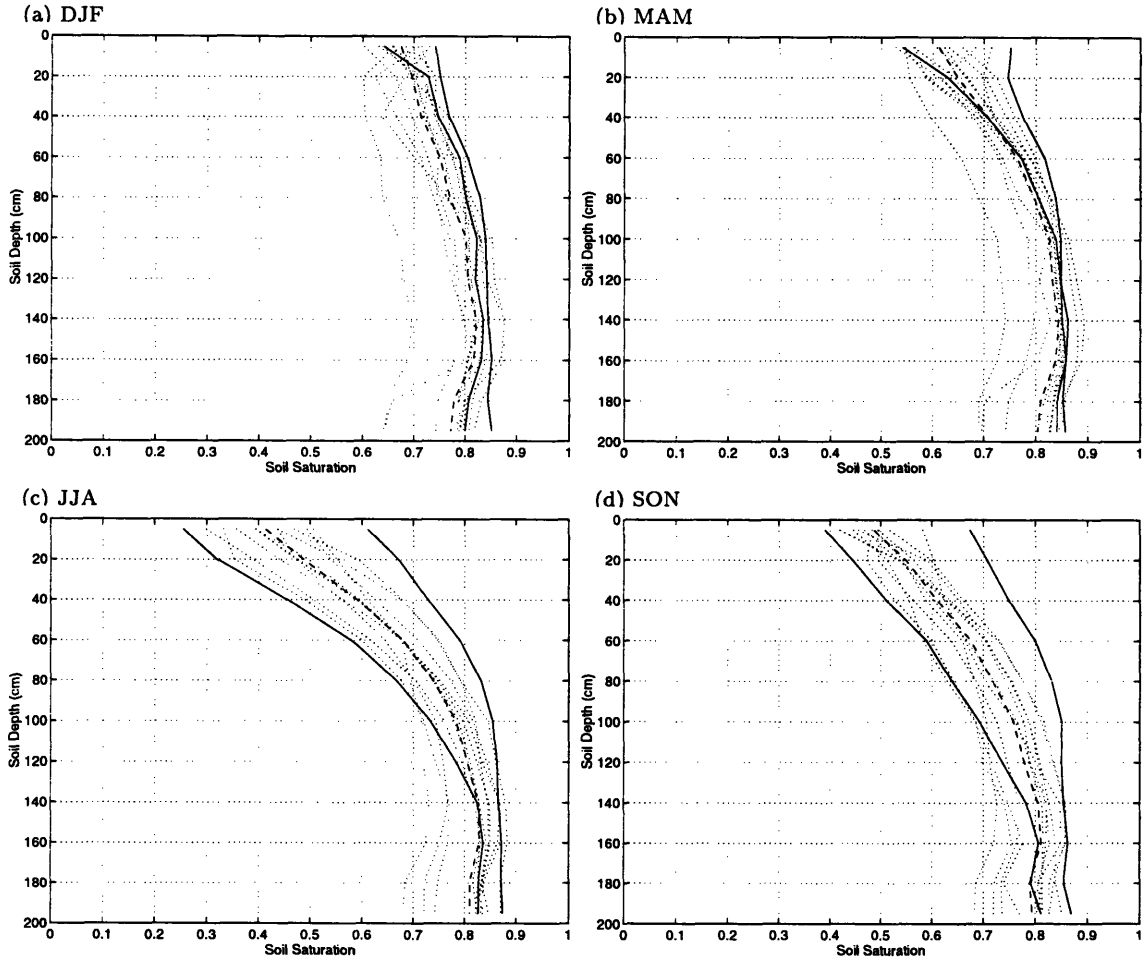

Figure 2-3: Illinois State Water Survey seasonal soil saturation as a function of depth for 1981 to 1993. Left solid line is the soil saturation for 1988, right solid line is for 1993, dotted lines are the remaining years, and dashed line is the average of all of the years. (a) December, January, and February; (b) March, April, and May; (c) June, July, and August; and (d) September, October, and November.

that becomes baseflow in the channels draining out of area A. The remaining portion of subsurface runoff is lost as unobserved groundwater flow and can be expressed as $G(t) = \mu B(t)$.

The evapotranspiration $E(t)$ is estimated by the following relation:

$$E(t) = E_p \frac{W}{W_{\max}}, \tag{2.4}$$

where E_p is the potential evapotranspiration rate in millimeters per month. E_p is estimated from observed surface air temperature since there is a lack of measurements required for other more accurate methods of estimation.

The model parameters, $W_{\max}$, μ, α, and m were calibrated using observed precipitation, temperature, and runoff from a 3° by 3° area in Oklahoma for the years 1960 to 1989. The calibrated model was applied to the 344 climate divisions across the U.S. in order to obtain values of soil moisture. The model was compared with 8 years (1984-1991) of observed ISWS soil moisture data. It was found that modeled soil moisture agrees best with the observed soil moisture in the top 1.3 meters of soil. Figure 2-4 shows a comparison of the monthly 13 year averaged ISWS soil moisture climatology and the simulated climatology for the same years over the state of Illinois. The model does a remarkable job in picking up the winter-spring maximum and the late summer minimum. Huang et al. (1996) attribute the observed phase shift between the two sets of data to the fact that temperature instead of net radiation is used to compute potential evapotranspiration. Figure 2-5 is a time series of HDG data compared to the observed ISWS data at 130 cm for 1981 through 1993 over Illinois. It is seen from the figure that HDG data picks up the monthly variability of soil moisture and does a good job of predicting soil moisture even in the extreme years of 1988 and 1993. Huang et al. (1996) computed the correlation coefficient between the modeled and the observed soil moisture data during May to September for 1984 to 1991 to be 0.84. The error in soil moisture observed from 1981 to mid-1983 may be due to fewer measurement stations being active during the early stages of the ISWS project (see Section 2.2.1). Considering that the model parameters were calibrated

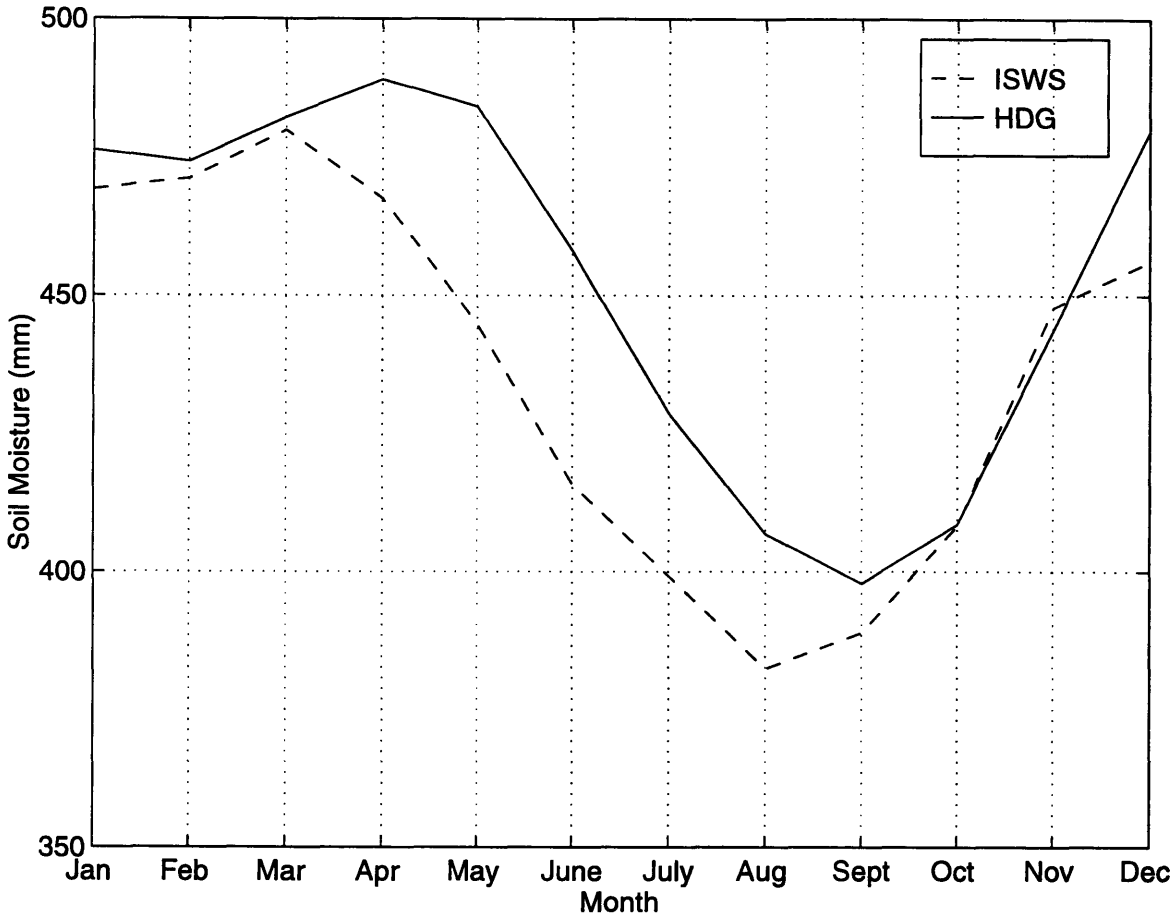

Figure 2-4: ISWS (dashed line) and HDG (solid line) soil moisture (mm) monthly climatology for 1981 through 1993 in Illinois plotted against month.

in a region of the U.S. completely different from Illinois, these two figures suggest that the model does a reasonable job in simulating the soil moisture climatology and anomalies.

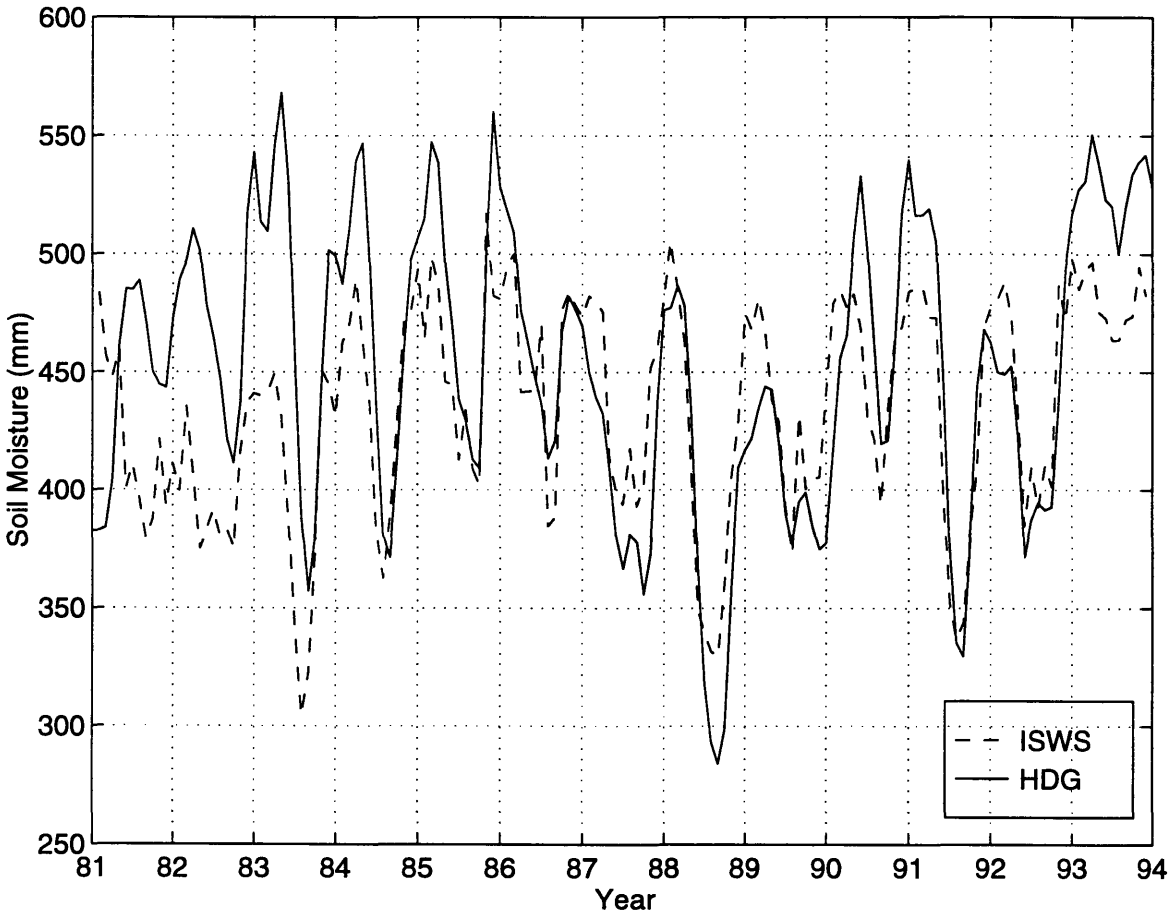

Figure 2-5: Time series of ISWS (dashed line) and HDG (solid line) soil moisture data (mm) for 1981 through 1993. Monthly values are plotted.

Chapter 3

Model Description

3.1 General Overview

The details of the model used in this study, Second-Generation Regional Climate Model (RegCM2), can be found in (Anthes et al. 1987). Hence only a brief description will be provided here. RegCM2 is a regional climate model that was originally developed by NCAR and PSU as Mesoscale Model version 4 (MM4). Since then, several of the MM4s physics parameterizations were modified to adapt its use to long-term climate simulations (see Giorgi, Marinucci and Bates (1993) and Giorgi, Marinucci, Bates and De Canio (1993)).

RegCM2 is a primitive equation, hydrostatic, compressible, σ-vertical coordinate model, where $\sigma = (p - p_{top}) / (p_s - p_{top})$, p is pressure, p_{top} is the pressure specified at the top of the model, and p_s is the prognostic surface pressure. The simulations in this study are performed over mid-latitudes. Hence, a Lambert conformal projection is adopted in the horizontal.

RegCM2 has a detailed representation of radiative transfer (Kiehl et al. 1987): It performs separate calculations of the atmospheric heating rates and surface fluxes for solar and infrared radiation under clear and cloudy sky conditions. The surface physics calculations are performed using the Biosphere-Atmosphere Transfer Scheme (BATS, Dickinson et al. (1986)). BATS is a state of the art soil-vegetation hydrological process model that has been developed for calculating the transfer of

energy, mass, and momentum between the atmosphere and the vegetated surface of the earth. It will be described in more detail in a Section 3.2. RegCM2 uses a planetary boundary layer model developed by Holtslag et al. (1990) and is described in Section 3.3. For this study, two different cumulus convection schemes are used: 1) Cumulus Cloud scheme developed by Grell (1993) and Grell et al. (1994) (referred to hereafter as GCC) and 2) Kuo-type cumulus parameterization described in Anthes (1977) and Anthes et al. (1987) (referred to hereafter as KUO). Both schemes will be described in greater detail in Section 3.4.

RegCM2 requires initial conditions and time-dependent lateral boundary conditions for wind components, temperature, surface pressure, and water vapor. The lateral boundaries are employed using a relaxation technique developed by (Davies and Turner 1977). The technique uses Newtonian and diffusion terms at the outermost four grid points. Furthermore, the model uses a split-time integration technique developed by Madala (1981).

The model can be used for a number of different types of applications. For example, it can be nested within a GCM to study the regional impacts of climate change such as global warming or it can also be used for simulation of specific short term events of a day or two.

3.2 Surface Physics

The surface physics computations in RegCM2 are performed using BATS version 1E (Dickinson et al. 1986). As previously mentioned, BATS describes the transfer of energy, mass, and momentum between the atmosphere and the vegetated surface of the earth. It contains three soil layers (a 10 cm surface layer, a 1 to 2 m. root zone, and a 3 m. deep soil layer), one vegetation layer (18 land cover/vegetation types), and one snow layer. It has prognostic equations for soil temperature and water content and in the presence of vegetation, canopy air temperature and foliage temperature. Figure 3-1 provides a schematic diagram of BATS. Table 3.1 is a list of each of the land cover/vegetation types. Many different parameters are associated with each land

Table 3.1: Land Cover/Vegetation classes

1.	Crop/mixed farming
2.	Short grass
3.	Evergreen needleleaf tree
4.	Deciduous needleleaf tree
5.	Deciduous broadleaf tree
6.	Evergreen broadleaf tree
7.	Tall grass
8.	Desert
9.	Tundra
10.	Irrigated Crop
11.	Semi-desert
12.	Ice cap/glacier
13.	Bog or marsh
14.	Inland water
15.	Ocean
16.	Evergreen shrub
17.	Deciduous shrub
18.	Mixed Woodland

cover/vegetation type (see Table 3.2). Four examples of how the vegetation classes are used in RegCM2 are provided in Figure 3-2 (taken from Dickinson et al. (1986)). In addition to the vegetation types, BATS has one of twelve soil properties ranging from very coarse (sand) to medium (loam) to very fine (heavy clay) assigned to it. Tables 3.3 and reftbl:BATSscol (taken from Dickinson et al. (1986)) give a description of the parameters associated with each soil class.

The governing soil water equations for BATS are as follows:

$$\begin{aligned}
\frac{\partial S_{sw}}{\partial t} &= P_r(1-\sigma_f) - R_s + \gamma_{w1} - \beta E_{tr} - F_q + S_m + D_w \qquad (3.1)\\
\frac{\partial S_{rw}}{\partial t} &= P_r(1-\sigma_f) - R_s + \gamma_{w2} - E_{tr} + S_m + D_w \\
\frac{\partial S_{tw}}{\partial t} &= P_r(1-\sigma_f) - R_s - E_{tr} - F_q + S_m + D_w \\
\frac{\partial S_{tw}}{\partial t} &= P_r(1-\sigma_f) - F_q + S_m + D_s
\end{aligned}$$

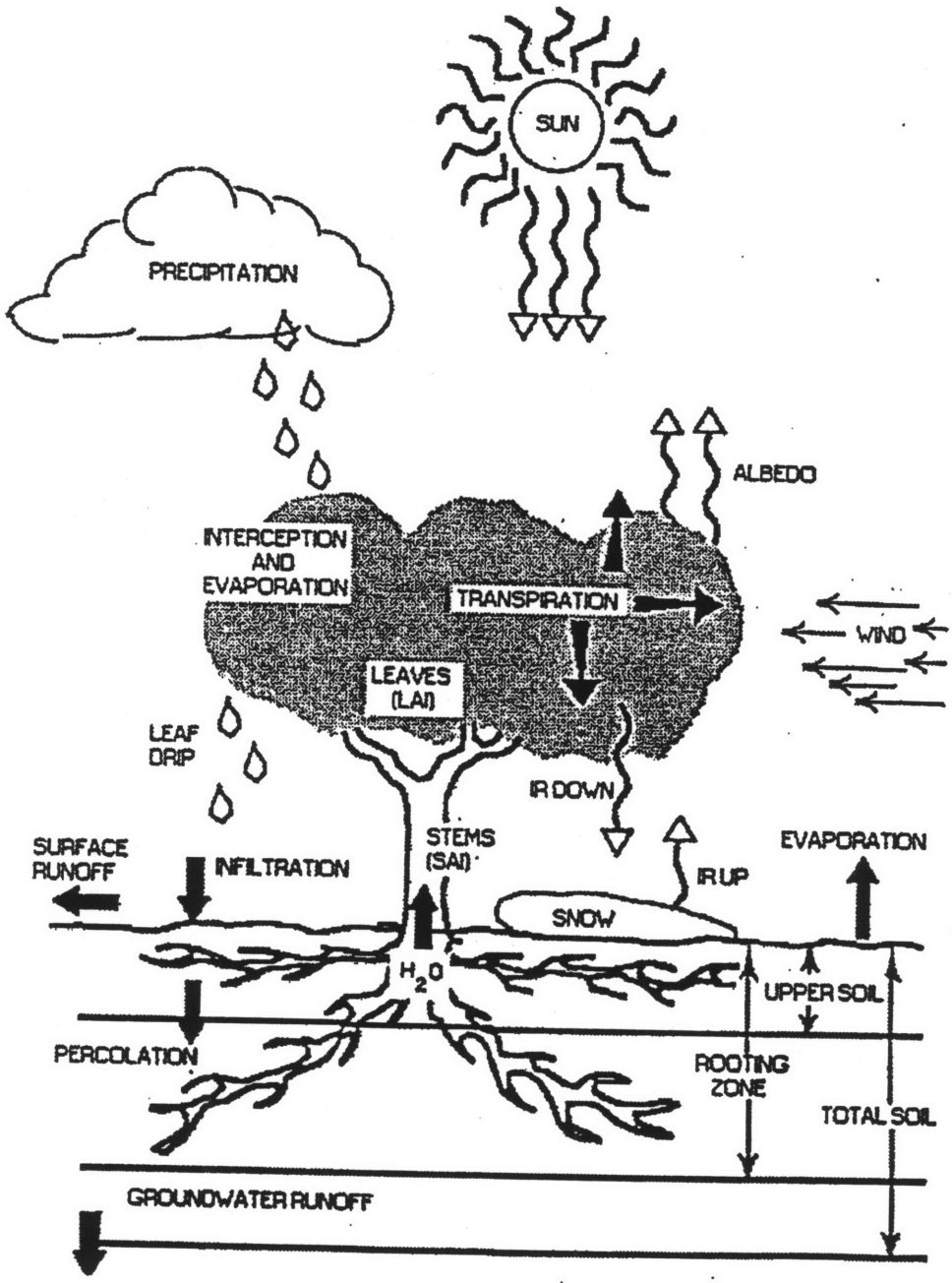

Figure 3-1: Schematic Diagram of Biosphere-Atmosphere Transfer Scheme. Taken from Dickinson et al. (1986).

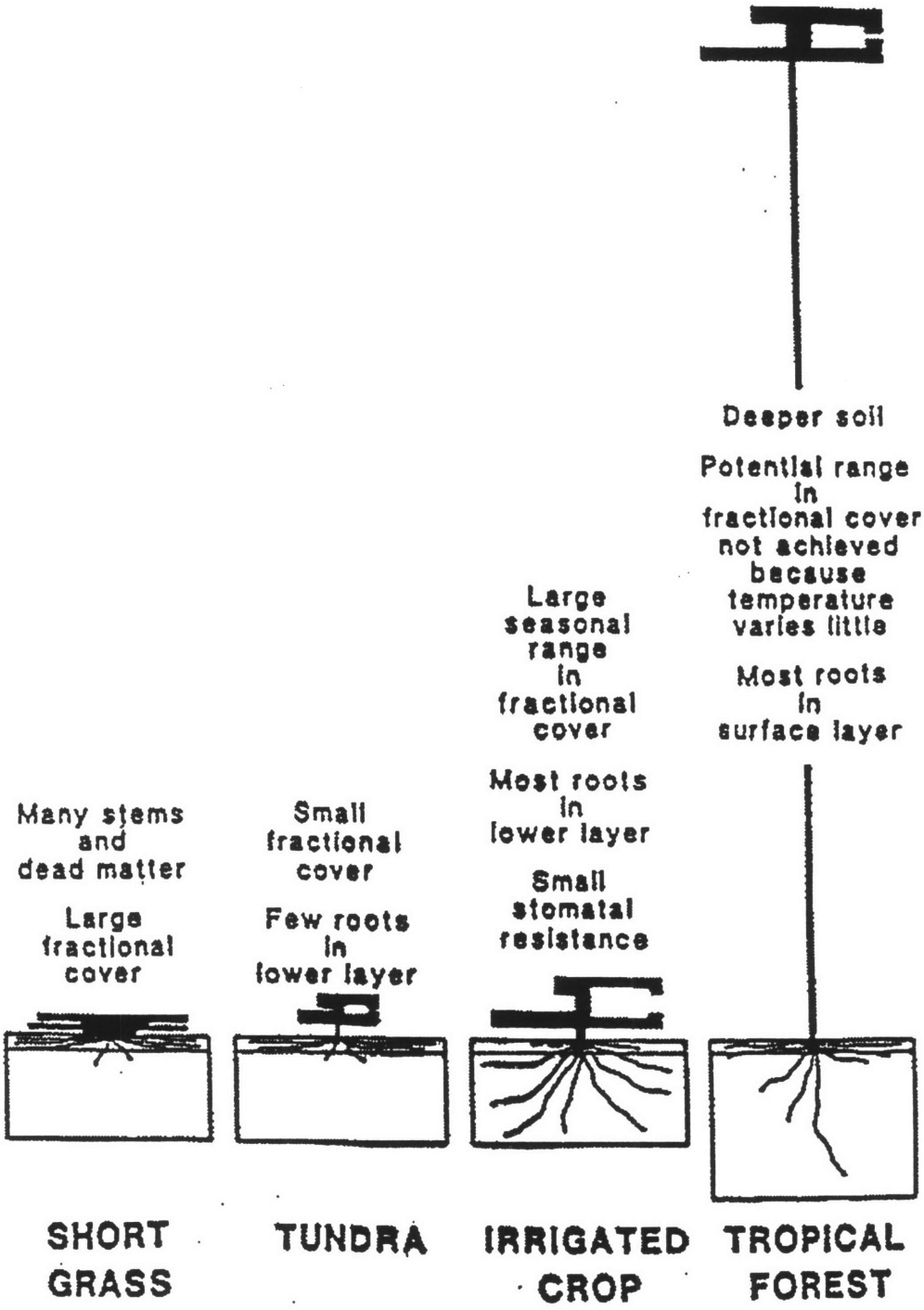

Figure 3-2: Four examples of how the land cover/vegetation classes are used in RegCM2 and BATS. Taken from Dickinson et al. (1986).

Parameter	Land Cover/Vegetation Type																	
	1	2	3	4	5	6	7	8	9	10	11	12	13	14	15	16	17	18
Max fractional vegetation cover	0.85	0.80	0.80	0.80	0.80	0.90	0.80	0.00	0.60	0.80	0.10	0.00	0.80	0.00	0.00	0.80	0.80	0.80
Difference between max fractional vegetation cover and cover at 269 K	0.6	0.1	0.1	0.3	0.5	0.3	0.0	0.2	0.6	0.1	0.0	0.4	0.0	0.0	0.2	0.3	0.2	
Roughness length (m)	0.06	0.02	1.00	1.00	0.80	2.00	0.10	0.05	0.04	0.06	0.10	0.01	0.03	0.0024	0.0024	0.10	0.10	0.80
Root zone soil layer depth (m)	1.0	1.0	1.5	1.5	2.0	1.5	1.0	1.0	1.0	1.0	1.0	1.0	1.0	1.0	1.0	1.0	1.0	2.0
Upper soil layer depth (m)	0.1	0.1	0.1	0.1	0.1	0.1	0.1	0.1	0.1	0.1	0.1	0.1	0.1	0.1	0.1	0.1	0.1	0.1
Fraction of water extracted by upper layer roots	0.3	0.8	0.67	0.67	0.5	0.8	0.8	0.9	0.9	0.3	0.8	0.5	0.5	0.5	0.5	0.5	0.5	0.5
Min stomatal resistence (s/m)	120	200	200	200	200	200	200	200	200	200	200	200	200	200	200	200	200	200
Max Leaf Area Index	6	2	6	6	6	6	6	0	6	6	6	0	6	0	0	6	6	6
Min Leaf Area Index	0.5	0.5	5	1	1	5	0.5	0	0.5	0.5	0.5	0	0.5	0	0	5	1	3
Vegetation albedo for wavelengths $< 0.7\ \mu$ m	0.10	0.10	0.05	0.05	0.08	0.04	0.08	0.20	0.10	0.08	0.17	0.80	0.06	0.07	0.07	0.05	0.08	0.06
Vegetation albedo for wavelengths $> 0.7\ \mu$ m	0.30	0.30	0.23	0.23	0.28	0.20	0.30	0.40	0.30	0.28	0.34	0.60	01.8	0.20	0.20	0.23	0.28	0.24
Stem (& dead matter) area index)	0.5	4.0	2.0	2.0	2.0	2.0	2.0	0.5	0.5	2.0	2.0	2.0	2.0	2.0	2.0	2.0	2.0	2.0
Inverse square root of leaf dimension ($m^{-1/2}$)	10	5	5	5	5	5	5	5	5	5	5	5	5	5	5	5	5	5
Light sensitivity factor ($m^2\ W^{-1}$)	0.02	0.02	0.06	0.06	0.06	0.06	0.02	0.02	0.02	0.02	0.02	0.02	0.02	0.02	0.02	0.02	0.02	0.06

Table 3.2: Description of land cover/vegetation parameters specified in RegCM2 and BATS. Reproduced from Dickinson et al. (1986).

Parameter	Texture Class (from sand (1) to clay (12))											
	1	2	3	4	5	6	7	8	9	10	11	12
Porosity	0.33	0.36	0.39	0.42	0.45	0.48	0.51	0.54	0.57	0.60	0.63	0.66
Min soil suction (mm)	30	30	30	200	200	200	200	200	200	200	200	200
Saturated hydraulic conductivity ($m\ s^{-1}$)	200	80	32	13	8.9	6.3	4.5	3.2	2.2	1.6	1.1	0.8
Ratio of saturated thermal conductivity to that of loam	1.7	1.5	1.3	1.2	1.1	1.0	0.95	0.90	0.85	0.80	0.75	0.70
Clapp and Hornberger exponent "B"	3.5	4.0	4.5	5.0	5.5	6.0	6.8	7.6	8.4	9.2	10.0	10.8
Wilting point	0.095	0.128	0.161	0.266	0.3	0.332	0.378	0.419	0.455	0.487	0.516	.542
Field Capacity	0.404	0.477	0.547	0.614	0.653	0.688	0.728	0.763	0.794	0.820	0.845	0.866

Table 3.3: Description of the parameters associated with soil texture specified in RegCM2 and BATS. Reproduced from Dickinson et al. (1986).

Parameter	Color Class (from light (1) to dark (8))							
	1	2	3	4	5	6	7	8
Dry soil albedo								
$< 0.7\mu$m	0.23	0.22	0.20	0.18	0.16	0.14	0.12	0.10
$> 0.7\mu$m	0.46	0.44	0.40	0.36	0.32	0.28	0.24	0.20
Saturated soil albedo								
$< 0.7\mu$m	0.12	0.11	0.10	0.09	0.08	0.07	0.06	0.05
$> 0.7\mu$m	0.24	0.22	0.20	0.18	0.16	0.14	0.12	0.10

Table 3.4: Description of the parameters associated with soil colors specified in RegCM2 and BATS. Reproduced from Dickinson et al. (1986).

where S_{sw} is the surface soil water in the upper layer of the soil, S_{rw} is the root zone soil water, S_{tw} is the total water in the soil column, P_r is the rate of precipitation falling as rain, R_s is surface runoff, γ_{w1} is the rate of transfer of water from soil layer one to soil layer two, γ_{w2} is the rate of transfer of water from soil layer two to soil layer three, E_{tr} is the transpiration, F_q is the moisture flux from the ground to the atmosphere, S_m is the rate of snow melt, D_w is the rate of excess water that drips from the leaves per unit land area, D_s is the rate of excess snow that drips from the leaves per unit land area, σ_f is the fractional foliage cover for each grid point, and β is the fraction of transpiration from the top soil layer.

Evaporation in the absence of vegetation is the minimum of the potential evapotranspiration F_{qp} and the maximum moisture flux from the surface that the soil can sustain F_{qm}. In a similar manner, the evaporation in the presence of vegetation is the minimum of the maximum transpiration that the vegetation can sustain E_{trmx} and the transpiration E_{tr} given the stomatal resistance r_s. The surface runoff R_s is computed by the following relation:

$$R_s = \left(\frac{\rho_w}{\rho_{wsat}}^4\right) G \tag{3.2}$$

where $\frac{\rho_w}{\rho_{wsat}}$ is the average of the volume of water in the top two layers, G is the net

water applied to the surface ($P_r + S_m + F_q$) in the absence of vegetation.

3.3 Boundary Layer Physics

BATS requires the use of an explicit planetary boundary layer (PBL) model with the lowest atmospheric level at approximately 40-m. The PBL adopted for RegCM2 was developed by Holtslag et al. (1990). The vertical eddy flux F_c for the quantity C (e.g. potential temperature, horizontal wind components, and water vapor mixing ratio) is given by

$$F_c = -K_c \left(\frac{\partial C}{\partial z} - \gamma_c \right), \tag{3.3}$$

where K_c is the vertical eddy diffusivity and γ_c is the countergradient transport. γ_c describes the nonlocal transport due to dry deep convection. The eddy diffusivity is given by

$$K_c = k w_t z \left(1 - \frac{z}{h} \right)^2, \tag{3.4}$$

where k is the von Kármám constant, w_t is the turbulent convective velocity (function of the friction velocity, height, and Monin-Obhukov length), and h is the PBL height.. h is iteratively computed by

$$h = \frac{Ri_{cr}[u(h)^2 + v(h)^2]}{(g/\theta_s)[\theta_v(h) - \theta_s]}, \tag{3.5}$$

where $u(h)$, $v(h)$, and $\theta_v(h)$ are the wind components and the virtual potential temperature at PBL height, g is gravity, Ri_{cr} is the critical bulk Richardson number, and θ_s surface air temperature. θ_s is computed by the following relation:

$$\theta_s = \theta_v(z_1) + K\frac{\phi_0^s}{w_t}, \tag{3.6}$$

where K is a constant equal to 8.5 and ϕ_0^s is the surface sensible heat flux. The second term on the right-hand side of the above equation represents the strength of convective thermals in the lower part of the PBL and is zero under stable conditions. Finally, γ_c for surface temperature or water vapor is expressed as

$$\gamma_c = K\frac{\phi_c^0}{w_t h}, \tag{3.7}$$

where ϕ_c^0 is the surface temperature or water vapor flux. This equation is applied between the top of the surface layer ($0.1h$) and the top of the PBL. Elsewhere and for horizontal wind velocities, γ_c is assumed to equal zero.

3.4 Convective Parameterizations

Moist convective processes typically occur on a scale that is smaller than the resolution of GCMs and RCMs and depend on a variety of physical forcings. Hence, the representation of these processes is difficult and often inadequate. RegCM2 has options for two different cumulus convection schemes, both of which are used in this study.

3.4.1 KUO Scheme

The KUO convective parameterization used in RegCM2 was initially developed by Anthes (1977) and simplified by Anthes et al. (1987). Convective activity is initiated when the moisture convergence in a column exceeds a given critical negative area threshold and the vertical sounding is unstable. A fraction of the moisture convergence, b, moistens the column by the following relation:

$$Q_c(x, y, \sigma) = bM(x, y)\alpha_q(\sigma), \tag{3.8}$$

where x and y are the east-west and north-south coordinates, respectively, M is the moisture convergence over the entire column, and $\alpha_q(\sigma)$ is the normalized vertical moistening function. $\alpha_q(\sigma)$ depends proportionally on the column's local relative humidity in such a way that more moisture is allocated to the drier grid points of the column. The fraction of moisture convergence that does not go into moistening the column, $1 - b$, precipitates out given by

$$P = M(x, y)(1 - b), \tag{3.9}$$

The b factor is a function of the average relative humidity $\overline{RH}$ of the sounding as follows

$$b = 2(1 - \overline{RH}), \tag{3.10}$$

for $\overline{RH} \geq 0.5$ and $b = 1$ otherwise.

The latent heating resulting from condensation is distributed between the cloud top and bottom by a parabolic heating profile function that allocates the maximum heating to the upper portion of the cloud layer as follows:

$$H_c(x, y, \sigma) = (1 - b)L_v M(x, y)\alpha_h(\sigma), \tag{3.11}$$

where L_v is the latent heat of condensation and $\alpha_h(\sigma)$ is a parabolic-shaped vertical heating function.

In stable conditions, all supersaturated water is instantaneously released.

Additional modifications by Giorgi and Bates (1989) and Giorgi (1991) have been employed to improve surface temperature and precipitation simulation. To eliminate "numerical point storms," a horizontal diffusion term and a time release constant have been added so that the redistribution of moisture and the latent heat release are not released instantaneously.

3.4.2 GCC Scheme

The GCC scheme of (Grell 1993) and (Grell et al. 1994) retains the main characteristics of the Arakawa-Schubert parameterization (Arakawa and Schubert 1974). In this parameterization, clouds are pictured as two steady-state circulations: an updraft and a downdraft. No direct mixing occurs between the cloudy air and the environmental air except at the top and bottom of the circulations. Mass flux is constant with height and no entrainment or detrainment occurs along the edges of the cloud. The originating levels of the updraft and downdraft are given by the levels of maximum and minimum moist static energy. The GCC scheme is activated when a lifted parcel attains moist convection. Condensation in an updraft is calculated by lifting a saturated parcel. The downdraft mass flux, m_0, depends on the updraft mass flux, m_b, by the following relation:

$$m_0 = \frac{\beta I_1}{I_2} m_b, \tag{3.12}$$

where I_1 is the amount of updraft condensation normalized by m_b, I_2 is the downdraft evaporation normalized by m_0, and β fraction of updraft condensation that reevaporates in the downdraft. Depending on the wind shear, β typically varies between 0.3 and 0.5. Both I_1 and I_2 are computed by lifting the saturated parcel. Rainfall is given by

$$R = I_1 m_b (1 - \beta). \tag{3.13}$$

The heating and moistening is determined both by the mass fluxes and the detrainment at the cloud top and bottom. In addition, the cooling effect of moist downdrafts is included.

Due to the simplistic nature of the scheme, any closure assumption can be used. For this study, the quasi-equilibrium assumption of Arakawa and Schubert (1974) is adopted, in that, it is assumed that clouds stabilize the environment as fast as the large-scale destabilizes it (Arakawa and Schubert 1974) and is expressed as

$$\frac{dAB_{tot}}{dt} = \frac{dAB_{LS}}{dt} + \frac{dAB_{CU}}{dt} \approx 0, \tag{3.14}$$

where AB is the available buoyant energy, LS stands for large-scale, CU stands for cumulus convection, and *tot* stands for total.

Chapter 4

Design of Numerical Experiments

The purpose of this study is to investigate the role that initial soil moisture conditions played in the drought of 1988 and the flood of 1993. The study is broken up into five different groups of experiments in order to test how initial soil moisture conditions affect precipitation and other surface variables over the Midwest. Each of the five groups are comprised of simulations using boundary conditions appropriate for the drought year of 1988 and the flood year of 1993. The first group of simulations are performed to investigate how sensitive the climate model is to extreme changes in soil moisture. In the second group, we investigate how the results of the simulations change when reasonable initial soil moisture values rather than extreme values are used. These initial values are chosen to be consistent with observations. For the third group, we look at how the timing of the initial soil moisture condition affects the regional climate simulation. In the fourth group, we investigate the sensitivity of precipitation to two KUO scheme parameters. And in the last group, we investigate how the spatial and temporal resolution of the boundary conditions affect the results of the control simulations. This chapter describes the model domain, initial and boundary conditions, and the design of each group of experiments.

4.1 Model domain

The model domain is centered around the state of Illinois at 40.5°N and 90°W. The model uses a Lambert conformal projection, with a domain size of 2050-km X 2500-km and horizontal grid point spacing of 50 km. At this resolution, the main topographic features of the domain are captured. The model domain and topography are shown in Figure 4-1. This region captures the primary area of drought in 1988 and flood in 1993. Figure 4-2 shows the surface land cover/vegetation types used by the model and Figure 4-3 shows a map of the soil types for the domain and Table 3.3 gives their description.

The predominant vegetation type of the domain is crops. Crops are characterized by a shallow root zone depth (1.0 m). Hence, the majority of the water for evapotranspiration is extracted from the upper portions of the soil. During the peak growing season (spring/summer), they achieve a relatively high maximum fractional vegetation coverage (85%) and leaf area index (6) and a relatively low minimum stomatal resistance (120 s/m). All of these parameters suggest that crops transpire more than the average vegetation type. The other dominant vegetation types of the model domain are: to the west short grass and evergreen shrubs (Texas only), to the north evergreen needleleaf trees and mixed woodland (Great Lakes only), and to the south and east deciduous broadleaf trees. The predominant soil types over the domain are representative of average texture parameters. The values for porosity, field capacity, wilting point, and saturated hydraulic conductivity are all around 50%, 70%, 35%, and 5 m/s, respectively (see Table 3.3). The dry and saturated soil albedos are approximately 0.18 and 0.08, respectively, for shortwave radiation, and 0.34 and 0.17 for longwave radiation, respectively (see Table 3.4).

4.2 Initial and Boundary Conditions

Sea surface temperature and meteorological initial and lateral boundary conditions (wind components, temperature, water vapor mixing ratio, and surface pressure),

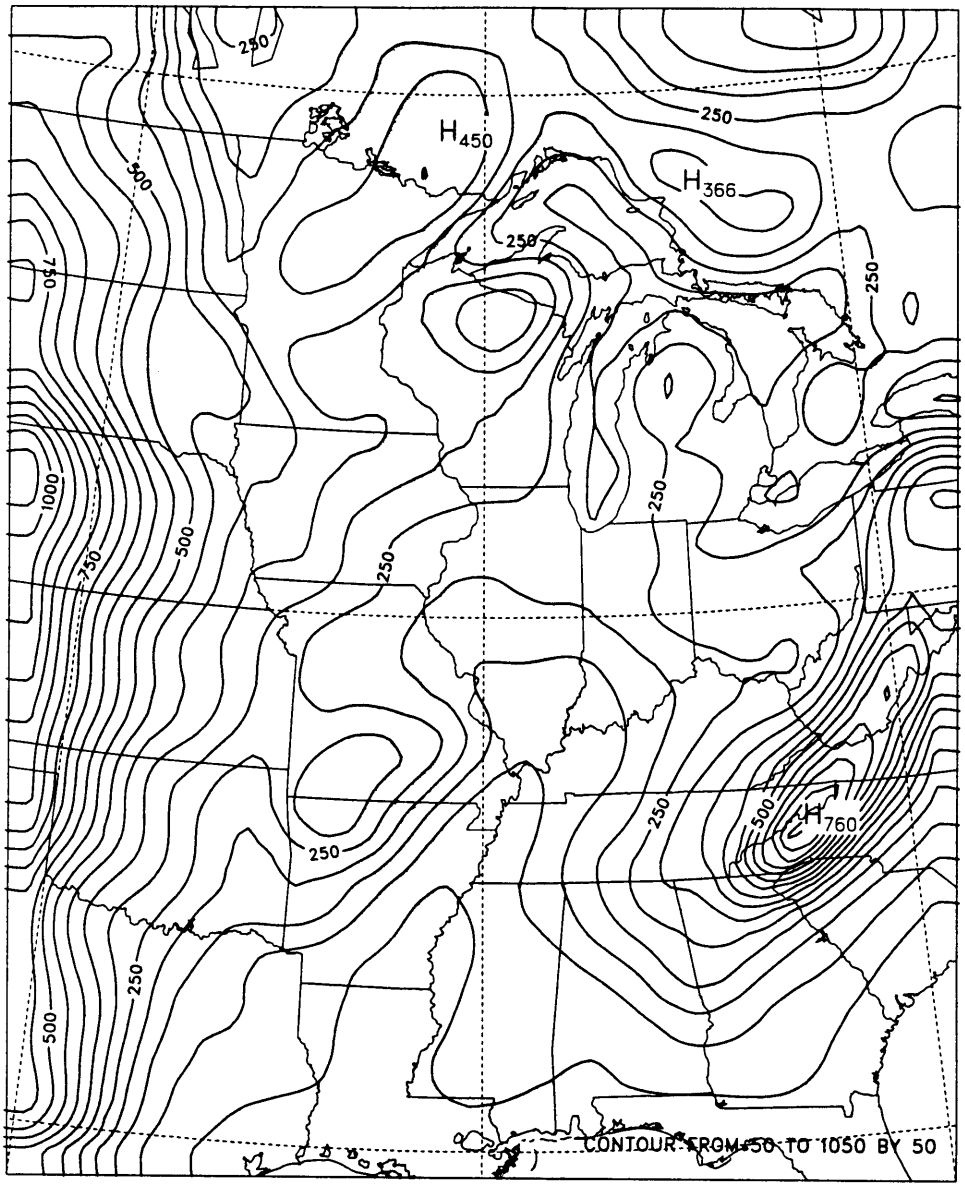

Figure 4-1: Model domain topography (m)

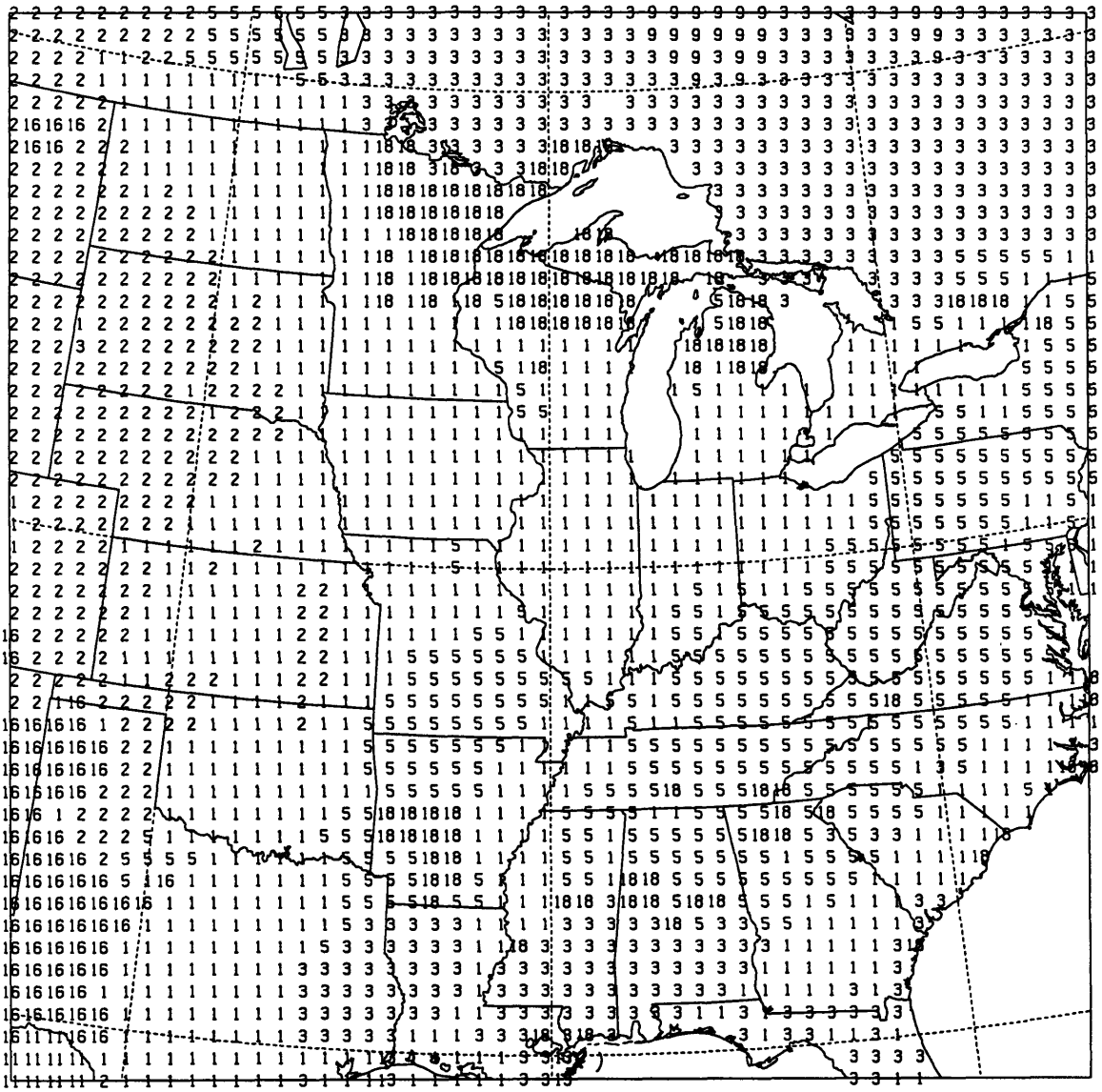

Figure 4-2: Land Cover/Vegetation map.

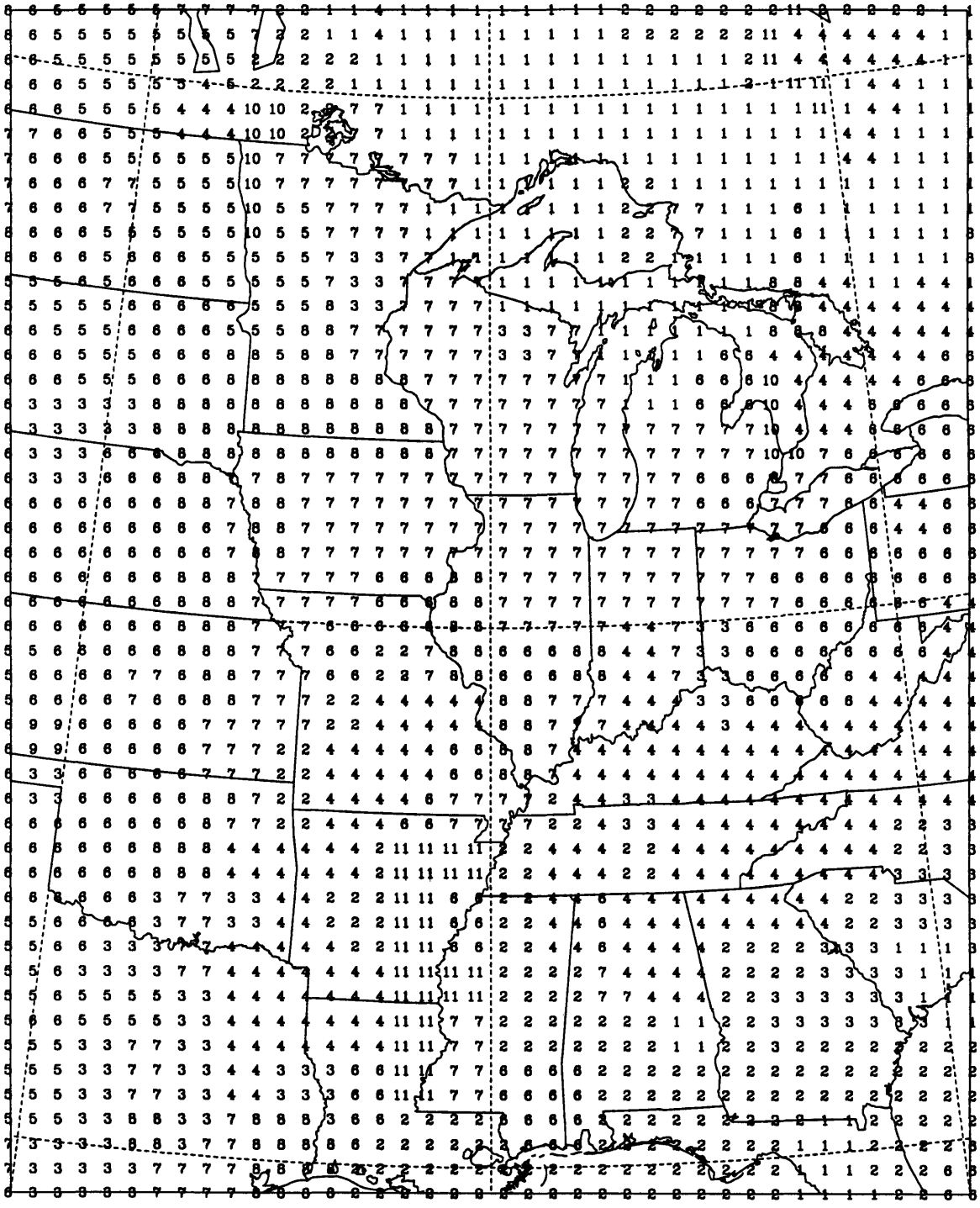

Figure 4-3: Map of Soil Textures.

necessary to drive the model, are interpolated from the ECMWF original IIIb global analysis of First Global Atmospheric Research Program Global Experiment data (Bengtsson et al. (1982); Mayer (1988); Trenberth et al. (1988)). The ECMWF data have a resolution of 2.5° X 2.5° (T43), are distributed at 15 pressure levels, and are available at intervals of 12 hours. In addition, ECMWF data at a horizontal resolution of 1.125° X 1.125° (T106) and 6-hour time intervals are also used in this study. ECMWF dataset is an assimilated dataset. Hence, the data is accurate in areas where observations are abundant. The data, however, is questionable in areas that lack observations, such as oceans and undeveloped regions. In the U.S., the ECMWF data should be representative of observations, except over the Rocky Mountains and Sierra Nevada where observations are scarce. For this study, most of the boundaries occur over regions abundant with observations. Hence, the temporal and spatial resolution of the boundary conditions may pose the largest source errors. Additional comments on the quality of this data can be found in Giorgi and Marinucci (1991).

To initialize the soil moisture in each layer of BATS, it is assumed that there is a linear relation between the ISWS data and the HDG data. In other words, the soil moisture, $S_{i,j,l}$, at a given layer, l, and grid point, i,j, is the ratio of the ISWS data at the desired layer to the HDG data over Illinois multiplied by the HDG data at the desired grid point:

$$S_{i,j,l} = \frac{ISWS_l^{avg}}{HDG_{ILL}^{avg}} * HDG_{i,j} \tag{4.1}$$

where $ISWS_l^{avg}$ is the ISWS soil moisture at level, l, averaged over Illinois, HDG_{ILL}^{avg} is the HDG soil moisture averaged over Illinois, and $HDG_{i,j}$ is the HDG soil moisture at grid point i,j. The HDG data is first interpolated to the domain grid and then used to compute the soil moisture. Over the state of Illinois, one factor is computed for each layer. This relation between ISWS and HDG data is used to generate a more realistic vertical soil moisture profile over the entire HDG domain. The factors (Table 4.1) are assumed to be constant over the entire domain of the experiment as

Table 4.1: Multiplication factors for specification of soil moisture at different layers. To obtain the soil moisture at a given level, multiply the factor times the HDG data value.

Date	880501	880701	880901	930501	930701	930901
10cm	0.055	0.042	0.060	0.075	0.066	0.069
30cm	0.174	0.132	0.179	0.205	0.191	0.198
50cm	0.315	0.265	0.331	0.340	0.326	0.337
70cm	0.474	0.432	0.514	0.484	0.470	0.484
90cm	0.636	0.616	0.715	0.624	0.615	0.631
110cm	0.798	0.809	0.925	0.763	0.760	0.778
130cm	0.959	1.010	1.146	0.899	0.903	0.923
150cm	1.121	1.218	1.378	1.035	1.045	1.068
170cm	1.281	1.427	1.619	1.169	1.186	1.212
190cm	1.436	1.634	1.858	1.301	1.327	1.354
200cm	1.514	1.734	1.970	1.368	1.398	1.427

shown.

Since the HDG soil moisture is a monthly dataset and each simulation begins on the first of the month, it is assumed the HDG soil moisture at the beginning of the month is the average of the prior and current month's data. Given the fact that ISWS data is measured approximately every two weeks, the HDG data should be sufficient to use over the rest of the domain. Although these are gross assumptions, use of the HDG data is much more reasonable than assuming the soil moisture is at its wilting point or field capacity uniformly over the entire domain and the depth of the soil. In addition, soil moisture variability, which may have played a role in the drought of 1988 and the flood of 1993 (Paegle et al. 1996), is represented by using these datasets. For the extreme simulations, the soil saturation at each grid point is initialized at the soil's minimum observed surface value for the dry simulations and maximum observed surface value for the wet simulations. These values are assumed to be uniform for the entire profile of the soil.

Table 4.2: Description of each setup used for the "Sensitivity to Soil Moisture Extremes" simulations. Table includes: Simulation name and date, initial soil saturation, convection scheme used, and boundary condition spatial and temporal resolution.

Run Name	Run date	Soil Moisture IC	Convection	BC Resolution
8807DRYKUOEXT	1-30 July, 1988	25%	KUO	T43 - 12hr
8807WETKUOEXT	1-30 July, 1988	90%	KUO	T43 - 12hr
8807DRYGCCEXT	1-30 July, 1988	25%	GCC	T43 - 12hr
8807WETGCCEXT	1-30 July, 1988	90%	GCC	T43 - 12hr
9307WETKUOEXT	1-30 July, 1993	90%	KUO	T43 - 12hr
9307DRYKUOEXT	1-30 July, 1993	25%	KUO	T43 - 12hr
9307WETGCCEXT	1-30 July, 1993	90%	GCC	T43 - 12hr
9307DRYGCCEXT	1-30 July, 1993	25%	GCC	T43 - 12hr

4.3 Experiments

4.3.1 Sensitivity to Soil Moisture Extremes

In recent years, many soil moisture sensitivity studies have been performed over the Midwestern United States. Most of them conclude that there is a positive feedback between soil moisture and precipitation. However, some conclude the there is a negative feedback or no feedback (see Section 1.2). In this first set of experiments, we hope to shed some light upon the reasons for the inconsistencies in numerical model results. To do so, a series of 30-day simulations for July 1988 and 1993 are performed using the two different convection schemes: GCC and KUO. The soil moisture in each layer is initialized at the observed low surface soil saturation over Illinois during the summer of 1988 (25% for the entire domain) for the dry runs and at the observed high for the summer of 1993 (90% for the entire domain) for the wet runs. These values are considered extreme because soil saturation is rarely observed at values as extreme as these. Furthermore, the entire domain is initialized uniformly with these values. The difference between the runs will demonstrate the sensitivity of the model, given a convection parameterization, to initial soil moisture conditions. Table 4.2 gives a description of the simulations performed in this portion of the study.

4.3.2 Reasonable versus Extreme Soil Moisture

The initialization of soil moisture in models is very important for an accurate representation of the land surface energy and water balance. Most soil moisture sensitivity studies have been initialized using extreme soil moisture initial conditions that are never observed. For example, Giorgi et al. (1996) initialize soil moisture in all levels of the soil at the wilting point for their dry runs and at the field capacity for their wet runs. At a further extreme, (Pan et al. 1995) represent wet perturbed soil moisture in their RCM simulations by maintaining surface evaporation at 99% of the potential evaporation with no dynamic feedback. Similarly, they represent dry perturbed soil moisture in their simulations by maintaining a surface evaporation at 1% of the potential evaporation. Here we attempt to assess the impact of initializing soil moisture at extreme values by comparing the results of the first group of simulations (Section 4.3.1) to simulations initialized with more reasonable values of soil moisture. For each year, two additional 30-day July simulations are performed using reasonable values of soil moisture: a control run and a perturbed run. The control simulations are initialized using the ISWS soil moisture data (for Illinois) and HDG soil moisture data (for the rest of the domain) for the given year. The perturbed simulations are initialized using ISWS and HDG soil moisture data from the opposite extreme year. See Table 4.3 for a description of the simulations.

4.3.3 Soil Moisture and Time of Year

As mentioned in Subsection 1.2.1, Findell (1997) found using observed soil moisture and precipitation data over the state of Illinois that the feedback of soil moisture and precipitation is a function of the time of year. More specifically, they found that soil moisture and subsequent precipitation show strongest correlation in the summer and little or no correlation for the rest of the year (see Figure 4-4). In addition, Oglesby (1991) in a GCM study found that a mid- to late-spring soil moisture anomaly impacts the following summer while a late-winter anomaly is corrected. To test these results, we perform a series of 30-day simulations with three different start dates for

Table 4.3: Description of each setup used for the "Reasonable versus Extreme Soil Moisture" simulations. Table includes: Simulation name and date, initial soil saturation, convection scheme used, and boundary condition spatial and temporal resolution.

Run Name	Run date	Soil Moisture IC	Convection	BC Resolution
8807CONKUO	1-30 July, 1988	1988 ISWS/HDG	KUO	T43 - 12hr
8807WETKUO	1-30 July, 1988	1993 ISWS/HDG	KUO	T43 - 12hr
8807DRYKUOEXT	1-30 July, 1988	25%	KUO	T43 - 12hr
8807WETKUOEXT	1-30 July, 1988	90%	KUO	T43 - 12hr
8807CONGCC	1-30 July, 1988	1988 ISWS/HDG	GCC	T43 - 12hr
8807WETGCC	1-30 July, 1988	1993 ISWS/HDG	GCC	T43 - 12hr
8807DRYGCCEXT	1-30 July, 1988	25%	GCC	T43 - 12hr
8807WETGCCEXT	1-30 July, 1988	90%	GCC	T43 - 12hr
9307CONKUO	1-30 July, 1993	1993 ISWS/HDG	KUO	T43 - 12hr
9307DRYKUO	1-30 July, 1993	1988 ISWS/HDG	KUO	T43 - 12hr
9307WETKUOEXT	1-30 July, 1993	90%	KUO	T43 - 12hr
9307DRYKUOEXT	1-30 July, 1993	25%	KUO	T43 - 12hr
9307CONGCC	1-30 July, 1993	1993 ISWS/HDG	GCC	T43 - 12hr
9307DRYGCC	1-30 July, 1993	1988 ISWS/HDG	GCC	T43 - 12hr
9307WETGCCEXT	1-30 July, 1993	90%	GCC	T43 - 12hr
9307DRYGCCEXT	1-30 July, 1993	25%	GCC	T43 - 12hr

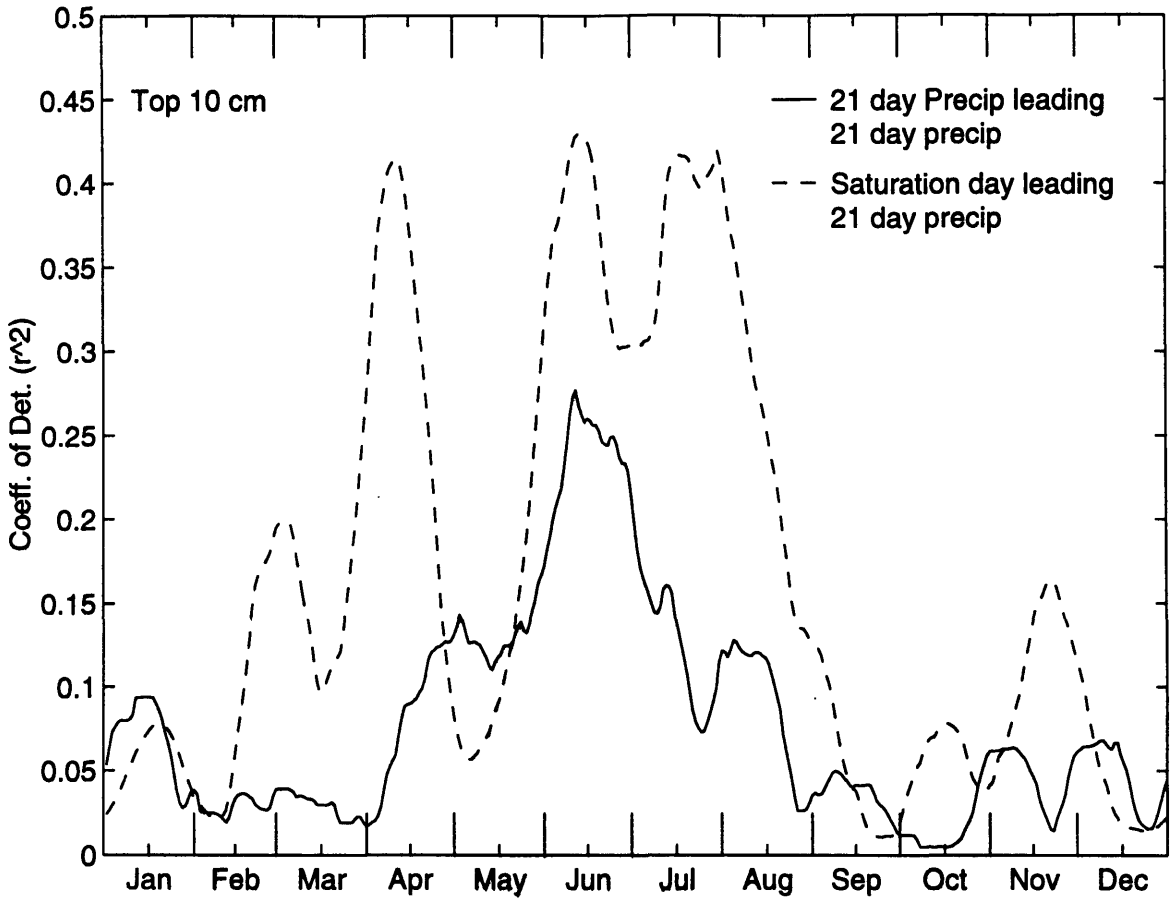

Figure 4-4: Correlation between initial soil moisture saturation (ISWS) from 0 to 10 cm and precipitation in the subsequent 21 days (solid line) compared to the correlation between adjacent 21 day precipitation windows (dashed line). Taken from Findell and Eltahir (1997).

both years: 1) Late-spring (May 1), 2) mid-summer (July 1), and 3) late-summer (September 1). Soil moisture is initialized using reasonable soil moisture values as described in the previous subsection. If the model can simulate the feedback and the timing of the feedback over Illinois, then more confidence can be placed on the results of the simulations. Table 4.4 gives a description of this series of simulations.

4.3.4 Model Sensitivity to Boundary Condition Resolution

The model, regardless of the convective parameterization does a poor job of capturing the spatial distribution of July rainfall (see Section 5.1). The temporal and spatial

Table 4.4: Description of each setup used for the "Soil Moisture and Time of Year" simulations. Table includes: Simulation name and date, initial soil saturation, convection scheme used, and boundary condition spatial and temporal resolution.

Run Name	Run date	Soil Moisture IC	Convection	BC Resolution
8805CONKUO	1-30 May, 1988	ISWS/HDG 1988	KUO	T43 - 12hr
8805WETKUO	1-30 May, 1988	ISWS/HDG 1993	KUO	T43 - 12hr
8807CONKUO	1-30 July, 1988	ISWS/HDG 1988	KUO	T43 - 12hr
8807WETKUO	1-30 July, 1988	ISWS/HDG 1993	KUO	T43 - 12hr
8809CONKUO	1-30 Sept, 1988	ISWS/HDG 1988	KUO	T43 - 12hr
8809WETKUO	1-30 Sept, 1988	ISWS/HDG 1993	KUO	T43 - 12hr
9305CONKUO	1-30 May, 1993	ISWS/HDG 1993	KUO	T43 - 12hr
9305DRYKUO	1-30 May, 1993	ISWS/HDG 1988	KUO	T43 - 12hr
9307CONKUO	1-30 July, 1993	ISWS/HDG 1993	KUO	T43 - 12hr
9307DRYKUO	1-30 July, 1993	ISWS/HDG 1988	KUO	T43 - 12hr
9309CONKUO	1-30 Sept, 1993	ISWS/HDG 1993	KUO	T43 - 12hr
9309DRYKUO	1-30 Sept, 1993	ISWS/HDG 1988	KUO	T43 - 12hr

resolution of the boundary conditions may be a reason for this. All of the previous simulations were driven by T43 (2.5° X 2.5°), 12 hour boundary conditions. This portion of the study investigates how increasing the spatial and temporal resolution improves the model results. A set of July simulations for 1988 and 1993 are performed using T106 (1.125° X 1.125°), 6 hour boundary conditions using both convective parameterizations. Table 4.5 gives a description of these simulations.

4.3.5 Model Sensitivity to KUO Scheme Parameters

This subsection investigates how two of the KUO scheme's parameters affect the distribution and volume of precipitation. The KUO scheme tends to produce too much precipitation over the northern portion of the domain and too little over the southern portion (see Figures 5-2 through 5-8). Paegle et al. (1996), Trenberth and Guillemot (1996), and others discuss the existence of a summertime low-level jet that travels northward from the Gulf of Mexico bringing moisture to the Midwest. If the KUO scheme is triggered earlier, maybe more of the moisture will be precipitated out in the southern portion of the domain before it reaches the north via the low-level

Table 4.5: Description of each setup used for the "Model Sensitivity to Boundary Condition Resolution" simulations. Table includes: Simulation name and date, initial soil saturation, convection scheme used, and boundary condition spatial and temporal resolution.

Run Name	Run date	Soil Moisture IC	Convection	BC Resolution
8807CONKUO	1-30 July, 1988	ISWS/HDG 1988	KUO	T43 - 12hr
8807CONKUOT106	1-30 July, 1988	ISWS/HDG 1988	KUO	T106 - 6hr
8807CONGCC	1-30 July, 1988	ISWS/HDG 1988	KUO	T43 - 12hr
8807CONGCCT106	1-30 July, 1988	ISWS/HDG 1988	KUO	T106 - 6hr
9307CONKUO	1-30 July, 1993	ISWS/HDG 1993	KUO	T43 - 12hr
9307CONKUOT106	1-30 July, 1993	ISWS/HDG 1993	KUO	T106 - 6hr
9307CONGCC	1-30 July, 1993	ISWS/HDG 1993	GCC	T43 - 12hr
9307CONGCCT106	1-30 July, 1993	ISWS/HDG 1993	GCC	T106 - 6hr

jet. Hence, a set of July simulations for both 1988 and 1993, with realistic initial soil moisture conditions, are performed with a reduced critical negative area in the sounding. The critical negative area threshold is reduced from 1.0 to 0.5. Another similar set of simulations are performed to see if decreasing the column moistening fraction, b, so that less moisture goes into moistening the column, results in more precipitation. The b factor is reduced by 25% by modifying Equation 3.10 as follows

$$b = 1.5(1 - \overline{RH}). \tag{4.2}$$

See Section 3.4.1 for a more complete description of the KUO parameterization. Table 4.6 gives a description of these simulations.

Table 4.6: Description of each setup used for the "Sensitivity of Precipitation to KUO Scheme Parameters" simulations. Table includes: Simulation name and date, initial soil saturation, convection scheme used, and boundary condition spatial and temporal resolution.

Run Name	Run date	Soil Moisture IC	Convection	BC Resolution
8807CONKUOT106	1-30 July, 1988	ISWS/HDG 1988	KUO - Standard	T106 - 6hr
8807NAKUOT106	1-30 July, 1988	ISWS/HDG 1988	KUO - Reduced Neg Area	T106 - 6hr
8807BFKUOT106	1-30 July, 1988	ISWS/HDG 1988	KUO - Reduced b factor	T106 - 6hr
9307CONKUOT106	1-30 July, 1993	ISWS/HDG 1993	KUO - Standard	T106 - 6hr
9307NAKUOT106	1-30 July, 1993	ISWS/HDG 1993	KUO - Reduced Neg Area	T106 - 6hr
9307BFKUOT106	1-30 July, 1993	ISWS/HDG 1993	KUO - Reduced b factor	T106 - 6hr

Chapter 5

Results

This chapter discusses in detail the results of each set of numerical experiments described in Chapter 4. The Midwest region, shown in Figure 5-1, centered around Iowa, extending to most of Illinois and parts of Indiana, Wisconsin, Minnesota, South Dakota, Nebraska, Kansas, and Missouri, is the area that was most affected by the drought of 1988 and the flood of 1993. Some of the simulations are compared and contrasted to each other, while others are compared to other datasets. Two datasets are used for the comparisons: U.S. Historical Climatology Network (USHCN) monthly precipitation and the ECMWF analysis. The USHCN data are managed by the National Climatic Data Center (NCDC) and the Carbon Dioxide Information and Analysis Center (CDIAC). The USHCN has 1221 stations from the U.S. Cooperative Observing Network within the continental United States. However, only approximately 400 stations for 1988 and 120 stations for 1993 were available for analysis. Note that the USHCN precipitation data are interpolated from station data to the model grid. This procedure may have exaggerated some of the observed peaks. In addition, the procedure may have produced unreliable values of precipitation along the coastal edges of the domain where there are few precipitation stations. However, the interpolated dataset provides a more than adequate representation of precipitation. Two ECMWF analysis datasets are used for this study and interpolated to the model grid. One is interpolated from a T43 grid and is available at 12-hour intervals and the other is interpolated from a T106 grid and is available at 6-hour

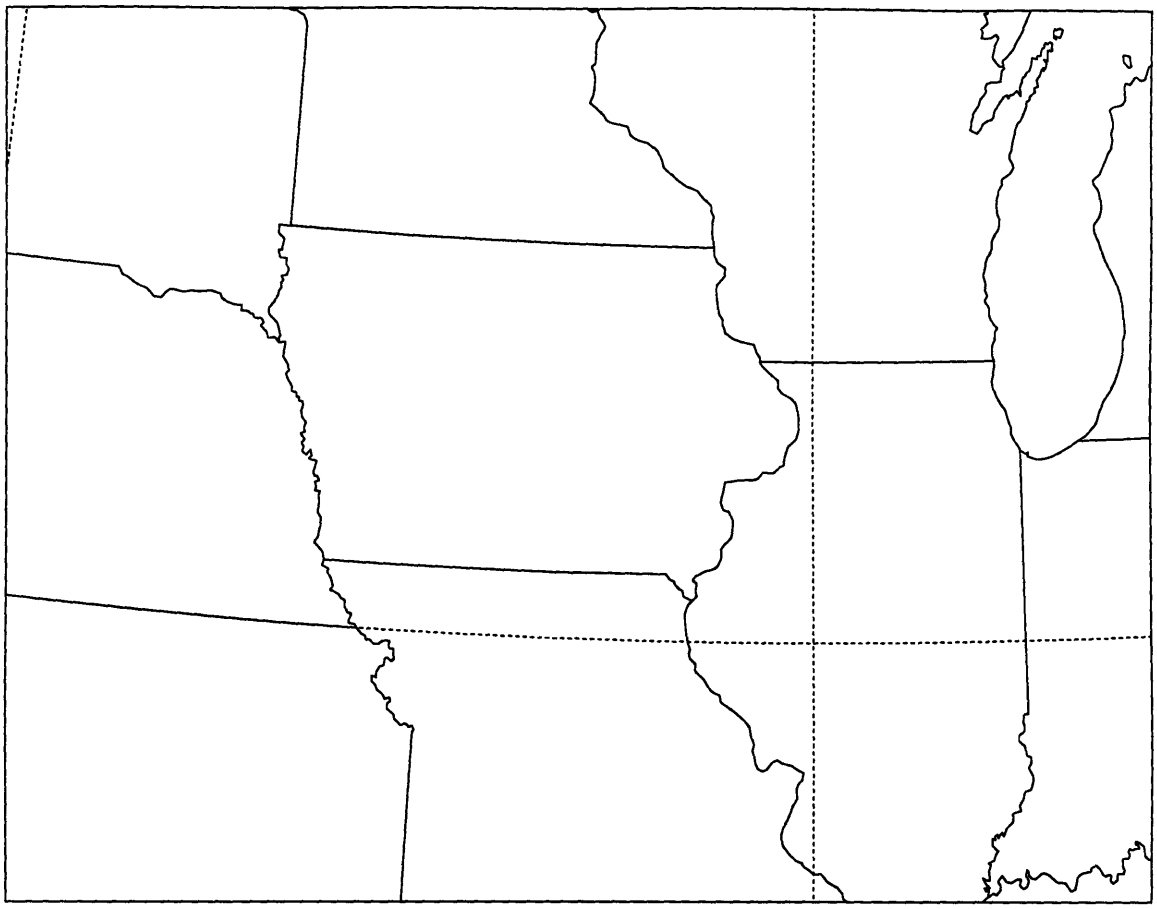

Figure 5-1: Map of the drought and flood stricken "Midwest" region used for the summaries.

intervals. Although the ECMWF analysis is an assimilated dataset, that should not affect the results since there is sufficient measured data over the domain of the simulations.

5.1 Comparison of Model Against Observations

This section compares the control simulations of May, July, and September of 1988 and 1993 simulations found in Table 4.4 (in Chapter 4 on the design of Numerical Experiments) to the U.S. Historical Climatology Network (USHCN) monthly precipitation and the ECMWF analysis data. Table 5.1 (in Chapter 4 on the design of Numerical Experiments) presents a summary of the observed and

Table 5.1: Precipitation (mm) of the control simulations compared to observations for the entire domain and the Midwest region.

Simulation	Precipitation			
	Entire Domain		Midwest Region	
	Observed	Simulated	Observed	Simulated
8805CONKUO	58.7	30.2	48.9	47.3
8807CONKUO	93.3	68.0	65.7	72.0
8809CONKUO	113.4	70.0	85.8	99.4
8805CONGCC	58.7	48.3	48.9	73.0
8807CONGCC	93.3	101.5	65.7	89.3
8809CONGCC	113.4	67.9	85.8	88.9
9305CONKUO	82.9	65.9	113.2	120.3
9307CONKUO	122.7	68.1	172.3	105.8
9309CONKUO	83.1	63.1	101.4	101.3
9305CONGCC	82.9	66.6	113.2	101.1
9307CONGCC	122.7	98.9	172.3	196.0
9309CONGCC	83.1	65.4	101.4	93.7

simulated precipitation over the entire domain and the affected Midwest region, and Table 5.2 presents a summary of some of the T43, 12-hour ECMWF analysis fields and simulated surface fields at 1,000 millibars over the Midwest. The figures and tables will be discussed in further detail in the following two sections.

Figures 5-2 through 5-8 show the total observed and simulated precipitation for both convection schemes for May, July, and September of 1988 and 1993, respectively. Regardless of the convective parameterization, the model does an unsatisfactory job of simulating the spatial distribution and total volume of precipitation in July when convection is prominent (described in detail in the following subsections). However, their performance in May and September of these years is much better. In all the simulations using the KUO scheme, the model does not simulate enough precipitation in the southern portion of the domain. In fact, in the area of the southern boundary no rainfall is simulated. Furthermore, the KUO scheme produces too much precipitation in the northern interior of the domain. On the other hand, the GCC scheme tends to miss the longitudinal location of the precipitation events. Both schemes, as a whole,

Table 5.2: 30-day mean mixing ratio (g/kg), temperature (C), and wet-bulb temperature (C) at 1,000 millibars of the control simulations and ECMWF analysis data for the Midwest region.

Simulation	Mixing Ratio		Temperature		Wet-bulb Temperature	
	ECMWF	Simulated	ECMWF	Simulated	ECMWF	Simulated
8805CONKUO	8.8	9.1	20.9	23.7	15.2	16.4
8807CONKUO	15.1	16.6	30.6	29.3	22.9	23.5
8809CONKUO	11.5	12.2	22.7	23.6	18.0	18.8
8805CONGCC	8.8	9.7	20.9	21.8	15.2	16.3
8807CONGCC	14.5	15.2	26.1	24.2	21.4	21.4
8809CONGCC	11.5	12.1	22.7	21.7	18.0	18.2
9305CONKUO	10.0	10.7	19.1	20.9	15.5	16.7
9307CONKUO	16.3	15.0	30.7	31.9	23.8	23.3
9309CONKUO	10.3	11.1	18.8	19.5	15.6	16.5
9305CONGCC	10.0	10.3	19.1	19.5	15.5	16.0
9307CONGCC	16.0	15.9	25.0	25.4	22.2	22.3
9309CONGCC	10.3	10.9	18.8	18.5	15.6	16.0

were able to recognize the difference between wet and dry months by simulating more precipitation in 1993 and less precipitation in 1988.

Figure 5-5 is a comparison of the soundings over the affected Midwest region (30 day mean) from the simulations using the KUO and GCC parameterizations to the ECMWF data for July 1988 and 1993. Clearly, the KUO scheme sgnificantly overestimates temperature ($\sim$3° C) below a σ-level of approximately 0.7 ($\sim$700 mb). On the other hand, the GCC scheme does a remarkable job of reproducing the ECWMF temperature data, except at σ-levels below 0.95 ($\sim$950 mb). Both schemes underestimate the mixing ratio near the surface by approximately 2 g/kg. Above a σ-level of 0.85, the GCC parameterization simulates mixing ratio reasonably well, while the KUO parameterization does not. Overall, the GGC scheme does a significantly better job than the KUO scheme of reproducing the ECMWF sounding. Both schemes, however, require significant improvements in the PBL.

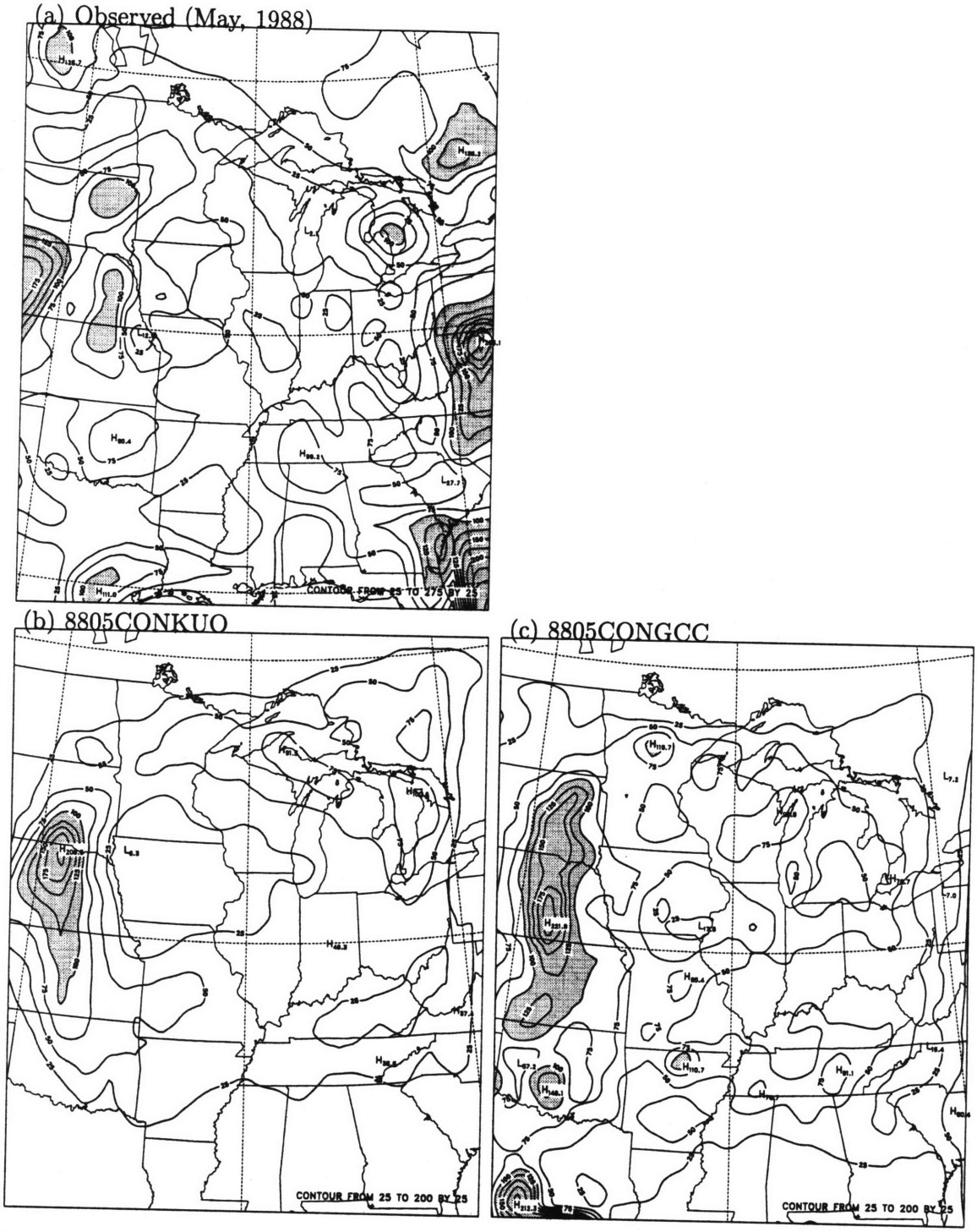

Figure 5-2: Total precipitation (mm). Comparison of the control simulations to observations. (a) Observed May, 1988; (b) 8805CONKUO; and (c) 8805CONGCC. Units are in millimeters, contour interval is 25 mm, and shading denotes values in excess of 100 mm.

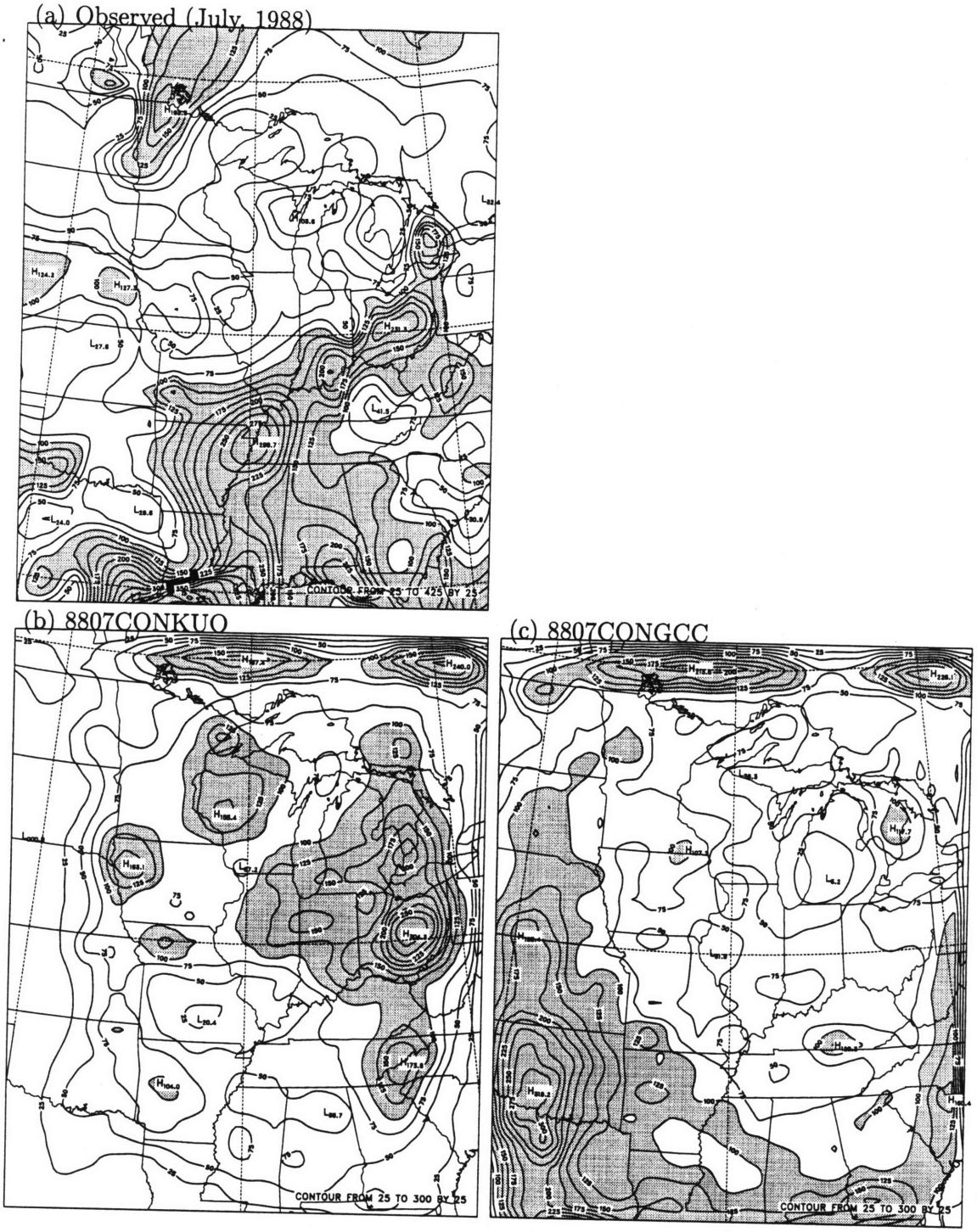

Figure 5-3: Total precipitation (mm). Comparison of the control simulations to observations. (a) Observed July, 1988; (b) 8807CONKUO; and (c) 8807CONGCC. Units are in millimeters, contour interval is 25 mm, and shading denotes values in excess of 100 mm.

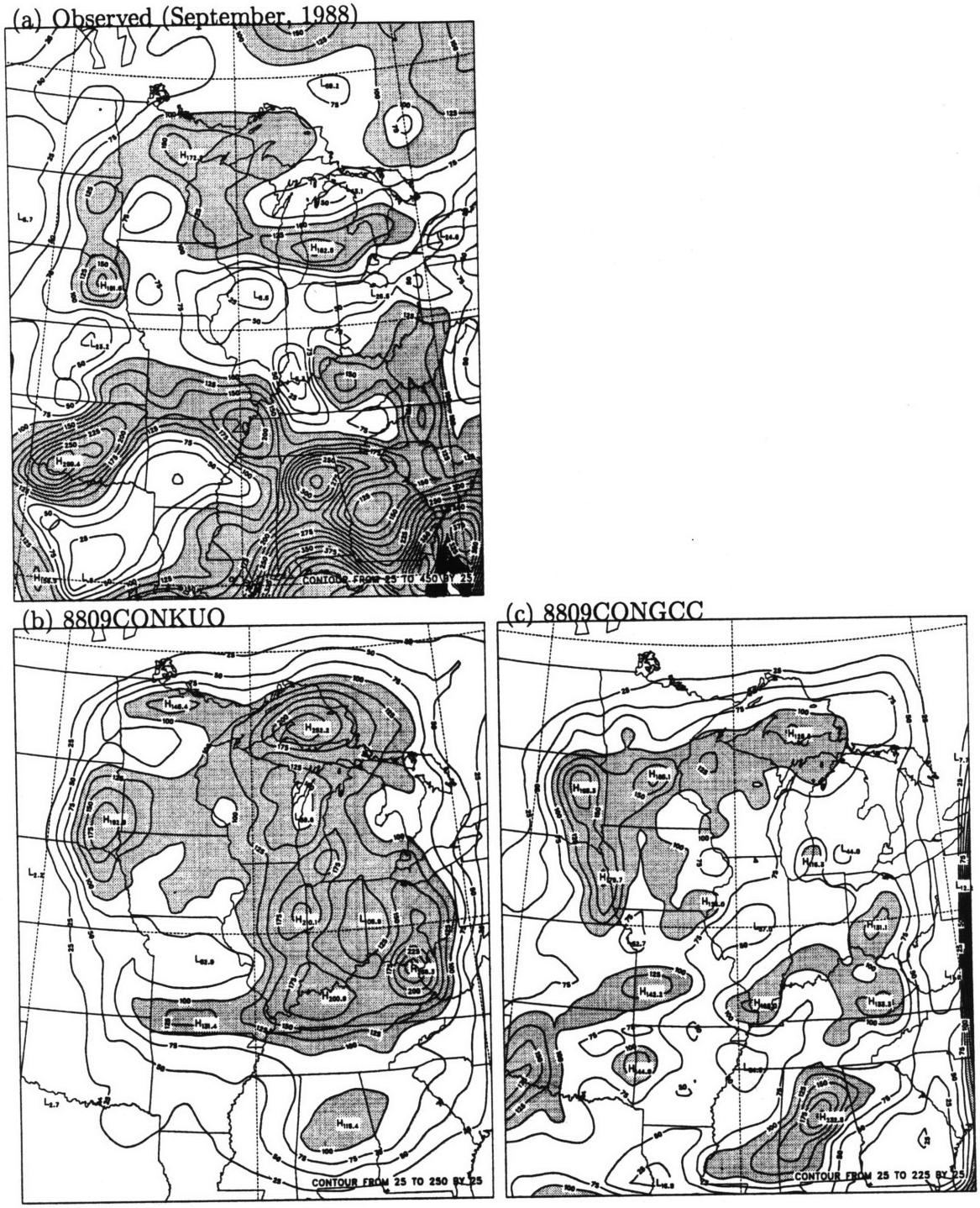

Figure 5-4: Total precipitation (mm). Comparison of the control simulations to observations. (a) Observed September, 1988; (b) 8809CONKUO; and (c) 8809CONGCC. Units are in millimeters, contour interval is 25 mm, and shading denotes values in excess of 100 mm.

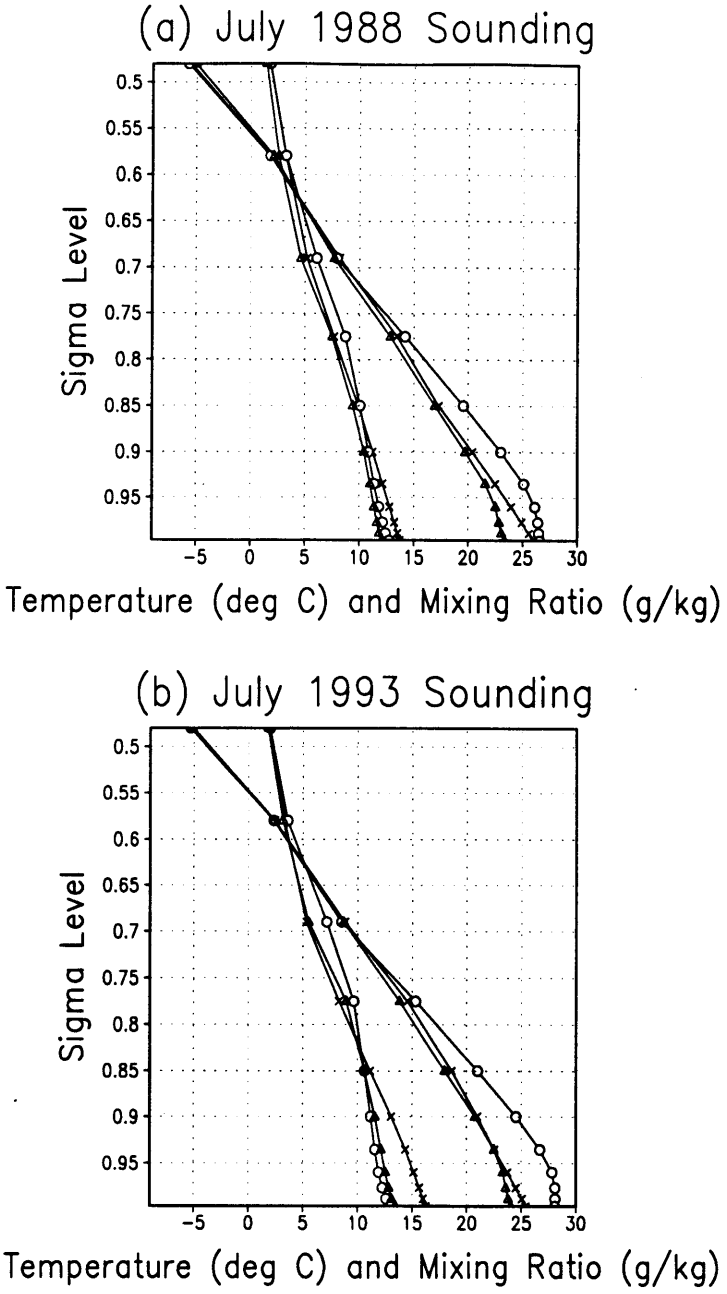

Figure 5-5: 30 day mean temperature and mixing ratio soundings over the affected Midwest region during July 1988 and 1993 for the ECMWF data (denoted by x), KUO simulation (denoted by o), and the GCC simulation (denoted by $\triangle$).
The x-axis is in units of degrees Celsius for temperature and grams per kilogram for mixing ratio. The y-axis is in units of σ-levels (σ-level = 1.0 is the surface).

5.1.1 1988 Control Simulations

1988 observations show a precipitation minimum centered around Iowa and Illinois for May, July, and September. From May to September, it is evident that the northward displaced storm track, discussed in Trenberth and Guillemot (1996), crept south towards its original position. In addition, the low-level jet (see Paegle et al. (1996)), which did not exist in May, seemed to develop in July and September but it did not extend far enough north to connect with the storm track.

In May (Figure 5-2), most of the domain showed little or no precipitation except for small peaks over Nebraska, Virginia, and other small isolated areas. Both the KUO and GCC schemes did a reasonable job of simulating the small rainfall peak that occurred over Nebraska, but neither scheme simulated the peak over Virginia. In addition, they were both able to predict the lack of rainfall over most of the domain. Overall (Table 5.1), both schemes, especially the KUO, underestimated precipitation for the entire domain. Over the Midwest region, the KUO simulated precipitation well, while the GCC scheme overestimated precipitation. When comparing the control simulations to the ECMWF data over the Midwest (Table 5.2), we found both schemes to be slightly moist and hot which imply a high wet-bulb temperature.

July of 1988 (Figure 5-3) was much wetter than May; the southern to mid-eastern portion of the domain had heavy rainfall but the northern and mid-western portions still remained relatively dry. A few peaks in rainfall occurred diagonally from eastern Arkansas to southern Ohio and another occurred between the border of Minnesota and Canada. The KUO scheme seems to have simulated the general location of the peaks in southern Ohio and northern Minnesota, but it incorrectly estimated their magnitudes. It did not, however, simulate any of the rainfall that occurred in the south. The GCC scheme was not able to represent the observed precipitation except for the peak at the Minnesota border. In addition, it produced a significant amount of precipitation over Oklahoma when very little was observed. Overall, the simulation using the KUO scheme significantly underestimated total precipitation over the entire domain and slightly overestimated precipitation over the Midwest

(Table 5.1). Similar to May, the surface of 8807CONKUO was slightly humid and hot (Table 5.2). The GCC scheme overestimated precipitation over the entire domain and midwest (Table 5.1). Furthermore, over the Midwest, the model simulated surface mixing ratio high and temperature low, yielding the correct wet-bulb temperature for the wrong reasons (Table 5.2).

In September of 1988 (Figure 5-3), there was heavy precipitation in the southern half of the domain with peaks over Alabama and Oklahoma and a relatively small broad local maximum over the northern U.S. The KUO scheme simulated too much precipitation in the interior of the domain and not enough around the edges, but was able to simulate some characteristics of the north. Overall, it grossly underestimated precipitation for the entire domain and slightly overestimated precipitation over the Midwest (Table 5.1). In addition, it was too humid and too hot over the Midwest (Table 5.2). The GCC scheme was able to do a reasonable job in simulating the small northern peaks and the southern highs in Alabama and Oklahoma but it was unable to simulate the overall high precipitation in the south. Hence, it significantly underestimated total domain precipitation. However, Midwest precipitation simulated well. The Midwest was too humid and cool again yielding a correct wet-bulb temperature for the wrong reasons.

Comparison of Figure 5-2(a) to Figure 5-2(b)(c), Figure 5-3(a) to Figure 5-3(b)(c), and Figure 5-4(a) to Figure 5-4(b)(c) show that both schemes do a satisfactory job of simulating precipitation in May and September and an unsatisfactory job in July. The main deficiency of the KUO scheme is its inability to simulate precipitation in the southern portion of the domain. Overall, the KUO simulations were too hot and too humid at the surface over the Midwest. Hence, they overestimated wet-bulb temperature. The GCC scheme was not able to represent the longitudinal placement of the precipitation peaks. It had no consistent errors in the analyzed surface fields. More on the inadequacies of the model will be discussed in detail in Chapter 6, Conclusions and Future Research.

5.1.2 1993 Control Simulations

In contrast to 1988, large amounts of precipitation occurred over the Midwest in May, July, and September of 1993 while relatively little occurred over the southern portions of the domain. The connection of the low broad storm track and low-level jet is evident during these months from the distribution of precipitation.

In May (Figure 5-6), a low-level jet produced a band of precipitation along the western edge of the Mississippi River with a smaller arm of precipitation crossing Arkansas and Tennessee. The largest peak was found over the borders between Iowa, Minnesota, and South Dakota and it extended over Wisconsin. A smaller peak occurred at the Missouri and Kansas border. The KUO scheme did a good job of simulating this band of precipitation. It even simulated the small arm of rainfall, although weaker in magnitude, across Arkansas and Tennessee. It did, however, shift the primary band too far westward and failed to simulate southern precipitation. Overall, 9305CONKUO underestimated total domain precipitation and simulated Midwest rainfall well (Table 5.1). In addition, it was too humid and hot (Table 5.2). The GCC scheme did a comparable job of simulating the distribution of May precipitation. It also shifted the primary band of precipitation westward. Overall, 9305CONGCC underestimated precipitation over the entire domain and the Midwest (Table 5.1). In addition, it simulated an atmosphere that is slightly moist and hot, as it did in 1988 (Table 5.2).

July of 1993 (Figure 5-7) had a similar rainfall distribution as May. The only difference was that July had much higher peaks. Peak rainfall was observed along the Mississippi River from the Gulf of Mexico to the southern Wisconsin. The largest peak, however, was observed over Kansas and Nebraska along the Missouri River. Both the Missouri and Mississippi Rivers experienced record high flooding during this month (Kunkel et al. 1994). The northern portion of the domain experienced a fairly uniform distribution of rainfall around 150 mm. The KUO scheme simulated the large amounts of rainfall in the northern portion of the domain, but it was not able to simulate the peaks. In addition, it simulated zero precipitation below 37° N. The

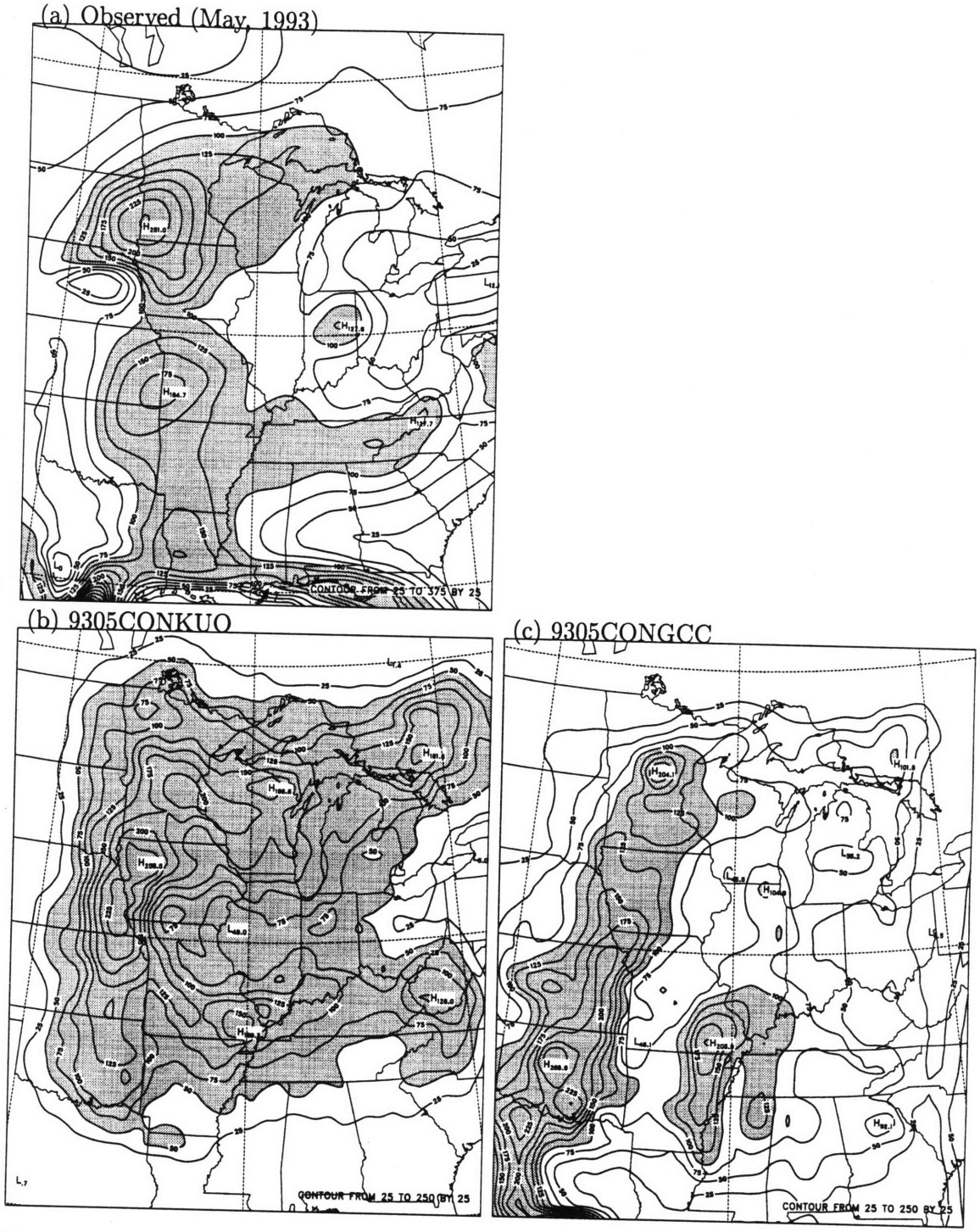

Figure 5-6: Total precipitation (mm). Comparison of the control simulations to observations. (a) Observed May, 1993; (b) 9305CONKUO; and (c) 9305CONGCC. Units are in millimeters, contour interval is 25 mm, and shading denotes values in excess of 100 mm.

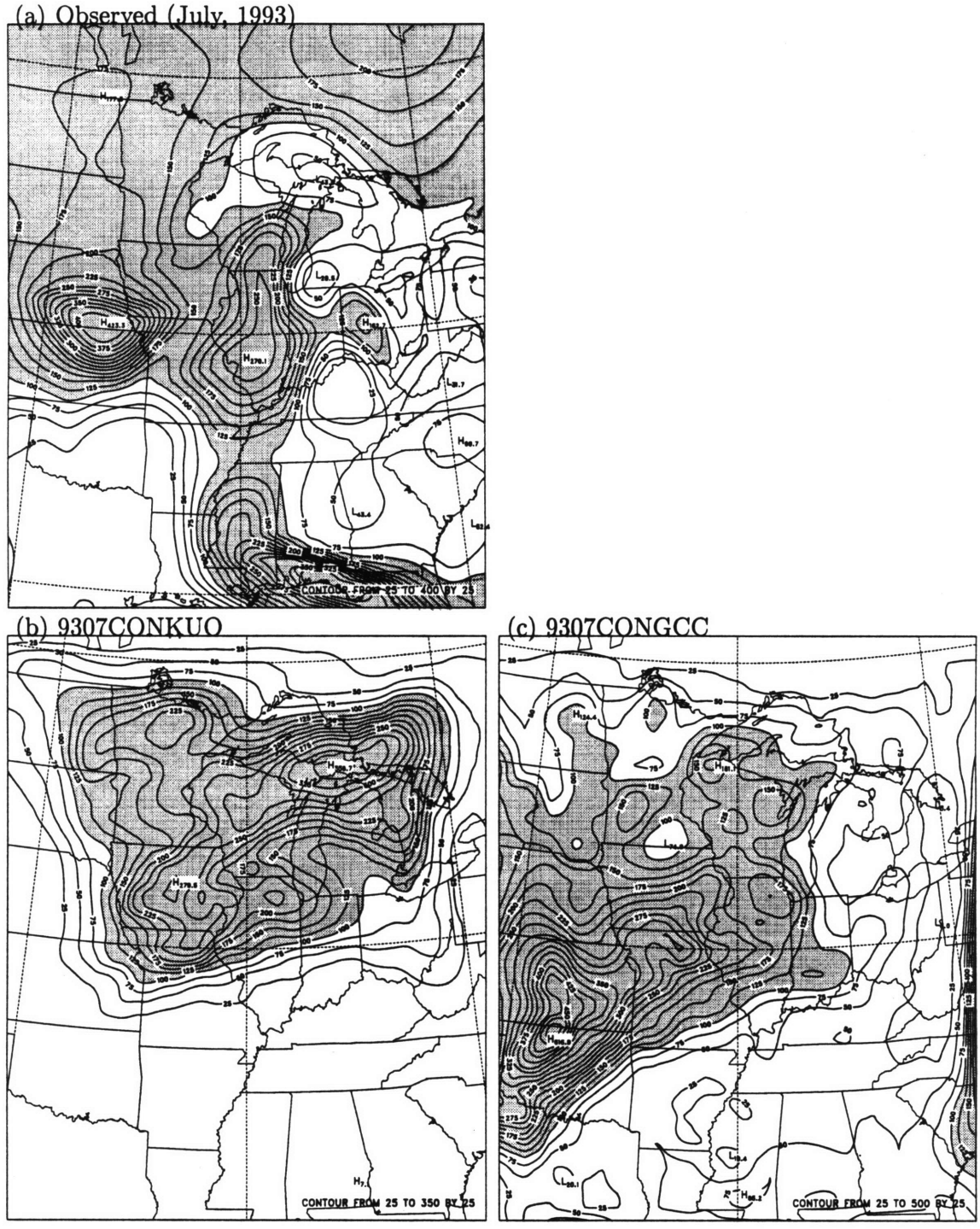

Figure 5-7: Total precipitation (mm). Comparison of the control simulations to observations. (a) Observed July, 1993; (b) 9307CONKUO; and (c) 9307CONGCC. Units are in millimeters, contour interval is 25 mm, and shading denotes values in excess of 100 mm.

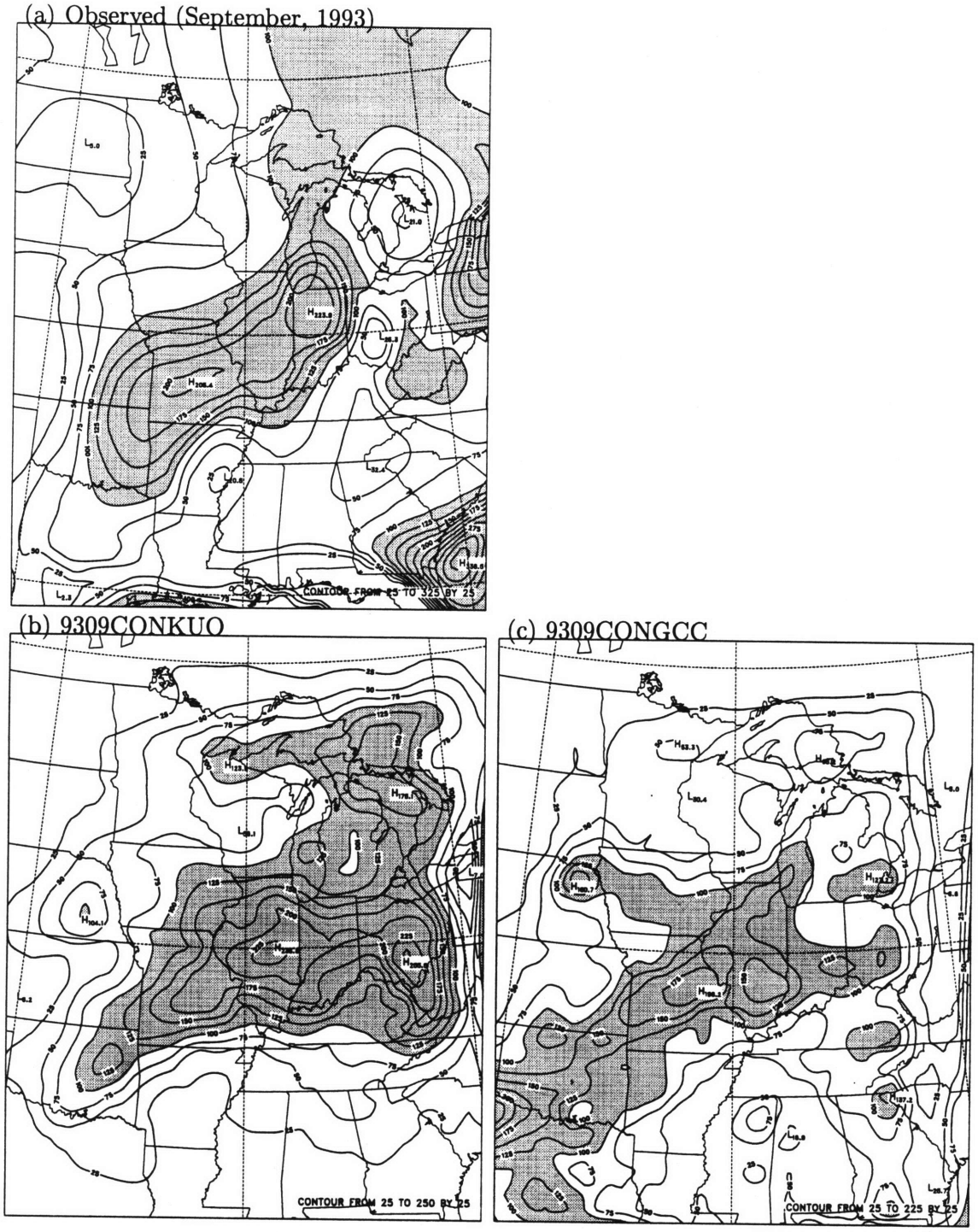

Figure 5-8: Total precipitation (mm). Comparison of the control simulations to observations. (a) Observed September, 1993; (b) 9309CONKUO; and (c) 9309CONGCC. Units are in millimeters, contour interval is 25 mm, and shading denotes values in excess of 100 mm.

overall volume over the entire domain and Midwest was underestimated (Table 5.1). 9307CONKUO was slightly dry and excessively hot over the Midwest (Table 5.2). The GCC scheme failed to simulate the southern and northern precipitation. But it was able to simulate the peak over Kansas and Nebraska, with a slight southward shift, and the peak over Illinois, with a westward shift. The total domain rainfall was low, and the Midwest rainfall was high (Table 5.1). Simulations using the GCC scheme underpredicted both mixing ratio and temperature over the Midwest (Table 5.2).

September of 1993 (Figure 5-8) experienced heavy precipitation diagonally from Oklahoma to Michigan. The rest of the domain received only moderate rainfall. Both schemes did a reasonable job in simulating the diagonal pattern of rainfall and in simulating the peak along Missouri and Illinois. The KUO scheme, however, added another peak in southern Ohio which was not observed. Over the entire domain, the KUO scheme underestimated precipitation (Table 5.1). Over the Midwest, it simulated precipitation volume well, mixing ratio too high, and temperature too high (Table 5.2). The GCC scheme underpredicted precipitation over the Midwest and entire domain. (Table 5.1). In addition, it simulated surface temperature well, however, it overestimated humidity (Table 5.2).

In comparing Figure 5-6(a) to Figure 5-6(b)(c), 5-7(a) to Figure 5-7(b)(c), and 5-8(a) to 5-8(b)(c), we found that both schemes do a reasonably satisfactory job of simulating precipitation in May and September, but they do an unsatisfactory job in July. Similar to 1988, the simulations using the KUO scheme tend to underestimate total domain precipitation. Over the Midwest, precipitation volume was simulated well for May and September but not for July. In addition, the model overestimated (except for 9307CONKUO) mixing ratio and temperature at 1,000 millibars over the Midwest, as it did in 1988 (Table 5.2). Hence, wet-bulb temperature was overestimated for all of the simulations. Similar to the KUO simulations, the GCC simulations underestimated total domain rainfall. However, the rainfall predictions over the Midwest were within 15% of the observed values (Table 5.1). No consistent errors were found when comparing the simulations to mixing ratio, temperature and wet-bulb temperature at 1,000 millibars.

Table 5.3: Total, convective, and non-convective precipitation (mm) of the extreme simulations for the entire domain and the Midwest region.

Simulation	Precipitation					
	Total		Convective		Non-Convective	
	Domain	Midwest	Domain	Midwest	Domain	Midwest
8807DRYKUOEXT	52.0	44.4	43.2	37.0	8.8	7.4
8807WETKUOEXT	76.4	100.2	68.5	91.4	7.9	8.8
8807DRYGCCEXT	97.9	78.6	81.0	65.8	16.9	12.8
8807WETGCCEXT	104.2	98.8	81.2	69.8	22.0	29.0
9307WETKUOEXT	72.7	118.8	67.4	108.0	5.3	10.8
9307DRYKUOEXT	44.0	57.4	39.5	47.5	4.5	9.9
9307WETGCCEXT	100.0	191.2	76.0	139.4	24.0	51.8
9307DRYGCCEXT	91.4	182.1	76.6	149.1	14.8	33.0

5.2 Sensitivity to Soil Moisture Extremes

This section describes the results of the simulations listed in Table 4.2 (in Chapter 4 on the Design of Numerical Experiments). More specifically, it investigates how sensitive RegCM2 is to extreme changes in soil moisture. Figures 5-9 and 5-10 present the precipitation and precipitation sensitivities from the extreme soil moisture initializations for both the KUO and GCC parameterizations for July 1988 and 1993, respectively. Table 5.3 presents a summary of the total, convective, and non-convective precipitation for the entire domain and the affected Midwest region for these simulations. Table 5.4 displays the sensitivities of these extreme simulations to several surface fields. Overall, simulations using the two convective parameterizations give significantly different results and are described below.

In July 1988, the difference in precipitation between the wet run and the dry run when using the KUO scheme is significantly positive for most of the domain (Figure 5-9). The primary precipitation system that extends northward from Ohio through Michigan and southwestern Ontario is extended westward across Indiana and Illinois in the wet simulation. In addition, another peak develops over southwestern Minnesota and southeastern South Dakota. Both of these additional peaks add precipitation to the drought affected region. Futhermore, most of the precipitation

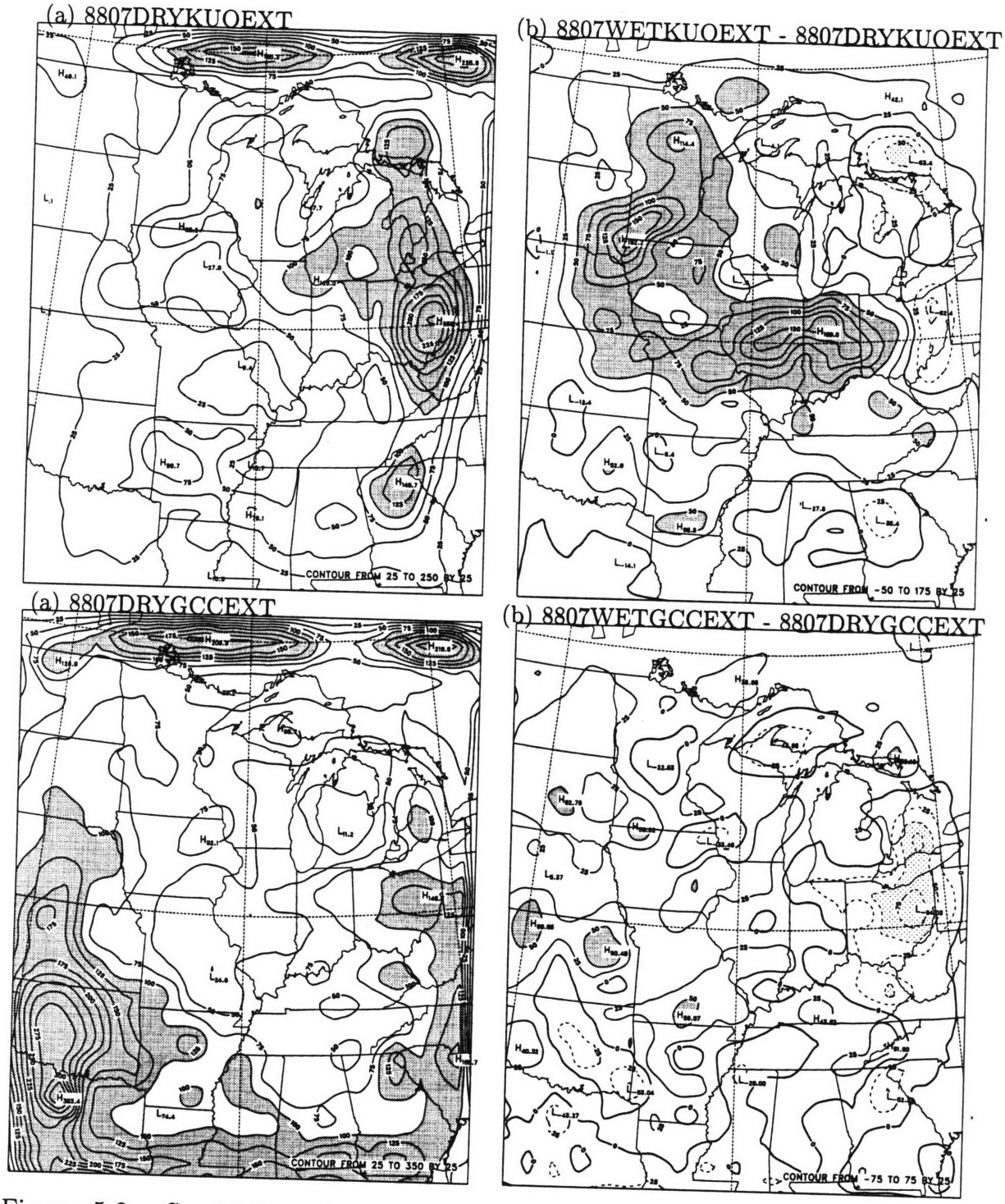

Figure 5-9: Sensitivity of precipitation to extreme changes in soil moisture. (a) 8807DRYKUOEXT; (b) 8807WETKUOEXT - 8807DRYKUOEXT; (c) 8807DRYGCCEXT; and (d) 8807WETGCCEXT - 8807DRYGCCEXT. Units are in millimeters, contour interval is 25 mm. On precipitation plots, dark shading denotes values in excess of 100 mm. On sensitivity plots, dark shading denoted values in excess of 50 mm and light shading denotes values less than 50 mm.

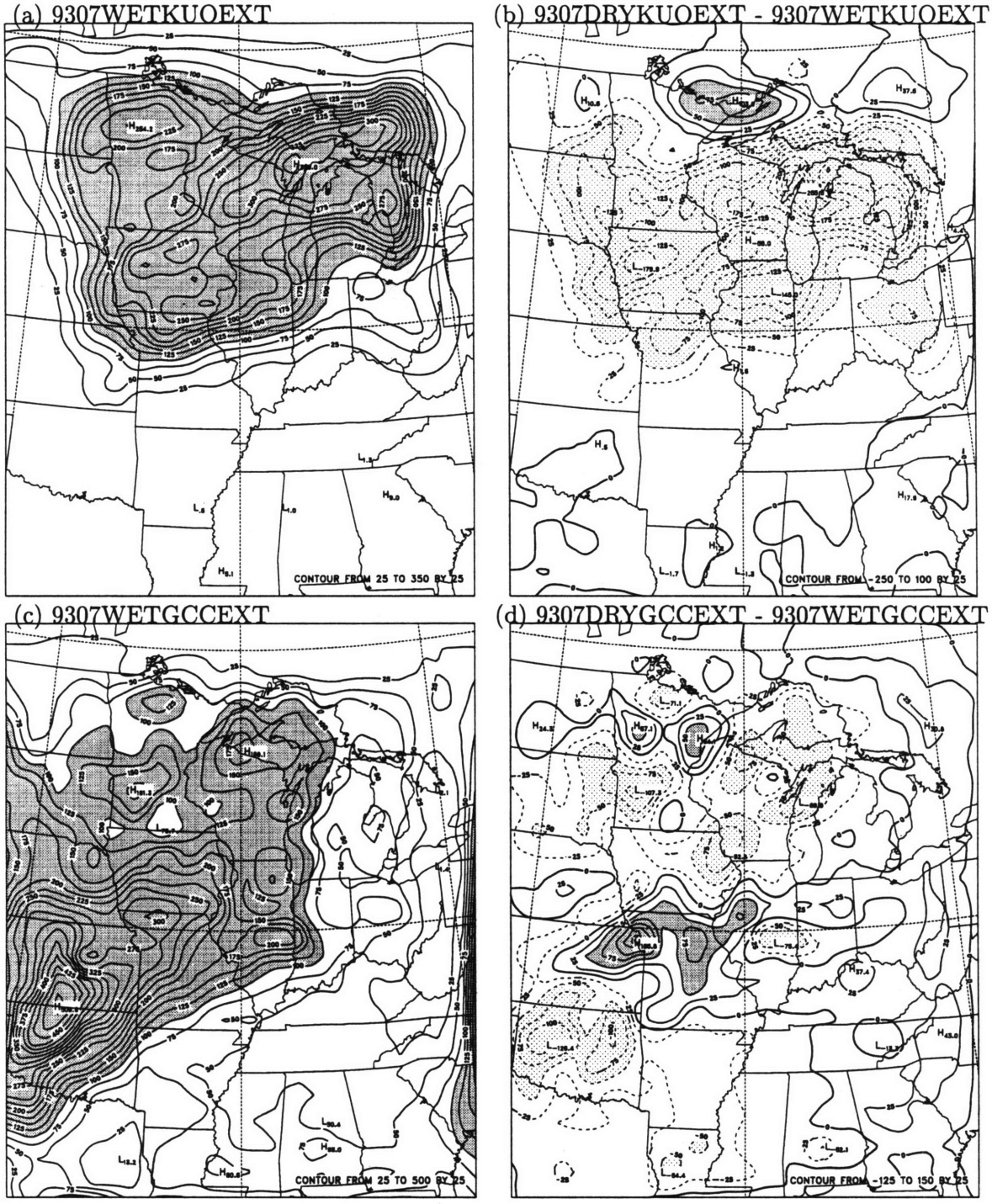

Figure 5-10: Sensitivity of precipitation to extreme changes in soil moisture. (a) 9307DRYKUOEXT; (b) 9307DRYKUOEXT - 9307WETKUOEXT; (c) 9307WETGCCEXT; and (d) 9307DRYGCCEXT - 9307WETGCCEXT. Units are in millimeters, contour interval is 25 mm. On precipitation plots, dark shading denotes values in excess of 100 mm. On sensitivity plots, dark shading denoted values in excess of 50 mm and light shading denotes values less than 50 mm.

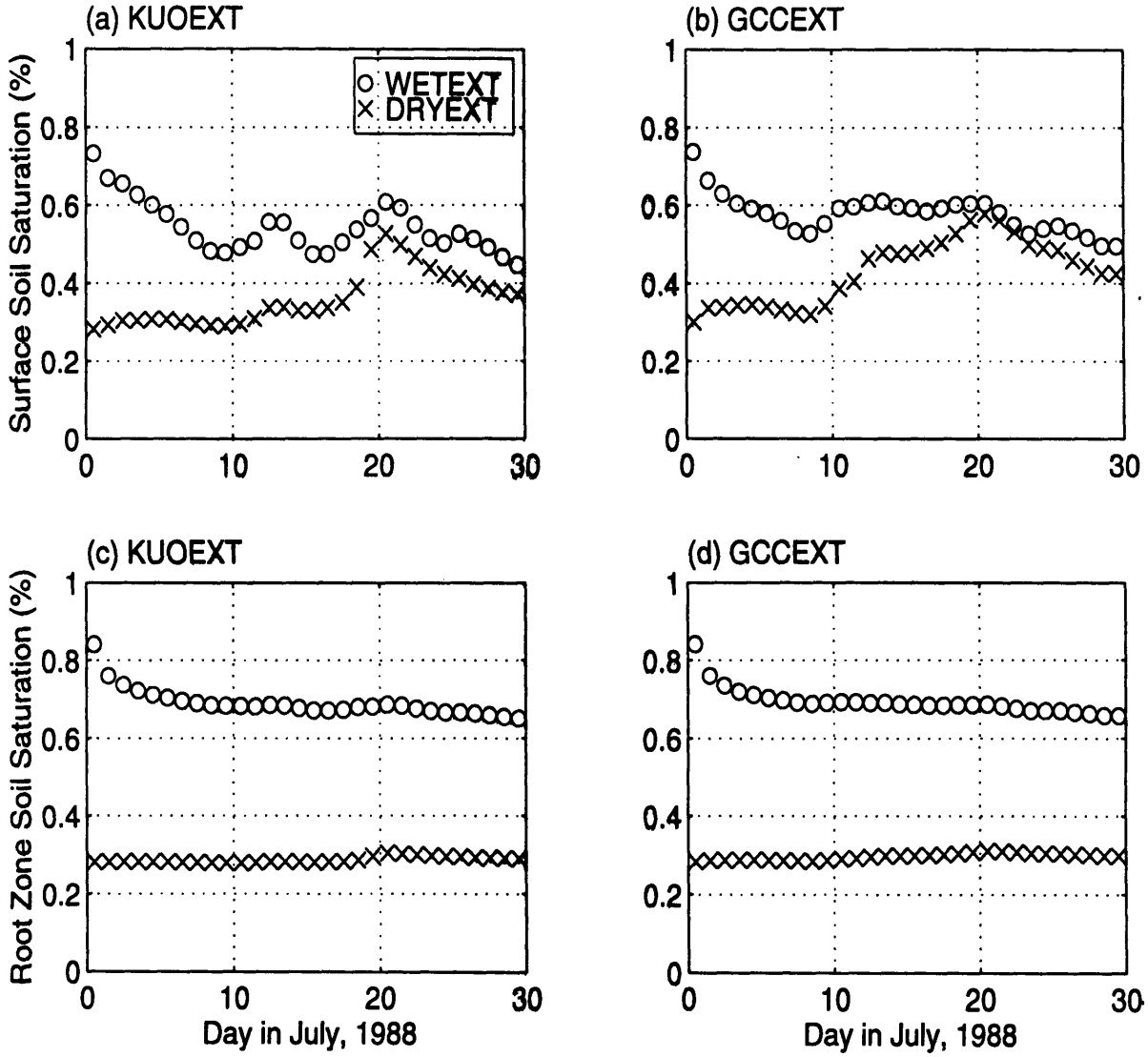

Figure 5-11: Surface and root zone soil saturation (%) daily time series for the extreme soil moisture initializations for July of 1988. (a) Surface zone (8807KUOEXT); (b) Surface zone (8807GCCEXT); (c) Root zone (8807KUOEXT); and (d) Root zone (8807GCCEXT).

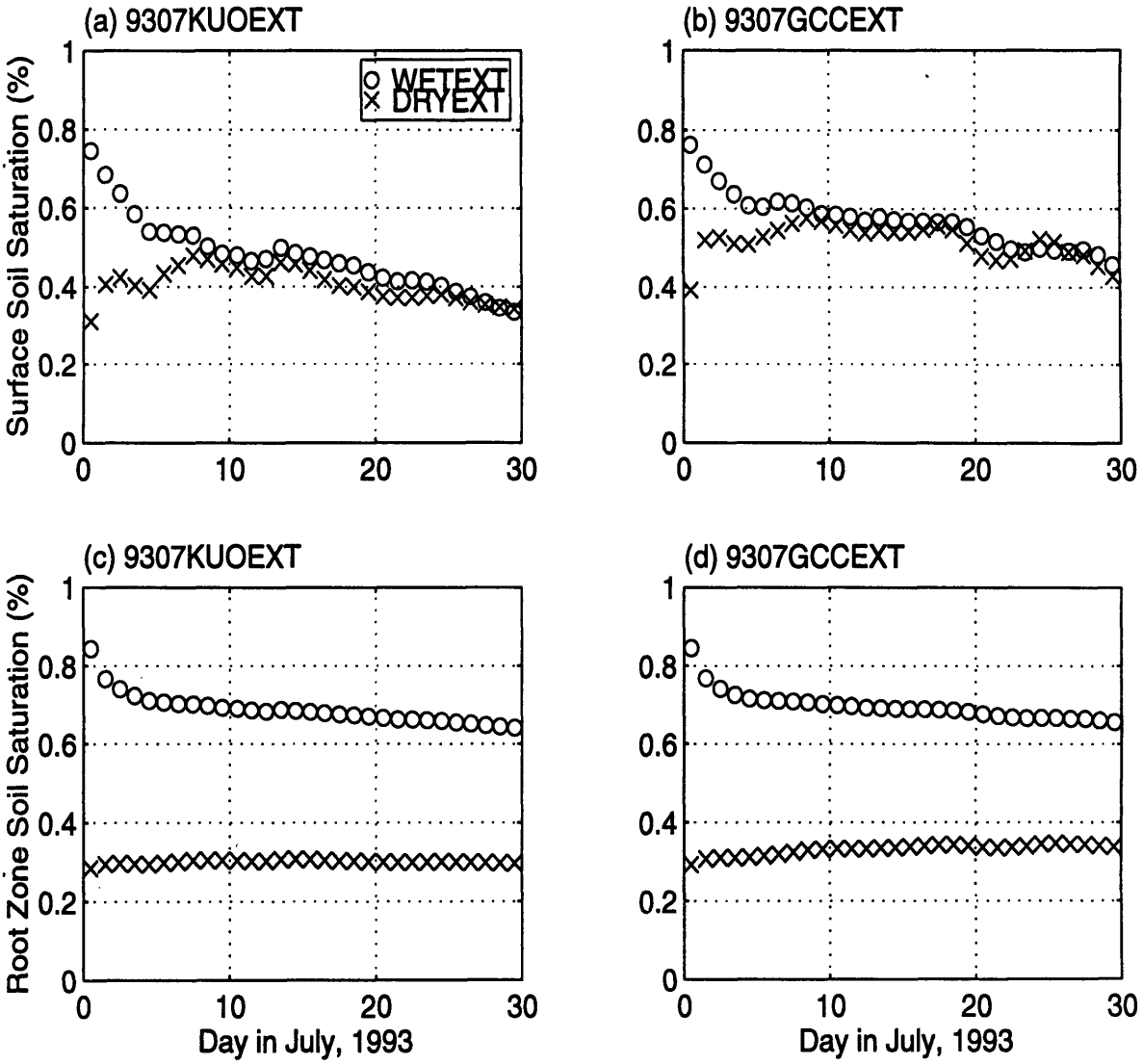

Figure 5-12: Surface and root zone soil saturation (%) daily time series for the extreme soil moisture initializations for July of 1993. (a) Surface zone (9307KUOEXT); (b) Surface zone (9307GCCEXT); (c) Root zone (9307KUOEXT); and (d) Root zone (9307GCCEXT).

Table 5.4: 30-day mean mixing ratio Q (g/kg), temperature T (C), and wet-bulb temperature Tw (C) at 1,000 millibars and precipitation *ppt* (mm) of the wet and dry extreme simulations for the Midwest region.

Simulation	Q		T		Tw		ppt	
	Wet	Dry	Wet	Dry	Wet	Dry	Wet	Dry
8807KUOEXT	17.3	12.4	28.5	32.8	23.8	21.7	100.2	44.4
8807GCCEXT	15.4	13.2	23.7	28.5	21.4	21.1	98.8	78.6
9307KUOEXT	17.1	12.9	30.1	33.2	24.2	22.2	118.8	57.4
9307GCCEXT	16.1	15.4	24.7	26.6	22.2	22.2	191.2	182.1

increase comes via convective processes (Table 5.3), since there is little change in non-convective precipitation. In addition to precipitation, mixing ratio, temperature, and wet-bulb temperature display a strong sensitivity to soil moisture (Table 5.4). The large increase in mixing ratio with wet soil moisture outweighs the decrease in temperature, netting a significant increase in wet-bulb temperature. This increase in wet-bulb temperature is consistent with the large increase in precipitation (see Eltahir and Pal (1996)).

In July 1988, there is a weak sensitivity of precipitation to extreme changes in soil moisture when using the GCC scheme (Figure 5-9). The northern portion of the system that extends north from Texas to Nebraska is slightly strengthened and widened due to the increase in soil moisture. On the other hand, the northern portion of the system that extends from Florida into Ohio disappears as a result of the increase. Contrary to the results of the simulation using the KUO scheme, the overall increase in precipitation that occurs from wet soil moisture conditions is primarily due to an increase in non-convective precipitation (Table 5.3). The decrease in temperature over the Midwest with increased soil moisture is virtually balanced by the increase in mixing ratio, yielding only a slight increase in wet-bulb temperature (Table 5.4). Thus, there is only a slight increase in rainfall.

The results for July 1993 are similar to the results from July 1988 when using the KUO parameterization. Precipitation is highly sensitive to changes in soil moisture. The large system that covers most of the northern half of the domain

for the extreme wet simulation experiences an overall weakening from the decrease in soil moisture, except north of Minnesota where a substantial increase occurs. Most of the decrease in precipitation for both the entire domain and the Midwest region comes from a decrease in convection (Table 5.3). The decrease in mixing ratio with low soil moisture outweighs the temperature increase (Table 5.4). Hence, wet-bulb temperature decreases and results in an decrease in precipitation.

With the GCC parameterization, the dry soil moisture simulations in July 1993 yielded an overall decrease in precipitation. Table 5.3 shows that for the Midwest region, convective precipitation slightly increased with dry conditions. When comparing the relative contribution of convective and non-convective precipitation, there exists a weak negative feedback between soil moisture and convective precipitation. This negative feedback is probably due to the increased sensible heat flux (buoyancy) that results from dry soil moisture conditions and that tends to trigger more convection in the buoyancy sensitive GCC parameterization as discussed in Giorgi et al. (1996). Table 5.4 shows that the surface fields in 1993 show less sensitivity to soil moisture than in 1988. The decrease in precipitation with dry soil moisture for the Midwest region is less than 5% which is consistent with the fact that there is no change in wet-bulb temperature.

Figures 5-11 and 5-12 are time series of surface and root zone soil saturation for July 1988 and 1993 extreme simulations over Illinois. The surface zone soil saturation for the wet and dry runs converge after 20 days at around 50%. According to Figure 2-2, this value is probably slightly high for the 1988 simulation and slightly low for the 1993 simulation. The soil saturation in the root zone stabilizes at 30% for the dry runs and 65% for the wet runs. Table 3.2 and Figure 4-2 indicate that Illinois is predominantly crop/farm land and has a rooting depth of one meter. Observations over Illinois indicate that the soil saturation at one meter for summer months ranges from 70% to 85%. The root zone soil saturation for the extreme wet simulations (initialized 90%) for 1993 does not compare with observations over Illinois in that it was excessively dry. Soil saturation for this simulation should have remained above 85%. The predictions of the soil saturation for the dry simulations, as well as the

1988 wet simulation are comparable to observations.

The contrasts in soil moisture-precipitation sensitivities between the two convective parameterizations raise many questions about the results of previous numerical modeling studies. The two different convection schemes give us two opposite conclusions. The conclusion from the simulations using the KUO scheme is that soil moisture played an important role in the drought of 1988 and the flood of 1993. In contrast, the results of the GCC simulations lead one to believe that the drought and flood were a result of large-scale forcings. It appears the KUO scheme places more emphasis on moisture while the GCC scheme places more emphasis on heating. More will be said on this in Chapter 6 (Conclusions and Future Research).

5.3 Reasonable versus Extreme Initial Soil Moisture

The initialization of soil moisture in models is very important for an accurate representation of the land surface energy and water balance. As mentioned earlier, most soil moisture sensitivity studies have been initialized using extreme soil moisture initial conditions that are never observed nature. Soil moisture in these studies is initialized not unlike those of Section 5.2. In this section, we attempt to assess the impact of initializing soil moisture at extreme values by comparing the results of the simulations in Section 5.2 to simulations initialized with more reasonable values of soil moisture. A list of these simulations can be found in Table 4.3 (Chapter 4). Figures 5-13 and 5-14 show the sensitivity of precipitation to reasonable changes in soil moisture and Table 5.5 displays summarized results for the Midwest region.

When comparing the results using the reasonable soil moisture initial conditions, we see that the feedback between soil moisture and precipitation weakens significantly. The same pattern is seen when looking at other soil moisture feedbacks such as temperature and humidity. Hence, the magnitude of the initial soil moisture difference does play a large role in the sensitivity of precipitation to soil moisture.

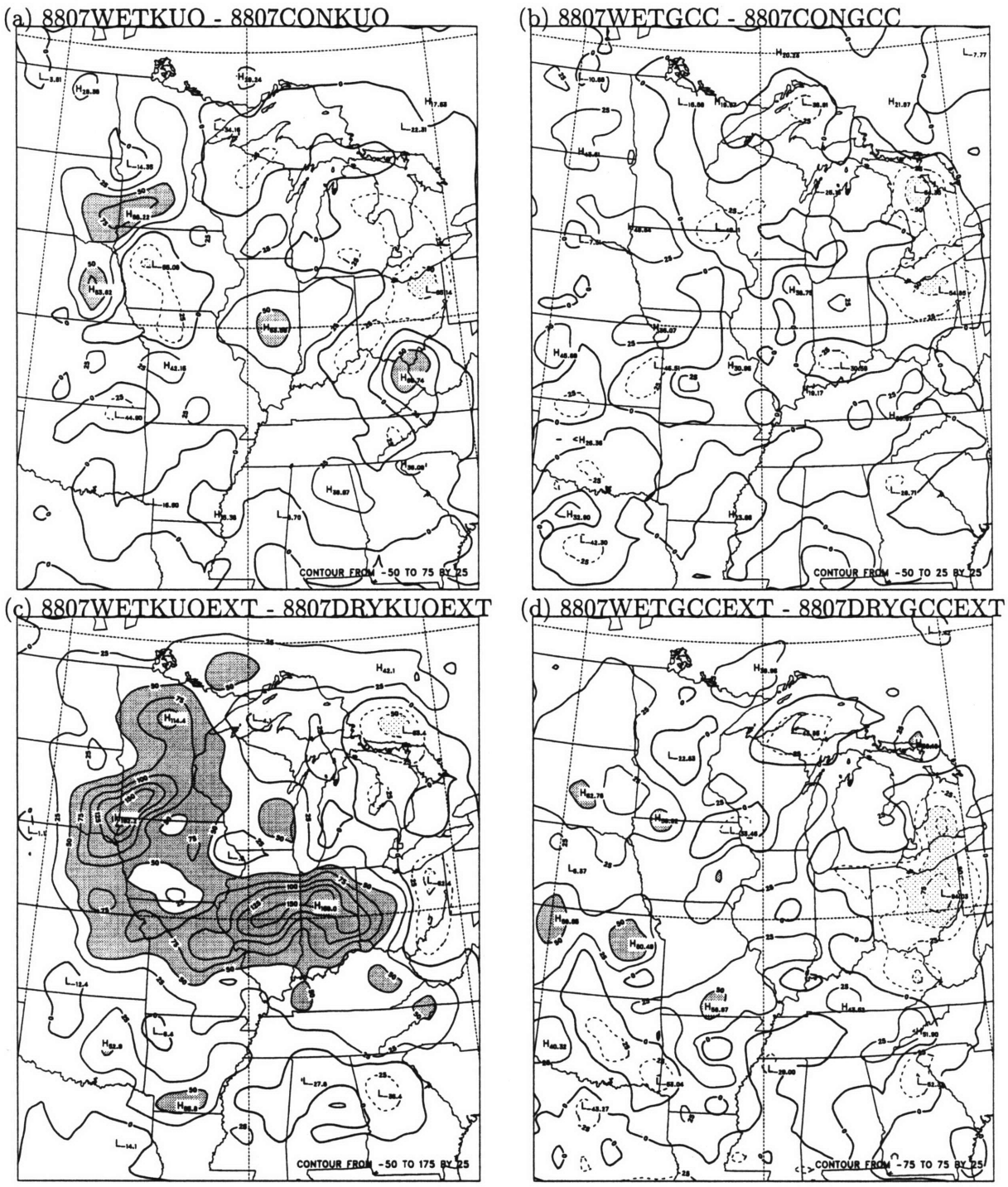

Figure 5-13: Sensitivity of precipitation to extreme and reasonable changes in soil moisture. (a) 8807WETKUO - 8807CONKUO; (b) 8807WETGCC - 8807CONGCC; (c) 8807WETKUOEXT - 8807DRYKUOEXT; and (d) 8807WETGCCEXT - 8807DRYGCCEXT. Units are in millimeters, contour interval is 25 mm., dark shading denotes values in excess of 50 mm., and light shading denotes values less than 50 mm.

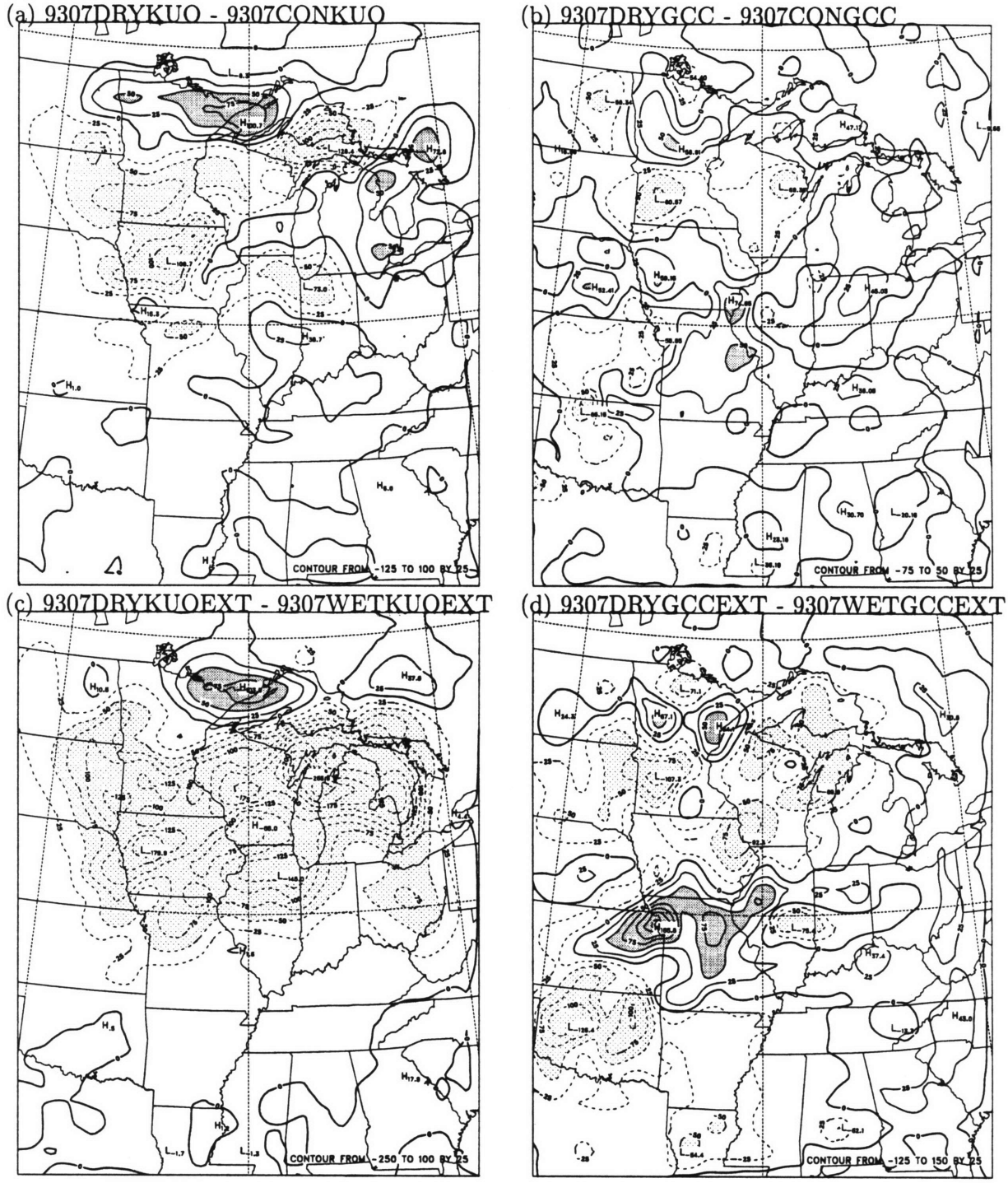

Figure 5-14: Sensitivity of precipitation to extreme and reasonable changes in soil moisture. (a) 9307DRYKUO - 9307CONKUO; (b) 9307DRYGCC - 9307CONGCC; (c) 9307DRYKUOEXT - 9307WETKUOEXT; and (d) 9307DRYGCCEXT - 9307WETGCCEXT. Units are in millimeters, contour interval is 25 mm., dark shading denotes values in excess of 50 mm., and light shading denotes values less than 50 mm.

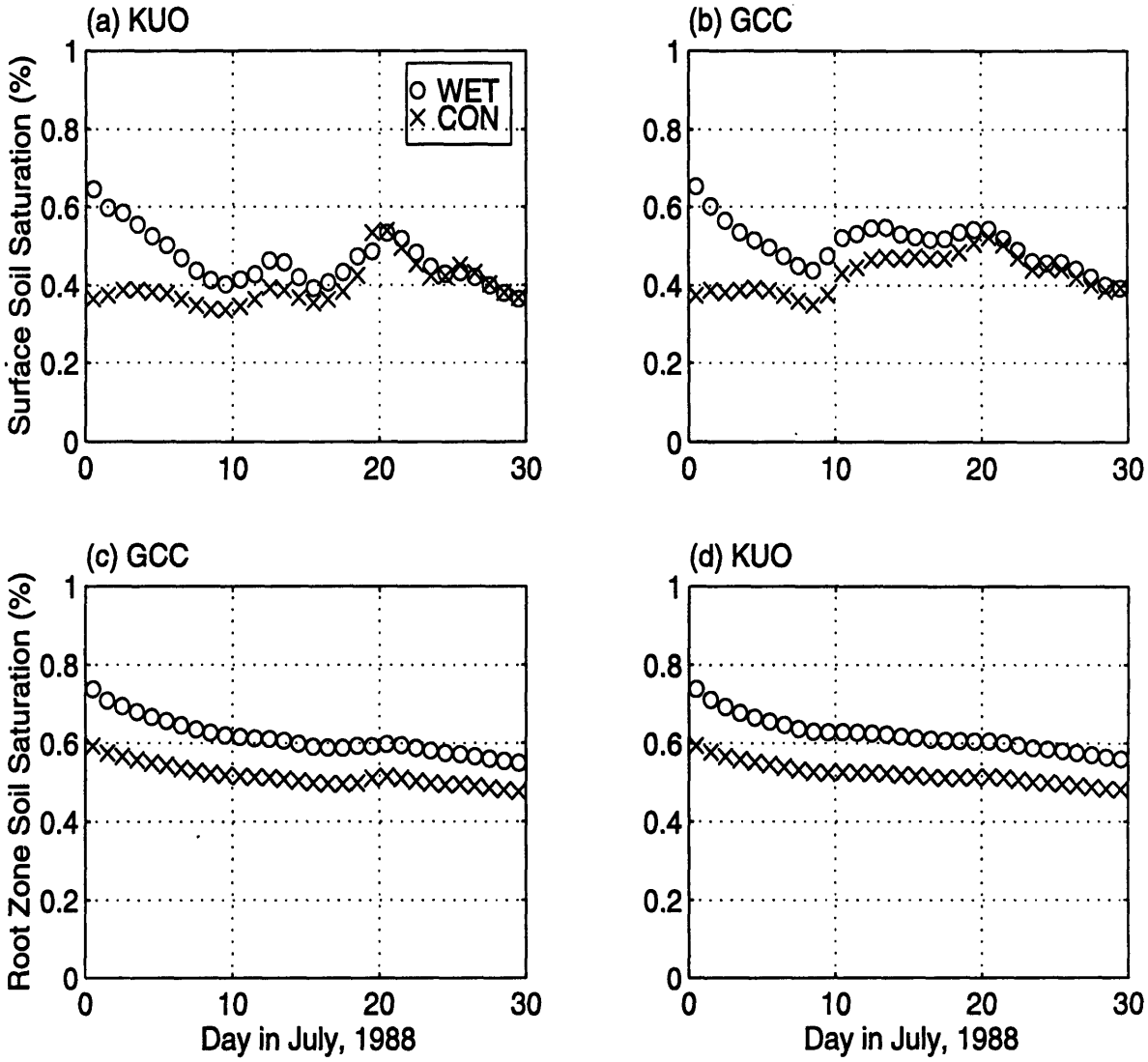

Figure 5-15: Surface and root zone soil saturation (%) daily time series for the reasonable soil moisture initializations for July 1988. (a) Surface zone (8807KUO); (b) Surface zone (8807GCC); (c) Root zone (8807KUO); and (d) Root Zone (8807GCC).

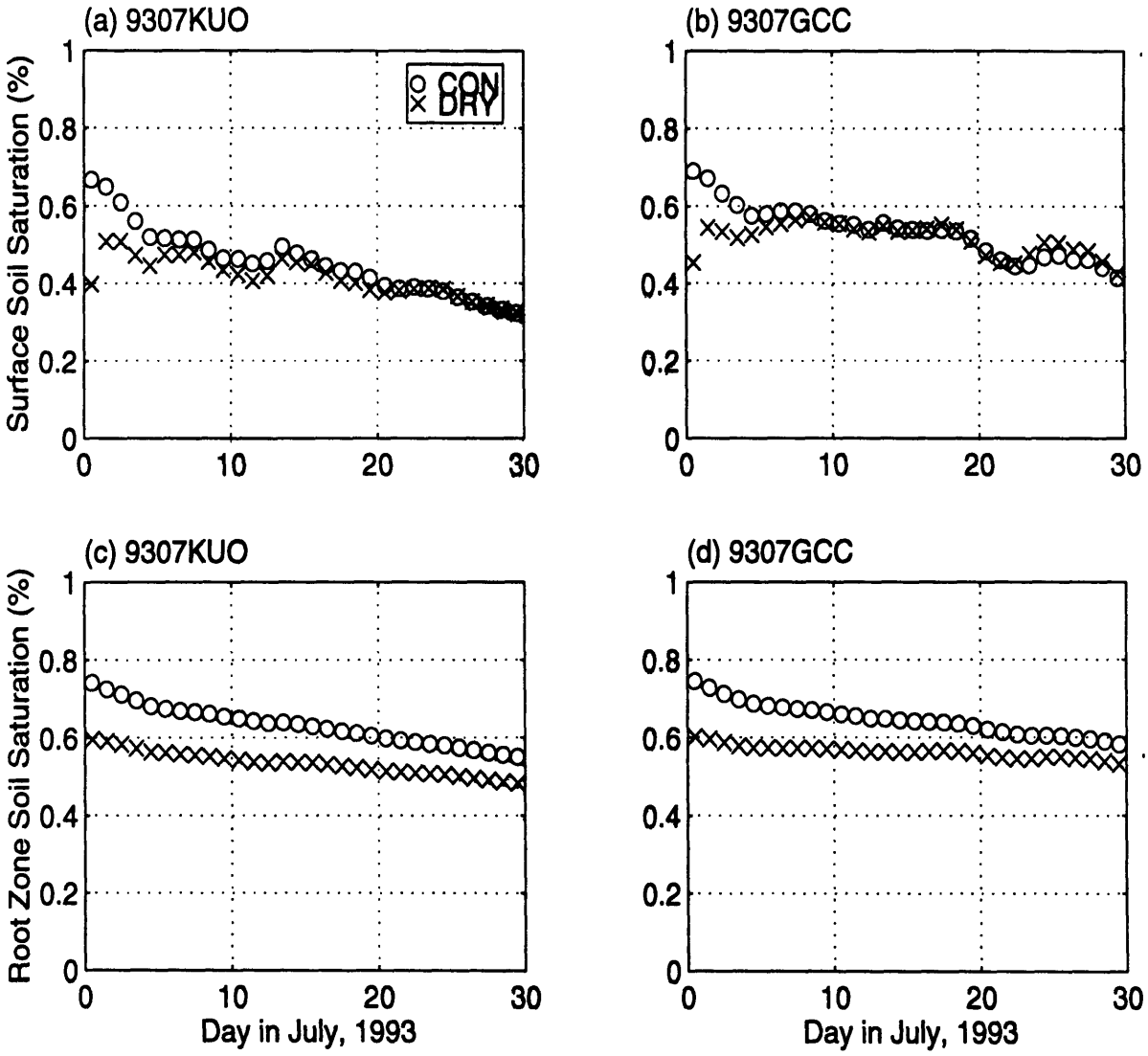

Figure 5-16: Surface and root zone soil saturation (%) daily time series for the extreme soil moisture initializations for July 1993. (a) Surface zone (9307KUO); (b) Surface zone (9307GCC); (c) Root zone (9307KUO); and (d) Root Zone (9307GCC).

Table 5.5: 30-day mean mixing ratio Q (g/kg), temperature T (C), and wet-bulb temperature Tw (C) at 1,000 millibars and precipitation *ppt* (mm) of the control and perturbed and extreme simulations for the Midwest region.

Simulation	Q		T		Tw		ppt	
	Cont	Pert	Cont	Pert	Cont	Pert	Cont	Pert
8807KUO	15.1	16.6	30.6	29.3	22.9	23.5	72.0	86.6
8807KUOEXT	12.4	17.3	32.8	28.5	21.7	23.8	44.4	100.2
8807GCC	14.5	15.2	26.1	24.2	21.4	21.4	89.3	93.1
8807GCCEXT	13.2	15.4	28.5	23.7	21.1	21.4	78.6	98.8
9307KUO	16.3	15.0	30.7	31.9	23.8	23.3	105.8	82.9
9307KUOEXT	17.1	12.9	30.1	33.2	24.2	22.2	118.8	57.4
9307GCC	16.0	15.9	25.0	25.4	22.2	22.3	196.0	194.4
9307GCCEXT	16.1	15.4	24.7	26.6	22.2	22.2	191.2	182.1

The significant increase in precipitation, during July 1988 in the case of the simulations using the KUO scheme, due to extreme changes in soil moisture, is not exhibited from reasonable changes. Small peaks over eastern South Dakota and southern Minnesota, Illinois, and eastern Kentucky contributed additional precipitation to the Midwest region. However, Iowa and Ohio suffered from a decrease in precipitation, reducing this increase. Similarly, mixing ratio, temperature, and wet-bulb temperature at 1,000 millibars over the Midwest all responded less to the reasonable soil moisture initializations (Table 5.5). Hence, there is only a 20% increase in rainfall as opposed to a 125% increase displayed with the extreme soil moisture initializations.

Simulations using the GCC parameterization, also showed a significant decrease in sensitivity to reasonable soil moisture initial conditions. No portion of the domain displayed a significant increase in precipitation (Figure 5-13). Ohio, however, displayed a weakly significant decrease. The Midwest precipitation sensitivity decreased from 25% to 4% as a result of reasonable soil moisture values (Table 5.5). The lack of significant increase in precipitation with reasonable soil moisture is consistent with the fact that there was no change in wet-bulb temperature.

The precipitation sensitivity over the Midwest region of the July 1993 simulations

employing the KUO scheme decreased from 50% to 20% when using reasonable soil moisture initial conditions (Table 5.5). Although this is a large decrease in sensitivity, precipitation in the Midwest is significantly sensitive to reasonable changes in soil moisture. Similarly, the feedback between mixing ratio and temperature weakens when the model is initialized with reasonable soil moisture values.

The GCC scheme, in July 1993, exhibited very little change in rainfall for the entire domain and the Midwest region with reasonable changes in soil moisture (Figure 5-14 and Table 5.5). Similarly, little change was observed in mixing ratio, temperature, and wet-bulb temperature over the Midwest region. The initialization with reasonable soil moisture values further weakened the already weak soil moisture - precipitation feedback from 5% to less than 1%.

Figures 5-15 and 5-16 are time series of surface and root zone soil saturation for July 1988 and 1993 simulations over Illinois. In July 1988, after one day of simulation, the surface zone soil saturation for the control run climbs from 25% to 40% for both convection schemes. Soil saturation, in the surface zone, however, was observed at approximately 25% for the entire month over Illinois (Figure 2-2). Some of the excessive moisture may be due to both schemes slightly overestimating precipitation over Illinois. However, this can not account for the entire difference. The root zone soil saturation for both convection schemes displays a decreasing trend throughout the entire simulation. However, soil saturation for the control simulation should be maintained at observed values (approximately 60% to 65%; Figure 2-2). Even with excessive rainfall simulated over this region, the root zone soil moisture dries too quickly. The 1993 simulations display a similar pattern to 1988. Soil saturation in the surface zone dries from 70% to 50% after only a few days. However, Figure 2-2 indicates that the soil saturation should remain above 60% for the entire simulation. The root zone saturation displayed a decreasing trend throughout the entire simulation. The wet simulation should have remained fairly constant at around 75% (Figure 2-2). The root zone soil saturation for all the simulations is too dry and the surface zone soil saturation is too high for 1988 and too low for 1993.

The above results show that the sensitivity of soil moisture to precipitation

is clearly responsive to the magnitude of the soil moisture anomaly. The KUO scheme, even with reasonable soil moisture changes, displays a significant precipitation feedback. Precipitation from the GCC scheme is also sensitive to the magnitude of the soil moisture anomaly. However, the sensitivity only played a role in July 1988, since July 1993 did not exhibit significant precipitation sensitivity with extreme soil moisture anomalies.

5.4 Soil Moisture and Time of Year

As mentioned in Subsection 1.2.1, Findell and Eltahir (1997) found, using the ISWS soil moisture data, that the feedback between soil moisture and precipitation is strongest in June and July. Hence, we should expect the July simulations to show a greater sensitivity to soil moisture than the May and September simulations. Figures 5-17, 5-13, 5-14 and 5-18 display the sensitivity of reasonable initial soil moisture conditions to precipitation as a function of the time of year given a convective parameterization.

Neither scheme exhibits a great deal of sensitivity to reasonable anomalies in soil moisture during May and September of both years. The KUO parameterization shows that the soil moisture - precipitation feedback is strong in the mid-summer and weak in the late spring and early fall. These results are consistent with the work of Findell and Eltahir (1997). Hence, the timing of the soil moisture anomaly is important in the initiation and maintenance of droughts and floods. A detailed discussion of these results will follow in Chapter 6.

5.5 Model Sensitivity to Boundary Condition Resolution

This section investigates if the spatial and temporal resolution of the boundary conditions improve the results of the control simulations. The purpose for doing this to find out if the resolution of the boundary conditions is the main cause of the

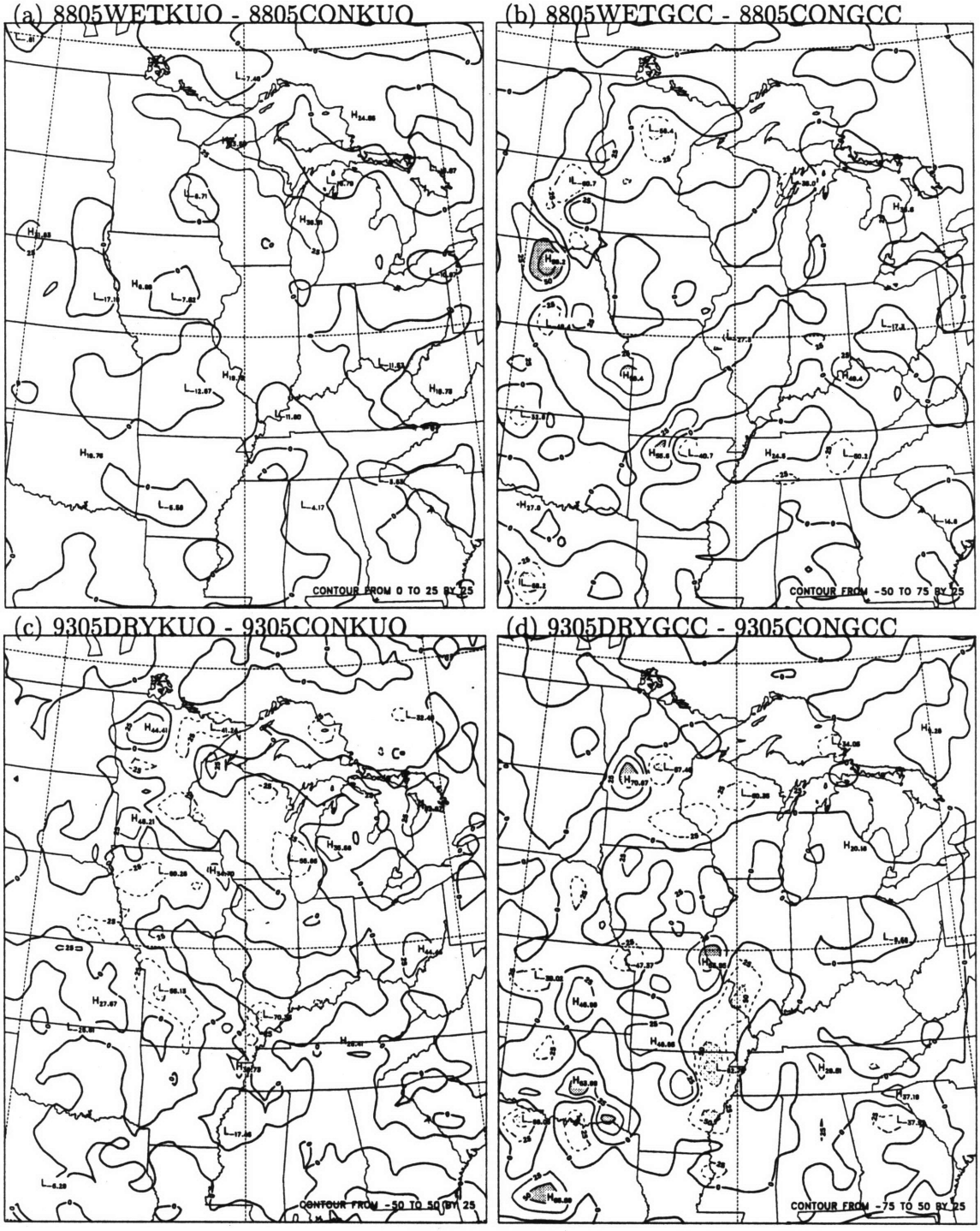

Figure 5-17: Sensitivity of precipitation to the timing of soil moisture anomaly. (a) 8805WETKUO - 8805CONKUO; (b) 8805WETGCC - 8805CONGCC; (c) 9305DRYKUO - 9305CONKUO; and (d) 9305DRYGCC - 9305CONGCC. Units are in millimeters, contour interval is 25 mm., dark shading denotes values in excess of 50 mm., and light shading denotes values less than 50 mm.

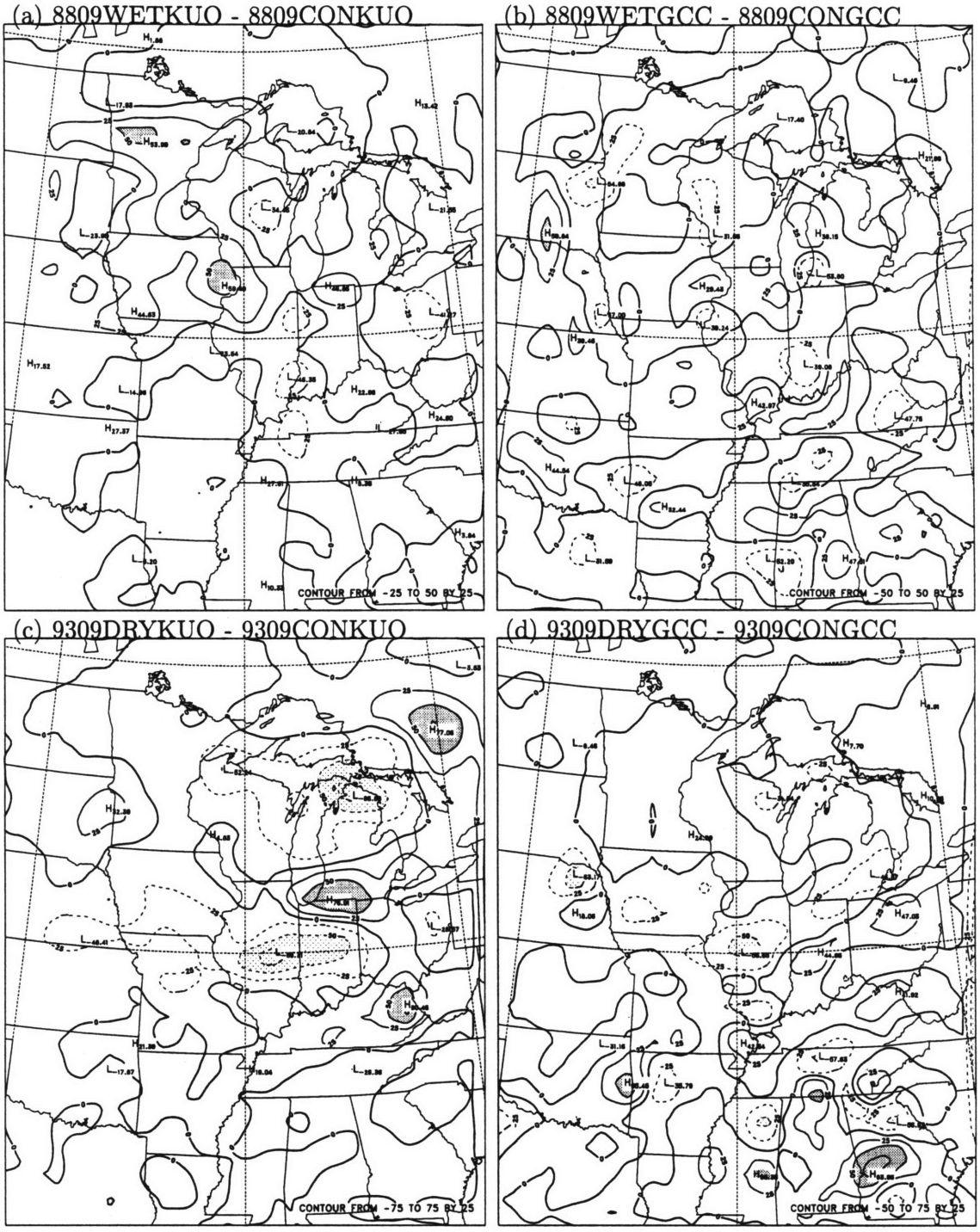

Figure 5-18: Sensitivity of precipitation to extreme changes in soil moisture. (a) 8809WETKUO - 8809CONKUO; (b) 8809WETGCC - 8809CONGCC; (c) 9309DRYKUO - 9309CONKUO; and (d) 9309DRYGCC - 9309CONGCC. Units are in millimeters, contour interval is 25 mm., dark shading denotes values in excess of 50 mm., and light shading denotes values less than 50 mm.

Table 5.6: 30-day mean mixing ratio, Q (g/kg), temperature, T (C), and wet-bulb temperature, Tw (C) at 1,000 millibars and precipitation, *ppt* (mm) of the control and perturbed simulations for the Midwest region.

Simulation	Q		T		Tw		ppt	
	Cont	Pert	Cont	Pert	Cont	Pert	Cont	Pert
8805KUO	8.9	9.2	22.5	21.7	15.8	15.9	47.3	52.4
8807KUO	15.1	16.6	30.6	29.3	22.9	23.5	72.0	86.6
8809KUO	13.4	13.6	22.7	22.0	19.5	19.4	99.4	106.3
8805GCC	9.2	9.4	20.9	20.3	15.6	15.6	73.0	78.9
8807GCC	14.5	15.2	26.1	24.2	21.4	21.4	89.3	93.1
8809GCC	12.5	12.7	20.9	20.4	18.3	18.3	88.9	92.4
9305KUO	10.7	10.4	20.9	21.2	16.7	16.6	120.3	114.8
9307KUO	16.3	15.0	30.7	31.9	23.8	23.3	105.8	82.9
9309KUO	11.7	11.7	19.8	20.7	17.0	17.3	101.3	91.8
9305GCC	10.4	10.4	19.4	19.7	16.1	16.2	101.1	100.7
9307GCC	16.0	15.9	25.0	25.4	22.2	22.3	196.0	194.4
9309GCC	11.3	11.2	18.6	19.4	16.4	16.6	93.7	89.9

poor simulation of precipitation.

Figure 5-19 shows observed precipitation and precipitation for the control (8807CONKUO) and the increased resolution boundary conditions (8807CONKUOT106) simulations. The increase in boundary conditions resolution weakened the primary precipitation system for the July 1988 simulations using the KUO scheme. This weakening improved the spatial distribution of rainfall in that it weakened a system that was exaggerated with the standard resolution boundary conditions. However, the total rainfall volume significantly decreased over the entire domain leaving only a small area of rainfall south of the Great Lakes region.

For the July 1988 (Figure 5-20) simulations using the GCC scheme, the increase boundary condition resolutions plays a minor role in the improvement or change the spatial distribution of precipitation. Signs of improvement are observed in that the model, with the high resolution boundary conditions, begins to capture the band of precipitation from Louisiana across to Ohio. However, it still simulates excessive precipitation in the western portion of the domain where little is observed.

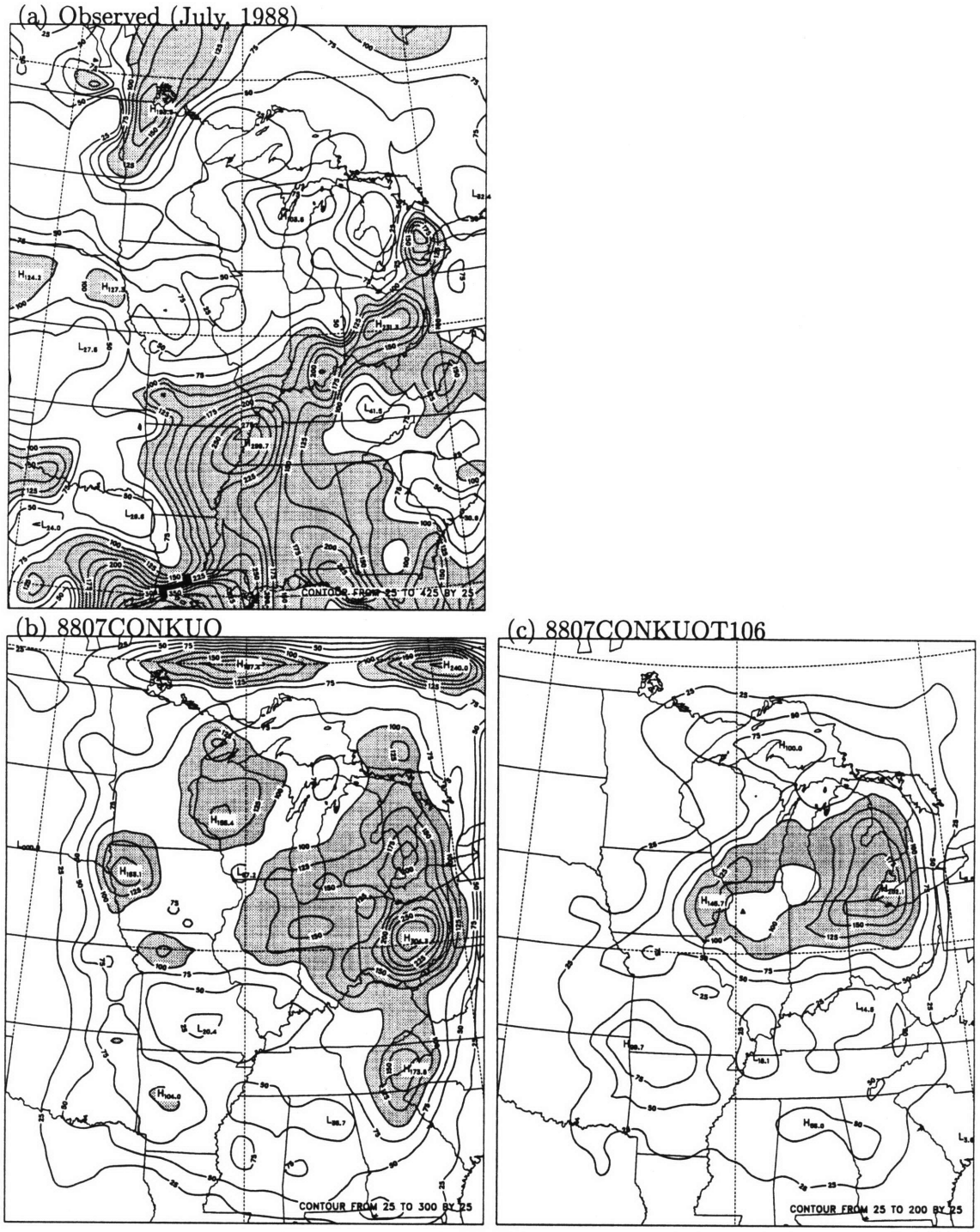

Figure 5-19: Sensitivity of precipitation to boundary condition resolution. (a) Observed (July, 1988); (b) 8807CONKUO; and (c) 8807CONKUOT106; Units are in millimeters, contour interval is 25 mm., and dark shading denotes values in excess of 100 mm.

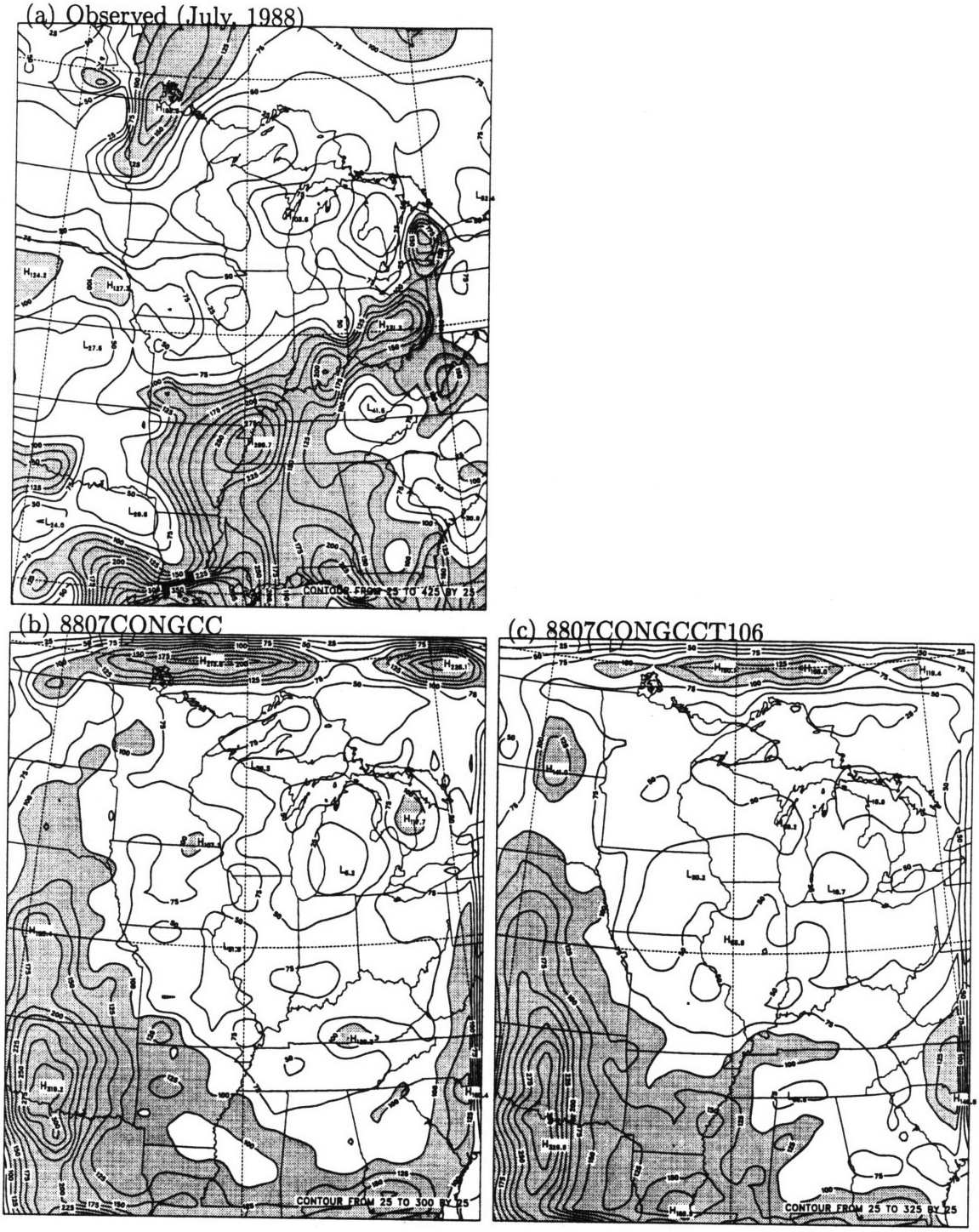

Figure 5-20: Sensitivity of precipitation to boundary condition resolution. (a) Observed (July, 1988); (b) 8807CONGCC; and (c) 8807CONGCCT106; Units are in millimeters, contour interval is 25 mm., and dark shading denotes values in excess of 100 mm.

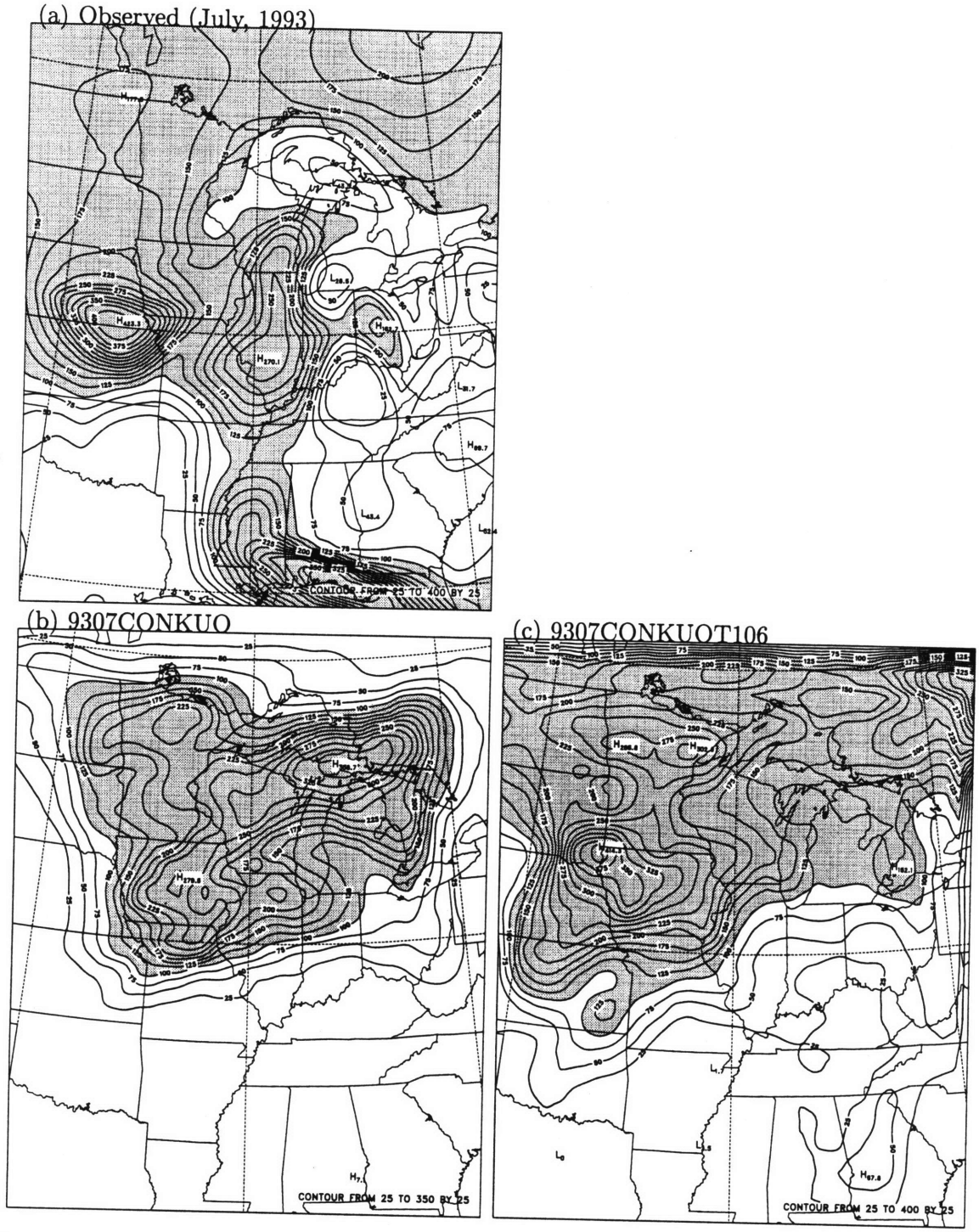

Figure 5-21: Sensitivity of precipitation to boundary condition resolution. (a) Observed (July, 1993); (b) 9307CONKUO; and (c) 9307CONKUOT106; Units are in millimeters, contour interval is 25 mm., and dark shading denotes values in excess of 100 mm.

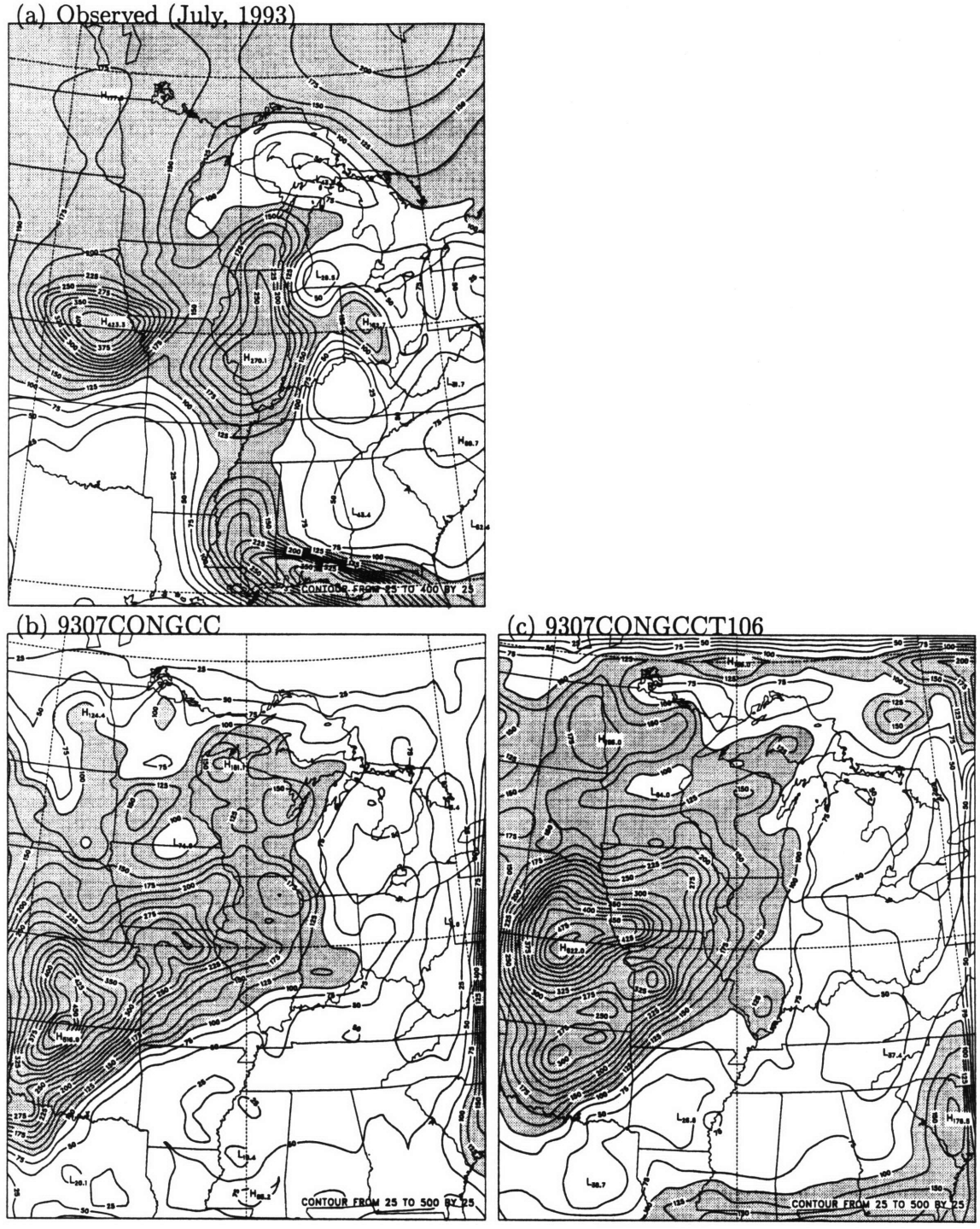

Figure 5-22: Sensitivity of precipitation to boundary condition resolution. (a) Observed (July, 1993); (b) 9307CONGCC; and (c) 9307CONGCCT106; Units are in millimeters, contour interval is 25 mm., and dark shading denotes values in excess of 100 mm.

In July 1993 (Figure 5-21), the spatial distribution of precipitation, using the KUO scheme, slightly improves from the increase in boundary condition resolution. The improved resolution increased rainfall over Canada where it was lacking using the standard resolution. In addition, the observed peak over Kansas and Nebraska was simulated with the high resolution boundary conditions.

Figure 5-22 shows that, similar to 1988, the improved boundary conditions had a weak effect on the rainfall distribution for July 1993. The only notable differences are the improved simulation of northern precipitation and of the location of the peak over Kansas and Nebraska.

Overall the improved resolution boundary condition simulations play only a minor role in the improvement of spatial distribution of July rainfall. Although minor improvements were observed, this did not come close to resolving the difficulty in simulating July precipitation accurately.

5.6 Model Sensitivity to KUO Scheme Parameters

This subsection investigates the role of two of the KUO scheme's parameters in how they affect the distribution and volume of precipitation. Figures 5-23 and 5-24 display precipitation for the control, critical negative area in the sounding reduction, and b factor reduction simulations as well as the observed precipitation.

For July of 1988, the changes in KUO scheme parameters have little effect on overall simulation of precipitation. As expected, the decrease in negative area threshold latitudinally lowers the precipitation center thus slightly improving the simulation of southern precipitation. It does not, however, improve the simulation of precipitation over the rest of the domain. Similarly, the reduction in the KUO scheme's b factor lowers the precipitation center. In addition, the reduction increases the overall precipitation closer to the observed value.

In July of 1993, the critical negative area reduction concentrated all of the

precipitation into a smaller area. This concentration does not seem to influence the overall results. Similarly, the b factor reduction does not significantly change the results of the simulation. It did, however, bring the domain total simulated precipitation near the observed value.

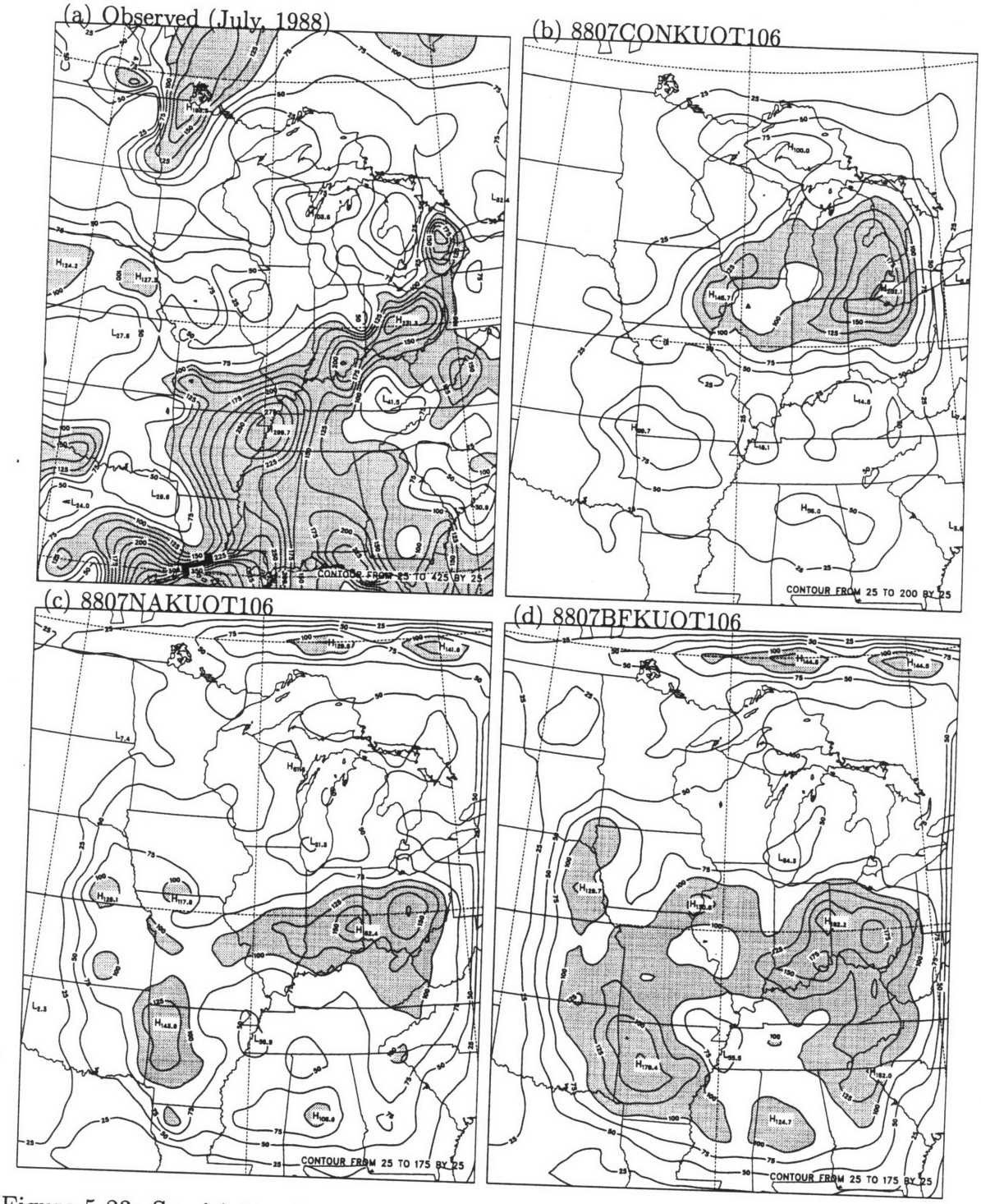

Figure 5-23: Sensitivity of precipitation to KUO Scheme Parameters. (a) Observed (July, 1988); (b) 8807CONKUOT106; (c) 8807NAKUOT106 (Reduced negative area threshold); and (d) 8807BFKUOT106 (Reduced *b*). Units are in millimeters, contour interval is 25 mm., and dark shading denotes values in excess of 100 mm.

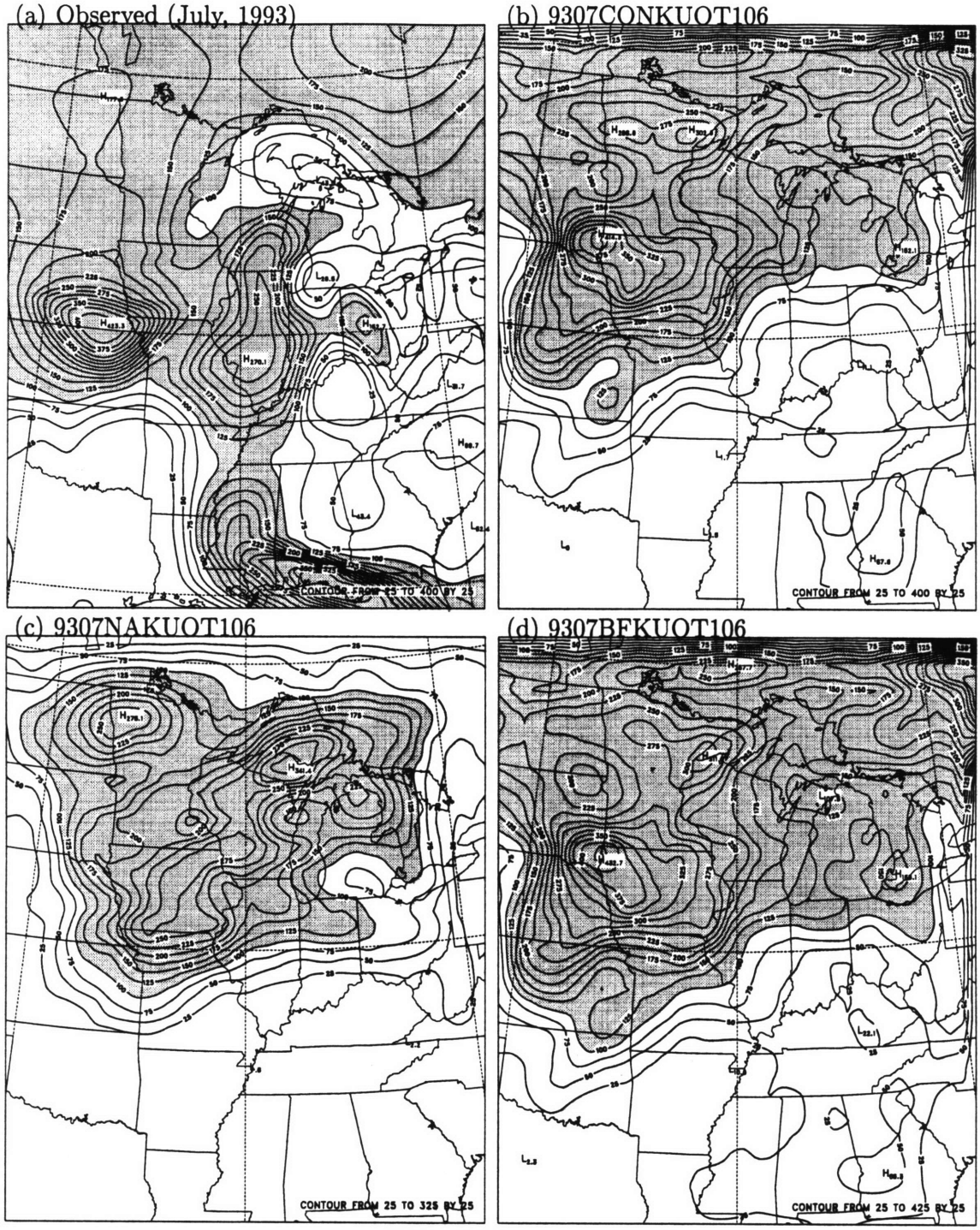

Figure 5-24: Sensitivity of precipitation to KUO Scheme Parameters. (a) Observed (July, 1993); (b) 9307CONKUOT106; (c) 9307NAKUOT106 (Reduced Negative area threshold); and (d) 9307BFKUOT106 (Reduced b). Units are in millimeters, contour interval is 25 mm., and dark shading denotes values in excess of 100 mm.

Chapter 6

Conclusions and Future Research

6.1 Conclusions

Several questions were addressed in this thesis: Were the extreme hydrologic events of 1988 and 1993 initiated and maintained by external forcings or were they due to internal mechanisms such as soil moisture? What role does the magnitude of the soil moisture anomaly play? Does the timing of the soil moisture anomaly affect the onset of such events? How does choice of the convective parameterization affect the results of numerical modeling studies of each event? And how does the spatial and temporal resolution of the boundary conditions affect these results of the RCM simulations?

In this study, we have attempted to understand the role that soil moisture played in the drought of 1988 and the flood of 1993 using a regional climate model (RegCM2). We initialized simulations with different magnitudes of soil moisture to develop an understanding of the magnitude of anomaly required to initiate and/or maintain such events. Additional simulations were performed with different initialization dates to see how the timing of the soil moisture anomaly affected the simulated climate. Furthermore, we used two different convective parameterizations (KUO and GCC) to determine whether the sensitivity of soil moisture to precipitation is influenced by these schemes.

Overall, regardless of the convection scheme used, the model does an adequate job in simulating the spatial patterns of precipitation in May and September of

both years. However, in July, when convective activity in mid-latitudes is at a maximum, both convective parameterizations do an unsatisfactory job of simulating the spatial distributions of rainfall. In addition, soil moisture in the surface and root soil layers do not match observations. More specifically, the surface layer, regardless of the simulation, seems to fluctuate around 40% and the root layer dries to values significantly lower than observed. In summary, some caution needs to be taken in interpreting the results and conclusions, especially for July.

Additional experiments were performed to see if the reason for the poor simulation of precipitation had to do with the resolution of the boundary conditions. We found that increasing the spatial resolution from 2.5 to 1.125 degrees and increasing the temporal resolution from 12 to 6 hours did not significantly improve the simulation of July precipitation.

Simulations using the KUO scheme tended to undersimulate precipitation in the southern portion of the domain and slightly overestimate it in the northern portion. A set of simulations were performed to see if lowering the KUO scheme's critical negative area of the sounding would cause the low-level jet that travels from the Gulf of Mexico north into the Midwest to trigger convection earlier so that moisture would precipitate out earlier. In July 1988, the reduced critical negative area of the sounding latitudinally lowered the primary area of precipitation but it did not come close to simulating southern precipitation adequately. In July 1993, the reduction concentrated and intensified the primary precipitation area. It did not, however, seem to improve the results. Another set of experiments were performed by lowering the KUO scheme's column moistening fraction, b. The effect of lowering b in July 1988 caused the northern precipitation center to broaden and shift south. For 1993, it simply intensified the precipitation areas. Overall, changing the b factor did not significantly improve the July results.

In conclusion, neither improving the boundary condition resolution nor adjusting some of the KUO scheme's parameters significantly improved the simulation of precipitation. Hence, other factors must be causing the poor spatial distribution of precipitation. Potential culprits are quality of the ECMWF boundary conditions,

the soil-vegetation hydrological process scheme (BATS), the convective and cloud parameterizations, and/or other inadequacies in the RegCM2. Clearly, more work needs to be done in the area of improving the simulation of precipitation and other surface fields. Once this is done, more credibility can be placed on the results of numerical modeling studies.

The accurate initialization of soil moisture in models is very important for an accurate representation of the land surface energy and water balance. As mentioned in Chapter 4.3.2, most soil moisture sensitivity studies using climate models have been initialized using extreme soil moisture initial conditions that are not consistent with observations even in the most anomalous years. Here we assess the impact of initializing soil moisture at extreme values by comparing simulations initialized at values similar to those observed in nature to simulations initialized at extreme values. We found that the simulated feedback between soil moisture and precipitation is dependent on the convective parameterization used. The KUO scheme is highly sensitive to extreme changes in soil moisture while the GCC scheme is moderately sensitive in 1988 and not sensitive in 1993. The feedback significantly weakens when using reasonable soil moisture initial conditions. The same pattern is seen when looking at other soil moisture feedbacks such as those involving temperature, humidity, and wet-bulb temperature. Hence, the magnitude of the soil moisture anomaly does play a significant role in the sensitivity of precipitation and other surface fields to soil moisture.

The two convective parameterizations give significantly different results. The KUO scheme shows a significant sensitivity of soil moisture to both total and convective precipitation; the additional moisture present from the wet simulations seems to enhance convection. Based on these results, soil moisture does play a major role in the persistence of the drought of 1988 and the flood of 1993. On the other hand, the GCC convective scheme shows little sensitivity, if any, of total precipitation to extreme changes in soil moisture. There is, however, a negative feedback between soil moisture and convective precipitation. This negative feedback is probably due to the increased sensible heat (buoyancy) that results from dry soil moisture and tends

to trigger more convection in the buoyancy sensitive GCC parameterization (Giorgi et al. 1996). This negative feedback, however, is countered by positive feedback of non-convective precipitation to soil moisture yielding a slightly positive feedback in total precipitation. Therefore, it would be safe to conclude that for the GCC simulations, the persistence of the drought of 1988 and the flood of 1993 were primarily a result of large-scale circulation anomalies. Based on these contrasting conclusions, it is evident that more effort needs to go into the developing and testing of convective parameterizations.

Each convective parameterization impacts surface fields differently. The KUO scheme seems to place more emphasis on moisture while the GCC scheme seems to place more emphasis on heating. In other words, soil moisture changes, when using the KUO scheme, affect humidity more than temperature. On the other hand, changes in soil moisture in GCC scheme impact temperature more than humidity. Eltahir and Pal (1996) showed that increased wet-bulb temperature, a measure of moist static energy, increases the frequency and magnitude of rainfall events in convective regimes such as the Midwest during the summer. Wet-bulb temperature is more sensitive to humidity than temperature. Hence, precipitation simulated by the model using the KUO scheme shows a greater sensitivity to soil moisture than the GCC scheme since the wet-bulb temperature is more sensitive in the KUO scheme. We found that the change in rainfall resulting from changes in soil moisture were strongly a function of wet-bulb temperature as suggested by Eltahir and Pal (1996).

The contrasting differences in soil moisture-precipitation sensitivities between the two convective parameterizations raises many questions about the results of previous numerical modeling studies. Most of these previous studies have employed the KUO parameterization. Hence, they have concluded that there is a strong positive feedback between soil moisture and precipitation. The differences in rainfall response to soil moisture can be attributed to the physical nature of each scheme. As mentioned in Subsection 3.4.1, the KUO scheme partitions the moisture convergence into a fraction that moistens the column (bM) and a fraction that precipitates ($(1-b)M$). None of the falling rainwater is allowed to reevaporate and cool the column. Therefore, an

increase in soil moisture (evapotranspiration) and, hence, the moisture convergence will result in an increase in precipitation. On the other hand, the GCC scheme allows for falling rainwater to reevaporate (see Subsection 3.4.2). Therefore, a reduction in the temperature of the sounding occurs (especially at lower levels) when precipitation occurs due to evaporative cooling. In other words, an increase in soil moisture (evapotranspiration) will cause significant cooling of the lower-levels from both the evaporation of soil water and the reevaporation of rainwater. Clearly, wet soil moisture conditions increase latent heat flux and decrease sensible heat flux. But their relative contribution seems to be the deciding factor in how soil moisture affects precipitation. For the KUO scheme, the increase in mixing ratio (latent heat flux) with wet conditions outweighs the decrease in temperature (sensible heat flux). Hence, an increase in net radiation results in an increase in moist static energy, yielding more precipitation. On the other hand, the decrease in temperature with wet conditions plays a more dominant role in the simulations using the GCC scheme. That is, the latent heat flux increase is almost balanced by the sensible heat flux decrease yielding little change in precipitation.

We found that the timing of the soil moisture anomaly is extremely important in simulating the extreme events. May and September simulations showed very little sensitivity to soil moisture while the July simulations showed significant sensitivity. Part of the reason for the lack of sensitivity is that the simulations were initialized with reasonable soil moisture conditions for the given month. For example, soil moisture for the May simulations was initialized at the May 1993 value for the wet run and the May 1988 value for the dry run. However, if the runs were initialized at the values observed in July 1988 and 1993, it is likely that more sensitivity would have been displayed. However, the primary reason for the lack of sensitivity in May and September is due to the fact that there is significantly less convective activity during these months than during July. However, additional simulations need to be performed to determine the relative contribution of these two reasons. In conclusion, given that observed anomalies in mid-spring did not seem to play a role in the onset of the drought and flood, it is unlikely that soil moisture can be solely responsible for the

initiation of such events.

6.2 Future Research

The goal of this study was to develop a more complete understanding of the soil moisture-precipitation feedback. In doing so, however, the study raised additional questions about the numerical models that have been used to study this feedback. It is commonly assumed that the sensitivity of a model represents the sensitivity of the climate system, even when the model does not reproduce the control state. This study demonstrated that the sensitivity of a model can significantly change with the convection scheme used. Therefore, extensive work needs to be performed to improve the simulation of precipitation and the deficiencies of the model. Once this is complete, more confidence can be placed on the conclusions of experiments performed with the model. The primary emphasis should go into the developing and testing of convective parameterizations. Additional improvement may also be required for the land process hydrologic and planetary boundary layer schemes.

There are numerous experiments that one can perform over the Midwestern U.S. to investigate the feedback between soil moisture and precipitation. The following is a description of a few experiments that may be useful in exploring this feedback:

This study has focused on the role of soil moisture as a point or spatially uniform source. The strength of the rain-producing mechanisms in the Midwest during the summer may be related to gradients in soil moisture. One possible avenue to explore is how the distribution of soil moisture affects the frequency and intensity of the rainfall events over the Midwest by performing numerical modeling experiments.

Another aspect that should be studied to further develop the understanding the soil moisture-precipitation feedback is to assess the relative importance of soil moisture anomalies and SST anomalies by separating the effects of SST from soil moisture. It is conceivable that extremes in Midwestern precipitation are primarily a result of SST anomalies, implying that soil moisture has no dynamic feedback on rainfall. It is likely, however, that both soil moisture and SST play an important role

in the summertime climate system of the Midwestern U.S. This can be explored by performing numerical modeling experiments and by performing data analyses.

Soil moisture is known to impact both the energy and water budget of the boundary layer. To develop a more theoretical understanding of the feedback between soil moisture and precipitation, numerical simulations can be performed by fixing radiative inputs to the model and perturbing soil moisture. By doing this, the impact of soil moisture on the energy budget can be separated from the water budget.

References

Anthes, R. (1977). A cumulus parameterization scheme utilizing a one-dimensional cloud model., *Monthly Weather Review* **117**: 1423–1438.

Anthes, R., Hsie, E. and Kuo, Y. (1987). Description of the Penn State/NCAR Mesoscale Model Version 4 (MM4)., *Technical Report TN-282+STR*, NCAR, Boulder, Colorado. pp. 66.

Arakawa, A. and Schubert, W. (1974). Interaction of a cumulus cloud ensemble with the large-scale environment, Part I., *Journal of Atmospheric Science* **31**: 674–701.

Atlas, R., Wolfson, N. and Terry, J. (1993). The effect of SST and soil-moisture anomalies on GLA model simulations of the 1988 U.S. summer drought., *Journal of Climate* **6**: 2034–2048.

Beljaars, A., Viterbo, P., Miller, M. and Betts, A. (1996). The anomalous rainfall over the United States during july 1993: Sensitivity to land surface parameterization and soil moisture anomalies., *Monthly Weather Review* **124**: 362–383.

Bell, G. and Janowiak, J. (1995). Atmospheric circulation associated with the Midwest floods of 1993, *Bulletin of the American Meteorological Society* **76(5)**: 681–695.

Bengtsson, L., Kanamitsu, M., Kallberg, P. and Uppala, S. (1982). FGGE 4-dimensional data assimilation at ECMWF., *Bulleten of the American Meteorogical Society* **63**: 29–43.

Betts, A., Ball, J., Beljaars, A., Miller, J. and Viterbo, P. (1996). The land surface-atmosphere interaction: A review based on observational and global modeling perspectives., *Journal of Geophysical Research* **101**: 7209–7225.

Castelli, F. and Rodriguez-Iturbe, I. (1996). On the dynamical coupling of large-scale spatial patterns of rainfall and soil moisture., *Tellus. Series A* **48A(2)**: 290–311.

Davies, H. and Turner, R. (1977). Updating prediction models by dynamical relaxation: An examination of the technique., *Quarterly Journal of the Royal Meteorlogical Society* **102**: 181–191.

Dickinson, R., Kennedy, P., Henderson-Sellers, A. and Wilson, M. (1986). Biosphere-Atmosphere Transfer Scheme (BATS) version 1E as coupled to the NCAR Community Climate Model., *Technical Report TN-275+STR*, NCAR, Boulder, Colorado. pp. 72.

Dirmeyer, P. (1995). Meeting on problems in initializing soil wetness: Review., *Technical Report Report No. 9*, COLA, Calverton, Maryland. pp. 33.

Dooge, J. (1988). Hydrology in perspective., *Hydrological Sciences Journal* **33(1)**: 61–85.

Eagleson, P. (1994). The evolution of modern hydrology (from watershed to continent in 30 years)., *Advances in Water Resources* **10(8)**: 1–16.

Eltahir, E. (1997). A soil moisture-rainfall feedback mechanism: 1. theory and observations., *Water Resources Research* **Submitted for Publication.**

Eltahir, E. and Pal, J. (1996). Relationship between surface conditions and subsequent rainfall in convective storms., *Journal Geopyhisical Research* **101**: 26,237–26,245.

Entekhabi, D., Rodriguez-Iturbe, I. and Bras, R. (1992). Variability in large-scale water balance with land surface-atmosphere interaction., *Journal of Climate* **5**: 798–813.

Entekhabi, D., Rodriguez-Iturbe, I. and Castelli, F. (1996). Mutual interaction of soil moisture state and atmospheric processes, *Journal of Hydrology* **184**: 3–17.

Findell, K. (1997). *On the role of soil moisture in floods and droughts in summer over the Mississippi basin*, Master's thesis, Massachusetts Institute of Technology.

Findell, K. and Eltahir, E. (1997). An analysis of the relationship between spring soil moisture and summer rainfall, based on direct observations from Illinois., *Water Resources Research* **33(4)**: 725–735.

Giorgi, F. (1991). Sensitivity of simulated summertime precipitation over the western United States to physics parameterizations., *Monthly Weather Review* **119**: 2870–2888.

Giorgi, F. and Bates, G. (1989). The climatological skill of a regional climate model over complex terrain., *Monthly Weather Review* **117**: 2325–2347.

Giorgi, F. and Marinucci, M. (1991). Validation of a regional atmospheric model over Europe: Sensitivity of wintertime and summertime simulations to selected physics parameterizations and lower boundary conditions., *Quarterly Journal of the Royal Meteorlogical Society* **117**: 1171–1206.

Giorgi, F., Marinucci, M. and Bates, G. (1993). Development of a Second-Generation Regional Climate Model (RegCM2). part I: Boundary-layer and radiative transfer processes., *Monthly Weather Review* **121**: 2794–2813.

Giorgi, F., Marinucci, M., Bates, G. and De Canio, G. (1993). Development of a Second-Generation Regional Climate Model (RegCM2). part II: Convective processes and assimilation of lateral boundary conditions., *Monthly Weather Review* **121**: 2814–2832.

Giorgi, F., Mearns, L., Shields, C. and Mayer, L. (1996). A regional model study of the importance of local versus remote controls of the 1988 drought and the 1993 floods over the central United States., *Journal of Climate* **9**: 1150–1162.

Grell, G. (1993). Prognostic evaluation of assumptions used by cumulus parameterizations., *Monthly Weather Review* **121**: 764–787.

Grell, G., Dudhia, J. and Stauffer, D. (1994). Description of the fifth generation Penn State/NCAR Mesoscale Model (MM5)., *Technical Report TN-398+STR*, NCAR, Boulder, Colorado. pp. 121.

Hollinger, S. and Isard, S. (1994). A soil moisture climatology of Illinois., *Journal of Climate* **4**: 822–833.

Holtslag, A., de Bruijn, E. and Pan, H. (1990). A high resolution air mass transformation model for short-range weather forecasting., *Monthly Weather Review* **118**: 1561–1575.

Huang, J., van den Dool, H. and Georgakakos, K. (1996). Analysis of model-calculated soil moisture over the U.S. (1931-93) and application in long-range temperature forecasts., *Journal of Climate* **9**: 1350–1362.

Kerr, R. (1989). Hansen versus the world on the greenhouse threat., *Science* **244**: 1041–1043.

Kiehl, J., Wolski, R., Briegleb, B. and Ramanathan, V. (1987). Documentation of radiation and cloud routines in the NCAR Community Climate Model (CCM1), *Technical Report TN-288+1A*, NCAR, Boulder, Colorado. pp. 109.

Kunkel, K., Changnon, S. and Angel, J. (1994). Climatic aspects of the 1993 Upper Mississippi River Basin flood., *Bulliten of the American Meteorogical Society* **75**: 811–822.

Madala, R. (1981). *Efficient time integration schemes for atmosphere and ocean models. Finite-Difference Techniques for Vectorized Fluid Dynamics Calculations*, Springer-Verlag. 56-76.

Mayer, T. (1988). Generation of CCM format history tape from analyzed data for selected periods RD2CFM Version 1., *Technical Report TN-322+STR*, NCAR, Boulder, Colorado. pp. 68.

Oglesby, R. (1991). Springtime soil moisture, natural climatic variability, and the North American Drought as simulated by the NCAR Community Climate Model 1., *Journal of Climate* **4**: 890–897.

Paegle, J., Mo, K. and Nogués-Paegle, J. (1996). Dependence of simulated precipitation on surface evaporation during the 1993 United States summer floods., *Monthly Weather Review* **126**: 345–361.

Pan, Z., Segal, M., Turner, R. and Tackle, E. (1995). Model simulation impacts of transient surface wetness on summer rainfall in the United States Midwest during drought and flood years., *Monthly Weather Review* **123**: 1575–1581.

Pan, Z., Tackle, E., Segal, M. and Turner, R. (1996). Influences of model parameterization schemes on the reponse of rainfall to soil moisture in the Central United States., *Monthly Weather Review* **124**: 1786–1802.

Ropelewski, C. (1988). The global climate for June-August 1988: A swing to positive phase of the southern oscillation, drought in the United States and abundant rain in monsoon areas., *Journal of Climate* **1**: 1153–1174.

Rowntree, P. and Bolton, J. (1983). Simulation of the atmospheric response to soil moisture anomalies over Europe., *Journal of the Royal Meteorological Society* **109**: 501–526.

Shukla, J. and Mintz, Y. (1982). Influence of land-surface evapotranspiration on the earth's climate., *Science* **215**: 1498–1500.

Trenberth, K. and Branstator, G. (1992). Issues in establishing causes of the 1988 drought over North America., *Journal of Climate* **5**: 159–172.

Trenberth, K., Branstator, G. and Arkin, P. (1988). Origins of the 1988 North American Drought., *Science* **242**: 1640–1645.

Trenberth, K. and Guillemot, C. (1996). Physical processes involved in the 1988 drought and 1993 floods in North America., *Journal of Climate* **9**: 1288–1298.